Stem cells as gene delivery system to create cardiac biological pacemaker

Sandra Kanani

Université de Nice Sophia Antipolis - UFR Science
Ecole Doctorale de Sciences Fondamentales et Appliquées

THÈSE

pour obtenir le titre de

Docteur en Science

de l'UNIVERSITE de Nice-Sophia Antipolis

Spécialité : "Physique"

présentée et soutenue par

Auteur: Sandra KANANI

TITRE :

Stem cells as gene delivery system to create cardiac biological pacemaker

Thèse dirigée par : Valentine KRINSKI et Alain PUMIR

Soutenu le: le 15 Décembre 2005

JURY

M. HAKIM	– DR CNRS , rapporteur
M. NARGEOT	– DR CNRS , rapporteur
M. PUMIR	– DR CNRS
M. KRINSKI	– DR CNRS
M. COULLET	– Professeur
M. MANGONI	– CR CNRS

Contents

Abstract

Keywords: biological pacemaker, stem cell model, oscillation, inactivation.

- By investigating stem cell models, we showed that induction of oscillation in normal ventricular myocytes by connecting stem cells to them is not possible. Induction of oscillations by stem cells was never demonstrated yet in well controlled conditions. Reported results [5],[4] demonstrate only increase of oscillation frequency (in cell culture or in whole hearts).

- Oscillations become possible only for myocytes with much lower than normal threshold for inducing oscillations. Approaches like decreasing of expression level of I_{K1} current in myocytes are successful.

- Other possible approach is connecting stem cells not directly to myocytes but to other types of cardiac cells with lower oscillation threshold. This induces oscillation without need to affect I_{K1} current. This transitional cells might be AV node cells, Purkinje cells or cells in the vicinity of the sinus node.

- To drive cardiac tissue, small size artificial pacemakers need deliver currents orders of magnitude larger than those used in cell pair or cell culture experiments. To avoid this, the size of the pacemaker created should be several times larger than the electrotonic constant λ.

- For pacemaker currents, most experimenters traditionally measure inactivation only. A description of a stem cell including inactivation only is not precise enough to study oscillations. Descriptions including both, activation and inactivation of pacemaker current should be used, contrary to tradition in this field.

Mots clefs : pacemaker biologique, les cellules souches, oscillation, inactivation.

- En étudiant des modèles de cellules souches, nous avons montré que l'induction des oscillations dans des myocytes ventriculaires normaux inexcitables n'est pas possible en les connectant à des cellules souches. Jusqu'à aujourdhui, cette induction n'a jamais été démontrée même sous de bonnes conditions. Les résultats référencés [5],[4] ne font apparaître qu'une augmentation de la fréquence d'oscillation (soit dans les cellules en culture, soit dans le coeur).

- Les oscillations ne deviennent possibles que pour les myocytes qui ont un seuil d'excitation des oscillations induites bien plus bas que la normale. Seules les méthodes qui diminuent le niveau d'expression de courant I_{K1} donnent des résultats.

- Il existe une autre approche, qui consiste à ne pas connecter directement les cellules souches à des myocytes, mais à d'autres types de cellules cardiaques avec un seuil d'excitation très bas. De cette façon, des oscillations sont induites sans avoir à modifier le courant I_{K1}. Ces cellules transitoires pourront être des cellules AV node, de Purkinje ou des cellules voisinant SA node.

- Pour amener un tissus cardiac à oscillation, les pacemakers artificiels de petite taille exigent des courants d'une magnitude bien plus élevée que dans les expériences menées avec des paires de cellules ou des cultures. Pour éviter ce problème, la taille des pacemakers artificiels doit être plus grande que la constante électrotonique λ.

- Pour le courantpacemaker, la plupart des expérimentateurs ont l'habitude de ne mesurer que l'inactivation. Cette seule mesure ne suffit pas pour étudier les oscillations. Les définitions incluant à la fois inactivation et activation du courant pacemaker doivent prévaloir contrairement à la tradition dans le domaine.

Chapter 1

Introduction

1.1 Electronic and biological pacemakers

We describe the state of art in the Genetic Biological Pacemaker following reviews [2],[3],[5],[7],[15],[28] ,[29],[31],[32],[33].

Although electronic pacemakers (fig.1.1) are highly successful and about one quarter of million per year are implanted in USA, they are not optimal. Among their shortcomings are [4]:

1. They impose limitations on the exercise tolerance and cardiac rate-response to emotion. There is no substitute currently available for the autonomic modulation of heart rate.

2. The limitations imposed on unit and electrode dimensions by increasing age and mass of the pediatric patient. The hardware must be tailored to the growth of the patient.

3. The placement site of the stimulating electrode in the ventricle and the resultant activation pathway may have beneficial or deleterious effects on electrophysiologic or contractile function.

4. The battery has a long-but-limited life expectancy, requiring testing and replacement at periodic intervals.

5. Intercurrent infection may require removal and/or replacement of the pacemaker.

6. Various devices including neural stimulators, metal detectors, and magnetic resonance imaging equipment have been reported to interfere at times with electronic pacemaker function.

These concerns have encouraged advances in electronic device development and manufacture as well as the search for alternatives to electronic pacemakers.

The major breakthrough here has been recent research in using genetical methods to create biologi-
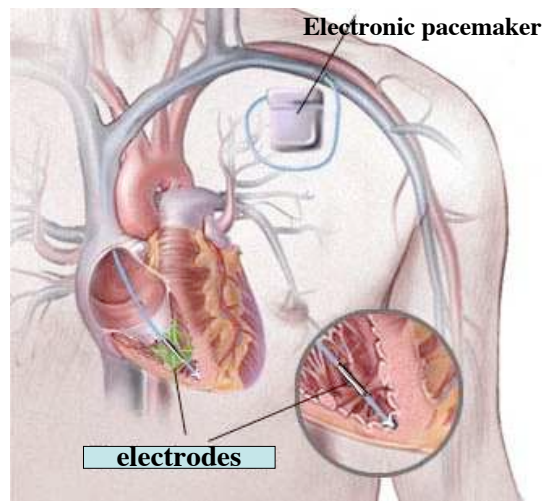
Figure 1.1: Electronic pacemaker

cal pacemakers. Yet now there is greater promise of cure, deriving from engineering novel functions into existing or newly generated cells. This research shares the techniques of gene therapy and cell therapy. This includes insertion of genes to replace those which are malfunctioning.

An important step in demonstrating proof of concept for gene- and cell-based therapies has been the study of potential triggers of the heartbeat, that is, the generation of biological pacemakers. The stimuli for designing biological pacemakers were:

1. the desire to improve on electronic pacemakers that are currently the state of the art for treating many rhythm disorders;

2. to use this paradigm as a template for developing other gene/cell-based strategies.

The most straight forward is to create a new sinoatrial node. The sinoatrial node is the primary biological pacemaker in the heart and a potential template for any biological pacemaker to be fabricated.

1.2   Paths for creating biological pacemakers

The natural pacemaker (sino-atrial node, or SA node) is situated not in ventricles but in atria (in the right atrium). But pacemaker activity exists also in many regions outside of the SA node such as in the AV node and in bundle branches in the ventricles. It contributes to reliability of oscillations: period of auto-oscillations in these regions is slower than in the SA node, and does not affect faster oscillation waves propagating from the SA node. If the SA node is damaged, these auto-oscillatory regions may keep periodic contractions of the heart.

Circulatory collapse ensues when these specialized cells are damaged by disease, a situation that currently necessitates the implantation of an electronic pacemaker.

From a medical point of view [2], there are two major problems to be treated: 1. a case when the SA or AV node does not work well, 2. a case when SA or AV are not functioning at all and are dead.

A general treatment might be either manipulating autonomic control or ion channel number, structure and function.

In my PhD, the focus is on creating a SA node from scratch.

1.3 Pacemaker(funny) ionic current I_f

Cardiac rhythmic activity is generated by "pacemaker" cells, which in mammals are located in the sino-atrial node (SA node).

During the four phases in a pacemaker cell for inducing oscillation they:

1. Set pace of heart beat

2. Fire spontaneously

3. Depolarize slowly to threshold

4. Depolarization caused by flow of Na^+ into the cell.

More precisely: action potentials of SA node cells have a special phase, called diastolic (or pacemaker) depolarization: at the end of an action potential, the pacemaker depolarization slowly takes the membrane voltage up to threshold for firing of a new action potential, thus inducing repetitive activity. In other words, the pacemaker cells of the heart initiate the heartbeat, sustain the circulation, and dictate the rate and rhythm of cardiac contraction.

The mechanism underlying the pacemaker depolarization was discovered by Brown, DiFrancesco and Noble [1]. They described a "funny" (I_f) current, so called because of its unusual properties. It is activated by hyperpolarization and not by depolarization unlike other currents, hence the designation "funny" current.

I_f is an inward current carried by Na^+ and K^+. It is activated on hyperpolarization at voltages in the diastolic range from a threshold of about $-40/-50$ mV. When at the end of an action potential the membrane repolarizes below this threshold, I_f is activated and supplies inward current, which induces the diastolic depolarization phase.

Sympathetic stimulation of SA node cells elevates cAMP levels and thereby shifts the voltage

dependence of I_f to more positive membrane potentials. This shift results in an increased I_f current, an accelerated pacemaker depolarization and hence, an increase in heart rate. In contrast, stimulation of SA node cells slows down the beating frequency, in part due to lowering of the cAMP concentration. cAMP binds directly to the I_f channel regulating its voltage dependance.

Hyperpolarization-activated cyclic nucleotide-gated (HCN) channel carries I_f.

Fig.1.2 shows an example of the pacemaker activity. In the Fig.1.2b the I_{K1} current is decreased. This is a key point and we will discuss this more in details in the "Models of different types of myocytes".
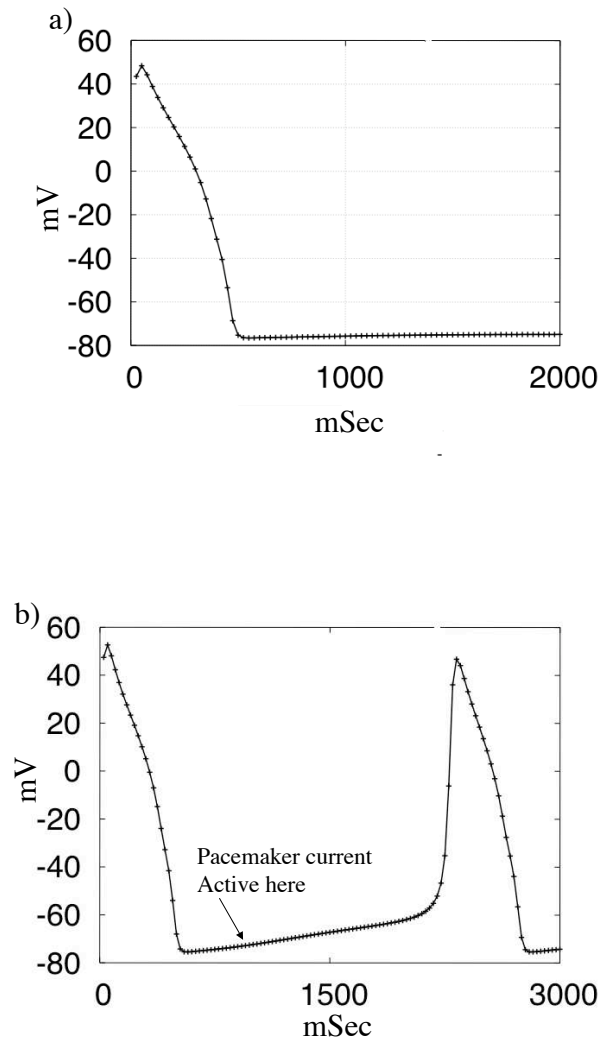
Figure 1.2: Pacemaker current: a) Action potential of a myocyte. b) Same in SA node cells.

1.4 Manipulating ion channel function to create pacemaker cells

Converting a normal cell into a pacemaker can be achieved either by an increase in inward currents (e.g., the pacemaker current I_f) or by a decrease in outward potassium currents. One such outward current is the inward rectifier I_{K1} [18],[23].

I_{K1} is a large current in ventricular myocardial cells, where it clamps resting membrane potential at a highly negative voltage, in other words, it stabilizes a strongly negative resting potential and should therefore suppress excitability. Any intervention that decreases I_{K1} below certain level, increases pacemaker rate. The same can be achieved by increasing I_f(e.g., by overexpressing a member of the HCN gene family)[17].

The approaches include use of naked plasmids or viral vectors to deliver the genetic construct of interest to a selected region of the heart and use of cells to deliver pacemaker constructs, whether the cells naturally incorporate them (e.g., embryonic stem cells) or can be loaded with them (e.g., mesenchymal stem cells).

1.5 Genetical approaches for creating biological pacemaker

Viruses can deliver the necessary genes [5]. Although the vectors have been replication-deficient adenoviruses that have little infectious potential, these incorporate the possibility of only a transient improvement in pacemaker function as well as potential inflammatory responses.

The use of retro-viruses and other vectors, although not attempted as yet for biological pacemakers, carries a risk of carcinogenicity and infectivity that is unjustified, given the current success of electronic pacemakers.

Attempts to use embryonic human stem cells to create pacemakers carry the problems of identifying appropriate cell lineages, the possibility of differentiation into lines other than pacemaker cells, and potential for neoplasia.

1.6 Characteristics to be embodied in a biological pacemaker

Characteristics needed to be in a biological pacemaker can be named as:

1. Create a stable physiologic rhythm for the lifetime of the individual

2. Require no battery or electrode and no replacement

3. Compete effectively in direct comparison with electronic pacemakers

4. Confer no risk of inflammation/infection

5. Confer no risk of neoplasia

6. Adapt to changes in physical activity and emotion with appropriate and rapid changes in heart rate

7. Propagate through an optimal pathway of activation to maximize efficiency of contraction and cardiac output

8. Have limited and preferably no arrhythmic potential

9. Represent cure, not palliation.

These considerations are not trivial. However, given the excellent successes of electronic pacemakers, anything less than the characteristics listed would not warrant the development of a biological alternative.

1.7   Stem cells used to create biological pacemaker

Adult human mesenchymal stem cells (hMSCs) are attractive for gene delivery applications [5]. The most important point is that these cells are immunoprivileged, in other words, they might not elicit the immune response that complicates transplantation [35].

Next, because the cells are readily available, and there are no objections to their use for research purposes. This is viewed as a major benefit to the work, which contemplates implanting human mesenchymal stem cells into hearts. In addition, it is believed that if the work advanced to the point of clinical trial, this property might facilitate the use of banked rather than autologous cells as a source for human administration.

hMSCs are multipotent and differentiate only further along mesenchymally derived lineages fig.1.3, the strategy is to use them as platforms to carry genes of interest to regions of the heart would need to couple with adjacent myocytes.

Human embryonic stem cells (hES) provide a rich source of material for initiating electrical activity in heart. The possibility that their use requires immunosuppressive treatment remains an issue.

Among the limitations common to both types of stem cell are concerns regarding their maintenance as stem cells vs their differentiation into other cell types.

For both human embryonic stem cells (hES) and human mesenchymal stem cells hMSC, it is important that the cells not evolve into unwanted cell lineages, as we would not want to see cartilage or lakes of hematopoietic cells in the heart. Similarly, issues regarding localization of cells vs migration elsewhere in the heart or in the body are critical[2].

Meanwhile, spontaneously excitable cardiomyocytes tissue from human embryonic stem cells hES are generated [26]. It was showed that they integrates structurally, electrically and mechanically with rat cardiac cells *in vitro*. They demonstrated that hES cardiomyocytes survive, integrate and function *in vivo* by showing that they pace ventricle in pigs with complete heart block.
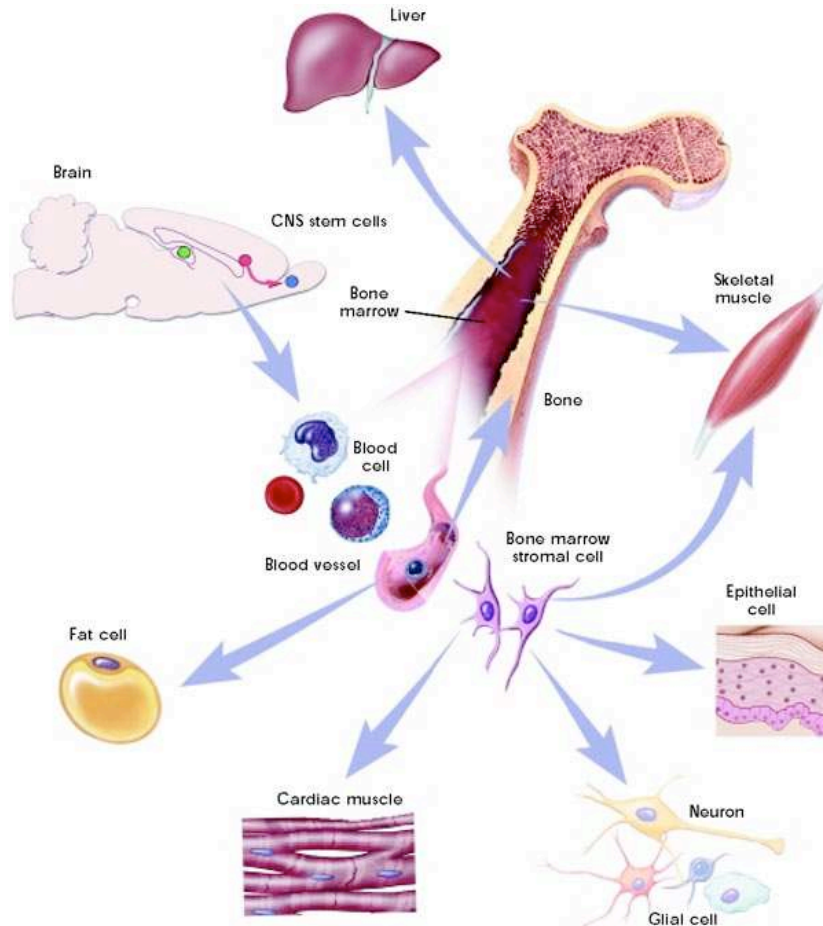
Figure 1.3: Stem cell can be converted to all kinds of cell in the body. We used mathematical modeling to choose most effective paths for experiments to use them to create cardiac pacemaker.

1.8 Stem cell experimental results

The paths to recreate the SA node [3] include introducing progenitor or stem cells into selected regions of the heart, so that they develop into cells having the characteristic physiologic function desired.

hMSCs transfected with a cardiac pacemaker gene, $mHCN2$ expressed high current activating in the diastolic potential range, confirming the expressed current as I_f -like. The stem cells ($hMSCs$)

form gap junctions with adjacent myocytes (Fig.1.4).

More precisely [5]: voltage ramp in Fig.1.4B ($V_1 = 100$, $V_2 = 0$ mV) applied to the canine myocyte evoked current flow through the patch pipettes attached in whole-cell mode to the myocyte, I_1, and hMSC, I_2. Currents recorded from the myocyte, I_1, represent the sum of two components, a junctional current and a membrane current in the myocyte. I_2, recorded from the voltage-clamped hMSC corresponds to the junctional current, I_j, between the hMSC myocyte pair.

Besides, the suggestion that coupling between myocyte and human mesenchymal stem cell resulted in effective pacemaker function was demonstrated *in vitro*, on a coverslip on which a small node of human mesenchymal stem cells transfected with either HCN2 alone was overlaid with neonatal rat myocytes [5]. The former developed beating rates approximately twice the rates of the latter (from 93±16 bpm to 161±4).

The difference between expressing HCN2 in adult and neonatal stem cells was investigated in [16]. An adenoviral construct (AdHCN2) of HCN2 was used to infect neonatal and adult rat ventricular myocytes to investigate the role of maturation on current gating. The expressed current exhibited an 18 mV difference in activation ($V_{1/2}$ was -95.9±1.9 in adult; -77.6±1.6 mV in neonate) comparable to the 22 mV difference between native I_f in adult and neonatal cultures ($V_{1/2}$ was -98.7 versus -77.0 mV).

Ventricular pacemaker current I_f shows distinct voltage dependence as a function of age, activating outside the physiological range in normal adult ventricle, but less negatively in neonatal ventricle [16].

These findings demonstrated that genetically modified hMSCs can mimick over expression of HCN2 genes in cardiac myocytes and represent a novel delivery system for pacemaker genes into the heart.

We will base our mathematical modeling on biological expriments that were done by Ira S. Cohen et al. [5]. They tested the ability of human mesenchymal stem cells (hMSCs) to deliver a biological pacemaker to the heart.

1.9   What Physics can do for such a problem?

Impressive results were obtained with stem cells to create an artificial biological pacemaker: human Mesenchymal Stem Cells (*hMSC*) transfected with HCN2 genes injected in canine left bundle branch provide ventricular escape rhythms that were mapped to the site of the injection [3].

In 15th annual Gordon K. Moe Lecture, M.Rosen described what is needed to see a biological pacemaker "In our lifetime" [3]:

- localization at site of implantation of stem cells vs migration to other sites;
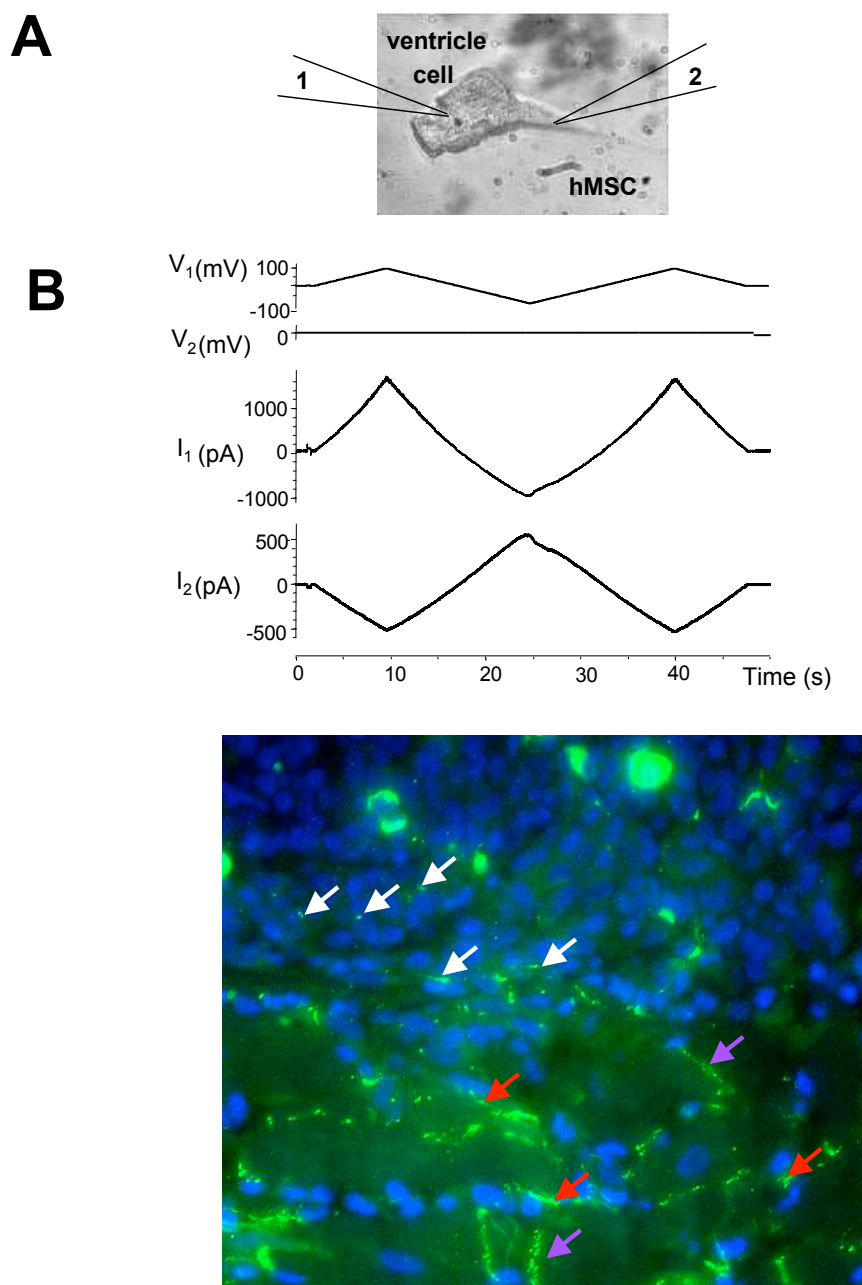
White=stem to stem, red=stem to myocardium, purple=intercalated disc

Figure 1.4: Stem cells form gap junctions with adjacent myocytes. See an analysis and more details in chapter "Stem cell model".

- evidence regarding persistence of the administered stem cell type vs differentiation into other cell types;

- evidence regarding persistence of pacemaker function (current and coupling).

In the list "what characteristics should be embodied in a biological pacemaker?", number one is:

- create a stable physiological rhythm for the lifetime of the individual.

On the physical language, it means: *robustness of oscillations.* This includes stability of oscillations and oscillation period against inevitable small variations of percentage of stem cells migrated to other sites; differentiated into other cell types; lost pacemaker function; decrease pacemaker current due to decrease of expression levels of pacemaker channels or gap junctions.

The period should be reasonably stable with respect to inevitable variations of many parameters affecting the biological pacemaker. It should tolerate the decrease of expression levels of pacemaker channels (HCN gene family) or gap junctions, of activity of peptides regulating gene expressions, loss of genes, small percentage of stem cells migrated to other sites; differentiated into other cell types; lost of pacemaker function by some cells.

Also there are several proteins like minK,MiRP1,... regulating level of expression of these HCN genes [24][10]. Factors like these proteins should be considered as a regulator for such biological pacemakers.

Even more important problem comparing to the factors mentioned above, is the "nucleation problem". The proteins and regulators can be a solution for a zero dimensional case (a stem cell transfected to HCN2 connected to a myocyte) but they are negligible in a three dimensional problem (real heart). In other words:

- The excitation threshold in three dimension is ~ 100 times larger than in zero dimension (For further details see chapter : two and three dimensional tissues).

- From 10^6 stem cells injected to myocytes, only 50 cells made gap junction connections with myocytes [5].

Achieving the construction of the biological pacemaker will require an expensive and a time consuming work or in other words, a large number of expensive genetical and electrophysiological experiments. A combination of experiments with theoretical predictions is to be used as a guide to decrease the number of experiments. Our aim is to create a theory to guide and help the plan of the experiments. This requires creation of precise and adaptable mathematical models based on concepts and results of [5]-[37].

1.10   HCN Channels (isoform family)

In cardiac muscle the pacemaker current is coded by a HCN gene family [32][9]. The name HCN stands for Hyperpolarization-activated Cyclic Nucleotides-gated channels that includes four iso-forms : HCN1, HCN2, HCN3, HCN4. The most pronounced difference between different isoforms is in distinct activation kinetics.

Fig.1.5B [32] shows inactivation curves of the HCN1-4 channels. The cells were clamped from a holding potential of -40 mV to voltages from -140 to -50 mV in 10 mV increments(see inlet in Fig.1.5B) for 200 mSec (HCN1), 2.5 Sec (HCN2 and 3) and 10 Sec (HCN4). Fig.1.5C Shows in activation kinetics of $HCN1 - 4$ (with number of experiments in the brackets).

Only stem cells transfected with HCN2 were used for designing an artificial biological pacemaker [3], [5], [7], [4]. We will begin our investigation with HCN2.

1.11 Aim of the work

In this thesis, our challenge is to replace a part of the expensive and time consuming experiments with theoretical understanding and numerical simulations.

For this, we:

- introduced for the first time a model for the stem cell transfected with a gene that codes the pacemaker current channel (HCN gene family).

- analyzed and compared three isoforms of this gene family (or channels): HCN1, HCN2, HCN4 (HCN3 is not present in the cardiac tissue).

- connected the stem cell to myocytes

- studied a cell pair, a two dimensional cell culture, and the three dimensional cardiac tissue

In the following chapter, we will present our model for a stem cell.
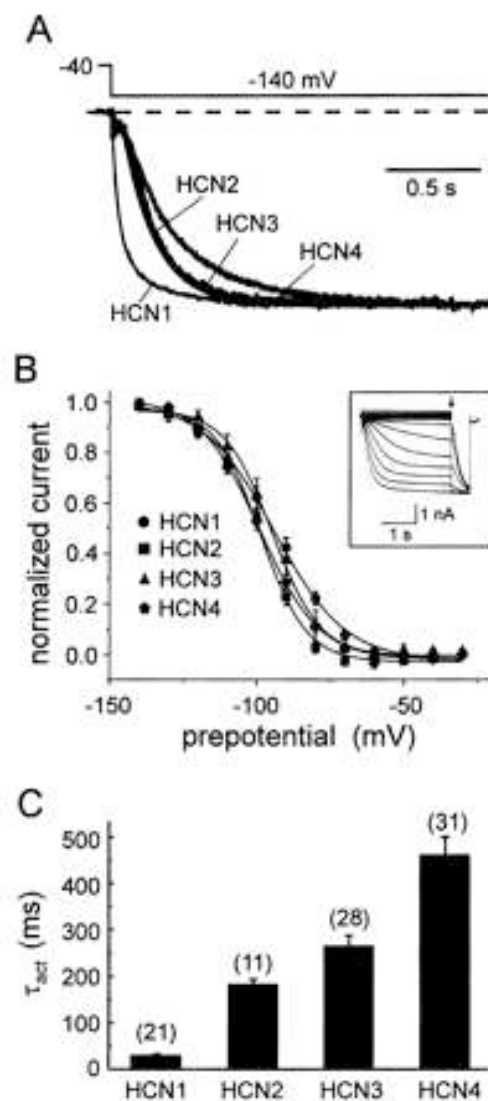
Figure 1.5: Electrophysiological properties of the HCN1-4 channels measured in voltage clamp mode. A) An example of a voltage clamp record. B) Voltage dependance of inactivation. Inlet shows scheme of the experiment. C) The inactivation time constants for $E = -140$ mV. In brackets is shown the number of experiments.

Chapter 2

Construction of the stem cell models

2.1   Models of stem cells transfected with HCN2

Because the experiments with artificial biological pacemaker were performed with stem cells transfected with HCN2 and these channels are strongly modulated by cAMP, we will start our investigations with this isoform.

We constructed models for a human Mesenchymal stem cell transfected with HCN2 gene from experimental data [5],[6]. The models permit to mimic experiments with levels of gene expressions not achieved yet in experiments and decide if the work to achieve this levels will significantly increase the quality of oscillations.

We describe here our two models: a model with two gating variables, activation and inactivation of the pacemaker current and a simplified model, including inactivation only.

Stem cell model with activation and inactivation (Stem-mh)

We described it as follows:

$$\frac{dE_s}{dt} = \frac{-N\sigma_f}{C}\, g_1^s g_2^s (E_s - E_r) \tag{2.1}$$

$$\frac{dg_i^s}{dt} = \frac{(\bar{g}_i^s - g_i^s)}{\tau_i^s(E_s)}, \quad i = 1,2 \tag{2.2}$$

E_s is the stem cell membrane potential, mV.
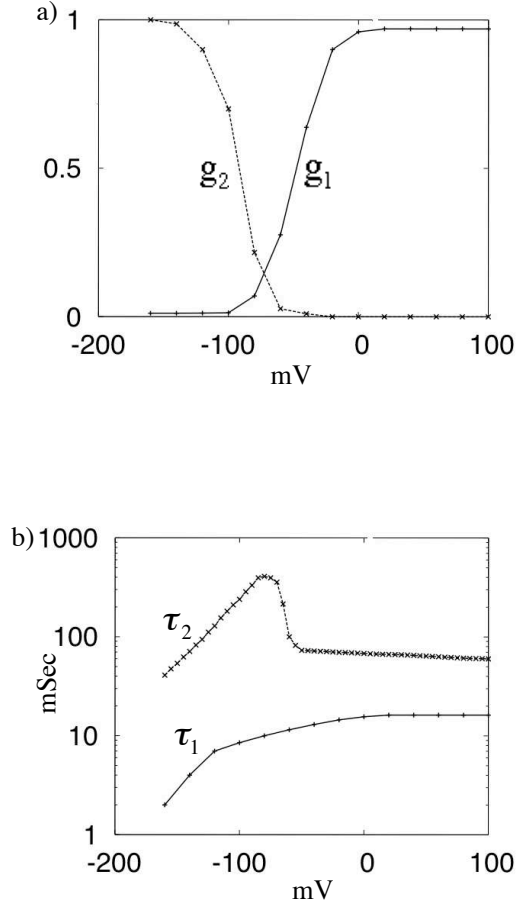
Figure 2.1: **Stem cell model with activation and inactivation.** a) activation (g_1 or m) and inactivation gating variables (g_2 or h). b) time constants.

g_1^s, g_2^s are activation and inactivation gating variables (notations m, h are used in Hodgkin-Huxley eqns[30]).

τ_1^s, τ_2^s are activation and inactivation time constants, Fig.2.1.

N is the number of pacemaker channels per cell,

$\sigma_f \sim 1pS$ is the conductivity of a single pacemaker channel,

$E_r \sim -40$ mV is the reversal potential. It is the membrane voltage at which there is no net flow of ions from one side of the membrane to the other.

A problem comes with respect to normal electrophysiological statements that the experimentalists in the field traditionally call "activation" the increase of the pacemaker (funny) current with negative voltages. This term induced questions how a model with inactivation only (without activation variable) can describe activation of the current. The explanation is: increase of the current in these

experiments is induced by removing inactivation at negative voltages (and not by activation, that is physically a different process).

We used symmetry of voltage dependence of gating variables $\bar{g}_i^s$ for constructing the model when the available experimental data were limited.

Stem cell model with inactivation only (Stem-h)

We describe it as follows:

$$\frac{dE_s}{dt} = \frac{-N\sigma_f}{C} g^s(E_s - E_r) \qquad (2.3)$$

$$\frac{dg^s}{dt} = \frac{(\bar{g}^s - g^s)}{\tau_2^s(E_s)} \qquad (2.4)$$

g_2 is given for complete model only and for the reduced model, $g^s = g_2 \times g_1$. Fig.2.2.

Since ratio $\epsilon = \frac{\tau_1^s}{\tau_2^s} \ll 1$, (Fig2.1b), it is natural to expect that a simplified model with inactivation only will give results close to the full model.
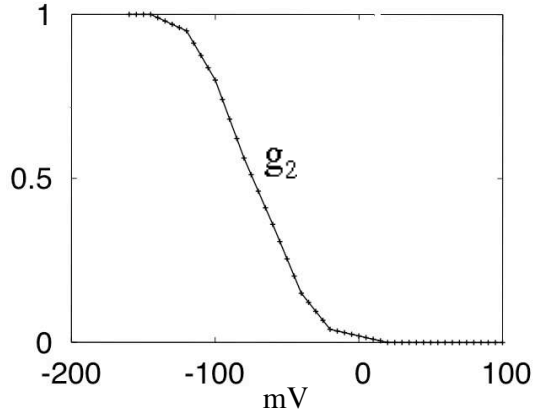
Figure 2.2: Inactivation gating variables (g_2 or h) for stem cell (stem-h)

2.1.1 How we constructed the stem cell models: generic features

We will start with the simpler model.

Stem cell model with inactivation only

We will repeat here equations of the model:

$$\frac{dE_s}{dt} = \frac{-N\sigma_f}{C} g^s(E_s) \times (E_s - E_r) \tag{2.5}$$

$$\frac{dg^s}{dt} = \frac{(\bar{g}^s - g^s)}{\tau_2^s(E_s)} \tag{2.6}$$

The right hand side of Eqns.2.5 is the pacemaker (funny) current I_f and is measured in the experiments [5]:

$$\frac{-N\sigma_f}{C} g^s(E_s) \times (E_s - E_r) = I_f(E) \tag{2.7}$$

The experiment records are shown in Fig.2.5.

As seen from Eqns2.5,2.6 and Fig.2.5, for construction of the simplified model, we needed to find the number of pacemaker channel per cell N and two functions:

$$g^s(E_s), \tau_2^s(E_s)$$

The values E_r, σ_f are known: $E_r \sim -40$ mV, $\sigma_f = 1$ pS.

We found N from the scaling condition that inactivation variable $g^s = 1$ for the most negative value of voltage ($E_s = -160$ mV). This gives $N = 6 \times 10^4$ pacemaker ionic channels per cell (See detailed calculations in the next chapter).

g^s was found from Eq.2.7 where now all values are known.

$\tau_2^s(E_s)$ was found as time constants of current records for every E_s in Fig.2.5B.

Stem cell model with activation and inactivation

The model is:

$$\frac{dE_s}{dt} = \frac{-N\sigma_f}{C} g_1^s(E) g_2^s(E) \times (E_s - E_r) \tag{2.8}$$

$$\frac{dg_i^s}{dt} = \frac{(\bar{g}_i^s - g_i^s)}{\tau_i^s(E_s)}, \quad i = 1, 2 \tag{2.9}$$

As seen from Eqns2.8,2.9 and Fig.2.1, for construction of the complete model, we needed to find four functions:

$$g_1^s(E_s), g_2^s(E_s), \tau_1^s(E_s), \tau_2^s(E_s)$$

Estimations of $g_1^s(E_s)$ and $g_2^s(E_s)$

The difficulty was:

$$I_f(E_s) \propto g_1^s(E_s) \times g_2^s(E_s)$$

and we had only one function measured in the experiment: $I_f(E_s)$. This can give only the product $G(E_s) = g_1^s(E_s) \times g_2^s(E_s)$ but not functions $g_1^s(E_s), g_2^s(E_s)$ separately. A standard approach to estimate them (used from the Hodgkin-Huxley times[30]), is to measure fast and slow ionic currents separately in a voltage clamp experiment. These measurements were not performed by the experimental team [5]("no manpower" to do it). So, we needed to find what data from the experimentally recorded currents could be used to supplement available $I_f \propto g_1^s \times g_2^s$.

I_f was measured in the experiment as a current induced in response to voltage step from -30 mV to variable levels E. In the same experiment, it is seen how the currents were modified by the end of this voltage step (so called "tail currents). We used these tail currents records to supplement available I_f records (see details in the next chapter). This gave us g_1^s and g_2^s independently.

Construction of the stem cell models: detailed analysis of the experiments

Estimation of g_2^s from tail currents records

In Fig.2.5B, tails currents were recorded as a response to the end of the voltage step that is from variable level E to $+20$ mV. The tail currents were measured at times t_0 such that:

$$\tau_1 << t_0 << \tau_2$$

Due to it, activation $g_1^s(E, t)$ reaches its steady value $g_1^s = \bar{g_1}^s(20mV)$, while inactivation is still close to its initial value before the end of the step, $g_2^s = g_2^s(E)$. So, the tail current measured is described by the equation:

$$I_{tail} = \frac{-N\sigma_f}{C} g_1^s(20\,mV) g_2^s(E_s)(20\,mV - E_r)$$

When I/I_{max} is represented as a dimensionless value, all multipliers except $g_2^s(E)$ disappear and the dependence on voltage is kept in $g_2^s(E_s)$ term only.

$$\frac{I_{tail}}{I_{max}} = \frac{g_2^s(E_s)}{g_2^s(E_{max})}$$

since $g_2^s(E_{max}) = 1$ (the scaling condition)

$$\frac{I_{tail}}{I_{max}} = g_2^s(E_s)$$

So tail current records [5] give inactivation g_2^s (separated from g_1^s).

Now g_1^s can be easily found from Eq.2.7

Estimations of τ_1 and τ_2

Estimations of τ_2

Since τ_2 is large (of the order of$\sim$ 500 mSec) it was easily estimated from current records in Fig.2.5B.

Estimations of τ_1

But there is a significant problem in estimation of τ_1.

τ_1 is of the order of$\sim$ 10 mSec, and this time scale is not resolved in the experiments, Fig.2.5B. More than that, if this time scale would be resolved, the fast current would be masked by the capacitance current. So experimentalists studying pacemaker current traditionally show only one component current records (slow component Fig.2.5B).

We needed to restore the fast component records based on generic features of the model.

A physiscist looking at the Eqns.2.8,2.9 would generically expect three components in

$$I_f = \frac{-N\sigma_f}{C} g_1^s(E_s, t) g_2^s(E_s, t) \times (E_s - E_r)$$

induced in response for a voltage step:

(1). An immediate response ($\tau = 0$ mSec) in $I_f = \frac{-N\sigma_f}{C} g_1^s g_2^s \times (E_s - E_r)$ due to jump in term $(E_s - E_r)$.

(2). A delayed response due to fast variable with $\tau \sim 10$ mSec.

(3). A delayed response with a larger time constant due to slow variable with $\tau \sim 100$ mSec.

These three components are not seen in Fig.2.5B. But their consequences can be found.
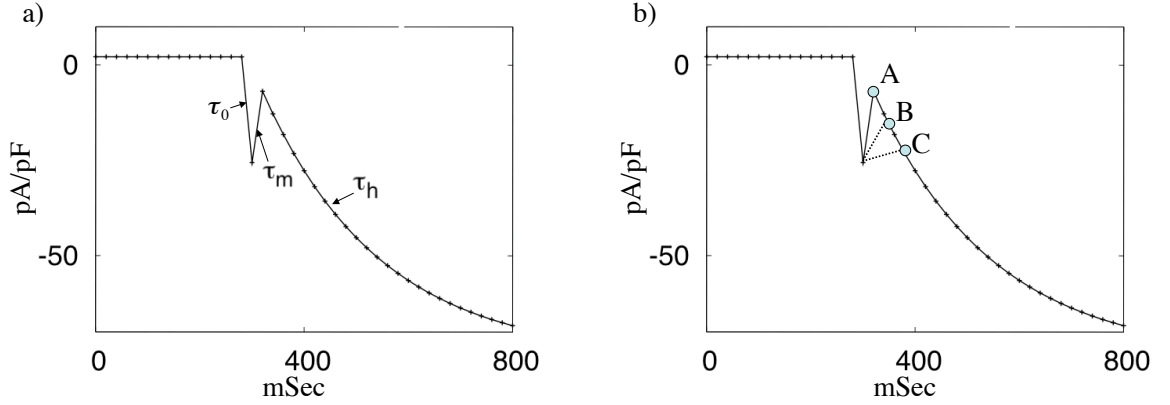
Figure 2.3: Measuring activation time τ_1 by matching the experimental records. a) Three components of the current that should be observed in the experiment with a higher time resolution. b) With try and error, the correct value of τ_1 corresponding to the experimental record was chosen.

Estimation of $\tau_1(E_s)$

The three components that should be observed here are shown in Fig.2.3. In Fig.2.3a, component τ_0 corresponds to the item (1) above, component τ_m corresponds to the item (2) and component τ_h corresponds to the item (3).

By varying component τ_1 in Fig.2.3b we may vary position of the initial point (A, B or C) of the slow current record. We chose the value τ_m so that it gives the position of the initial point of the slow current record in Fig.2.3b same as in experiment Fig.2.5. This was done for every voltage E and gave us the needed dependance $\tau_1(E)$.

2.1.2 Specific features: (*Calculating number of pacemaker and gap junction channels in source experiment; dimensionless and dimensioned variables*)

Number of pacemaker channels

It can be readily found from eq.2.7 for the steady value of the pacemaker current:

$$I_f(E) = \frac{-N\sigma_f}{C} g^s(E_s) \times (E_s - E_r)$$

Here $g^s(E_s)$ was found in the previous chapter, $I_f(E_s)$ is measured in the experiment and all other values are known except N. This gives :

$$N \sim 6 \times 10^5 \; channels \; per \; cell$$

See details in dimensionless and variables section.

Number of gap junction channels
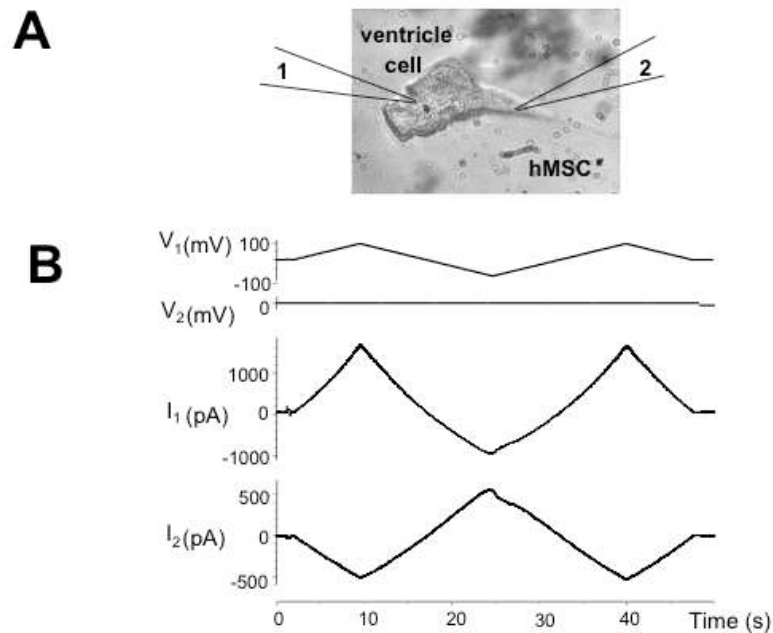
Figure 2.4: Voltage and current records from a stem cell connected to the myocyte

From Fig.2.4B the resistance between the Myocyte and the stem cell is:

$$R = 0.2 \times 10^9 \Omega$$

Since the conductivity of a single gap junction channel is 50 pS, this gives :

$$n = 100 \; gap \; junction \; channels \; per \; cell$$

Note that there is four orders of magnitude difference between numbers of gap junction and pacemaker channels per cell.

Dimensionless and dimensioned variables

Here we will give calculations of the numbers of channels per cell. This is an important step in designing a quantitative model.

Number of pacemaker channels

For voltage $E_s = -160$ mV the inactivation variable $g_2^s = 1$ (the scaling condition), then Eq.2.7 became $I_f = -N\sigma_f (-160 - E_r)$. where from :

$$N = \frac{I_f}{\sigma_f} (-160 - E_r) \tag{2.10}$$

Inserting values $E_r = -40$ mV and $\sigma_f = 1$ pS and value for I_f , one can obtain N.

In our model, the predicted currents correspond to an entire cell, but the experimentalists express their results in pA/pF. These two are related by the total capacitance, C=95 pF.

As an example, one of the currents recorded in Fig.2.5B is $I' = 76$ pA/pF which corresponds to $I_f = C \times I' = 95 \times 76 = 7220$ pA. If the value $I' = 76$ pA/pF was used it would give ~ 100 times error. The point is that N is defined as number of pacemaker channels per cell.

This, together with Eq.2.10, leads to the following calculation for the number of pacemaker channels.

$$N = \frac{7220(pA)}{1(pS)} 120(mV) \sim 6. \times 10^5 channels$$

Number of gap junction channels

In Fig.2.4B current flowing between stem cell and myocyte is $I_2 = 500$ pA and $\Delta E = 100$ mV. So the resistance of the gap junction channel between cells is:

$$R = \frac{\Delta E}{I_2} = \frac{100 \times 10^-3}{500 \times 10^-12} = 0.2 \times 10^9 \Omega$$

So the total conductivity between two cells $\sigma_{total} = 5 \times 10^-9$ S. Since the conductivity of a single gap junction channel is 50 pS, the number of gap junction channels per cell n is:

$$n = \frac{\sigma_{total}}{\sigma_1} = \frac{5 \times 10^{-9}}{50 \times 10^{-12}} = 100 \; channels$$
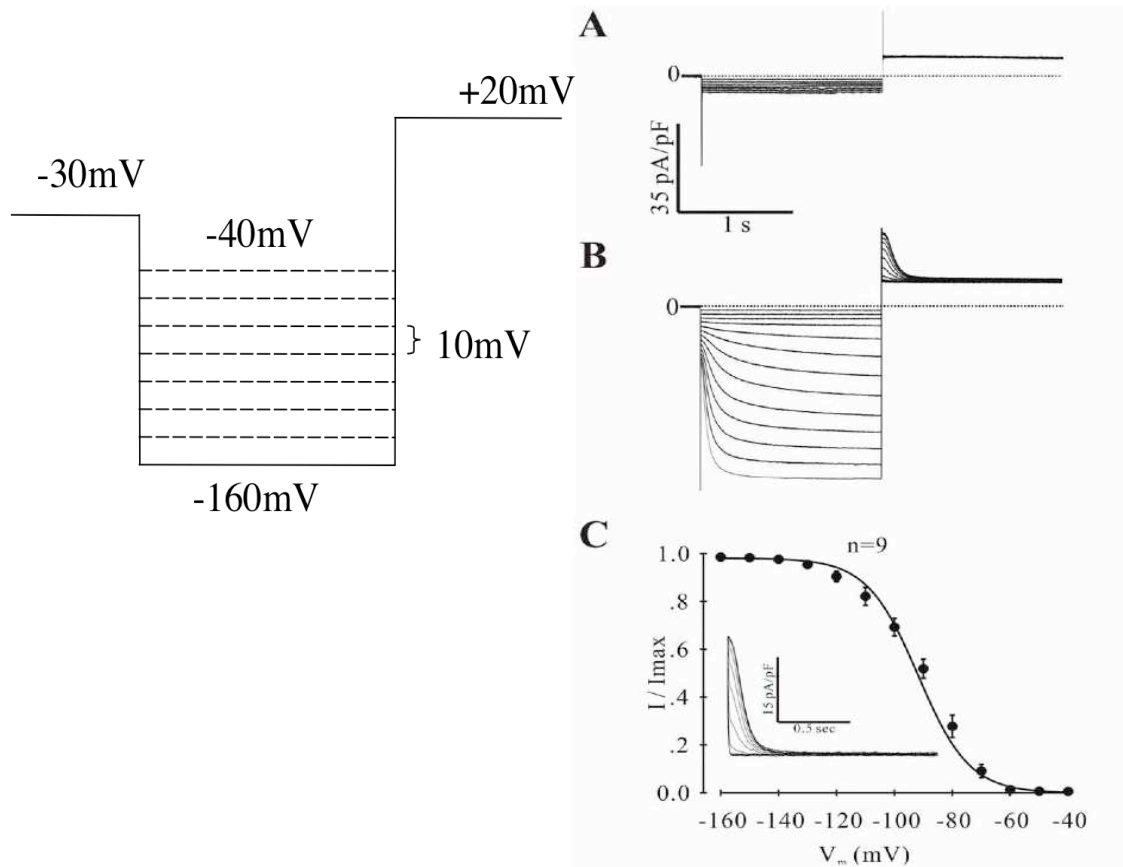
Figure 2.5: **Pacemaker current I_f in an experiment with stem cells hMSCs transfected with mHCN2 gene [5]**. Voltage protocol is shown on the left. Voltage was hold at -30 mV and hyperpolarized to voltages between -40 and -160 mV in 10 mV increments. (A) There is no current for non transfected stem cells. (B) Current I_f records in a transfected stem cell. (C) Dependance of steady value of the current I_f on voltage.

Currents generated by the stem-h model Eq.2.5,2.6 with the same experimental protocol as in Fig.2.5a are shown in Fig.2.6. It is seen that the model reproduces precisely the same current values as in the experiment Fig.2.5b [5].
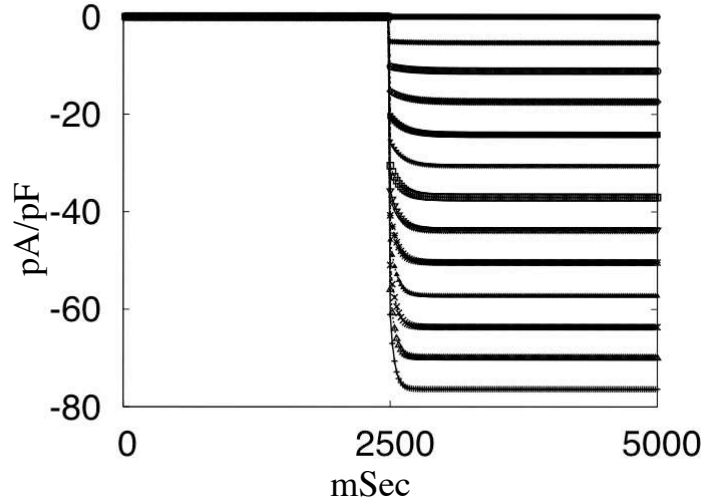
Figure 2.6: **Current records from the stem cell model**. Compare with Fig.2.5b.

2.2   Models of different types of myocytes

We need to investigate interaction of stem cells with myocytes of different types. No published models are sufficient for this (each of them describes a specific type of myocytes). So, we'll create models of several types of myocytes starting from an existing model.

Important characteristics of myocyte here are: whether it is self-oscillating (as a neonatal myocyte), or excitable (as a ventricular myocyte). For excitable myocytes, important is the threshold value of current that is needed from a stem cell to induce oscillations with desired period (T $\sim$ 1 sec); other characteristics and ionic currents are less important. To achieve this, it is sufficient to modify the level of expression I_{K1} (time independent Potassium) current.

Here, we work with several models of myocytes:

1. Normal myocytes (with high threshold I_{osc} for inducing oscillations).

2. Self oscillating neonatal type myocytes

3. Several transtional types.

We obtained these models by reducing expression level of I_{K1} current [1] to decrease I_{osc} and subsequent re-scaling all time constants in the model to keep APD same for all myocytes types.

I_{K1} was presented as:

$$I_{K1} = k \times I_{K1}^* \tag{2.11}$$

where I_{K1}^* is the current in original myocyte model and $k < 1$ is a coefficient. Fig.2.7 shows I_{K1} current in BR model. It is important to note that k=1 corresponds to the normal ventricular myocytes.
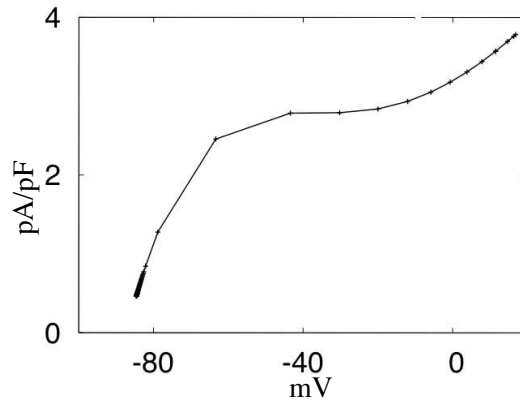
Figure 2.7: Time independent K^+ current, I_{K1}

The expression level of I_{K1} needed to obtain a specific myocyte type will be different for, say, a model of a human myocytes and an animal model.

For creation of a biopacemaker, the threshold I_{osc} for inducing oscillations (controlled by k) is the most important. Other details such as ionic currents and hence, the choice of an ionic model among many models published are less important comparing to this factor. Fig.2.8 shows how shape and resting potential changes according to level of expression of I_{K1}.

We obtained the models of different types of myocytes starting with the Beeler-Reuter (BR) [28] model. It describes the membrane potential, E_m, gating variables g_i^m controlling ionic chanels, and Ca concentration $[Ca]$:

$$\partial_t E_m = \frac{-I_{ion}}{C}(E_m, g_i^m) + D\nabla^2 E_m \tag{2.12}$$

$$\partial_t g_i^m = \frac{(\bar{g}_i^m - g_i^m)}{\tau_i^m(E_m)}, \quad i = 1, 6 \tag{2.13}$$

$$\partial_t [Ca] = -10^{-7} i_{Ca} + 0.07(10^{-7} - [Ca]) \tag{2.14}$$

---

[1] I_{K1} is the time independent Potassium current in the original BR model.

Where:

$$i_{Ca} = g_{Ca}g_5^m g_6^m (E_m - E_{Ca})$$

$$g_{Ca} = 0.09mS/cm^2$$

$$E_{Ca} = -82.3 - 13.0287\ln[Ca].$$

The diffusion term D in Eq.2.12 represents the electric coupling between cells. $D \sim 10^{-3}cm^2/mSec$. The model in one and two dimension was calculated with $dx = 0.1$ mm, $dt = 0.001$ mSec. (dx was chosen due to the cell size $\sim 100 \times 10 \times 10\mu$)

In Fig.2.8a a normal AP in a myocyte is seen, while in Fig.2.8b we have changed I_{K1} (or k).
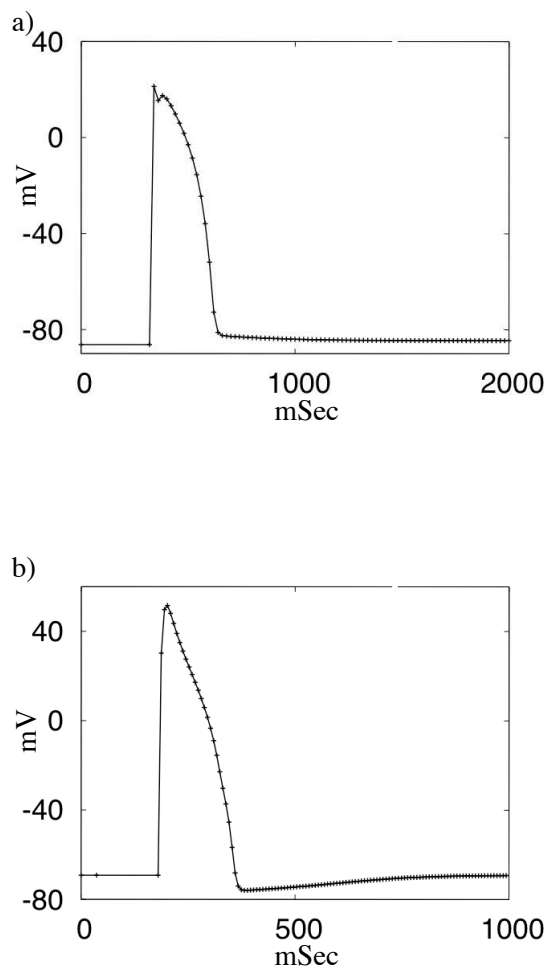
Figure 2.8: a) AP in the original BR model. b)AP shape and resting potential for a myocyte $k = 0.25$ (modified BR model).

A myocyte with k=1 corresponds to the original BR equation.

Excitation threshold current is $I_{exc} = 2$ pA/pF
Oscillation threshold current is $I_{osc} = 2.01$ pA/pF

While a myocyte with k=0.3 has both thresholds with an order of magnitude less:

Excitation threshold is $I_{exc} = 0.17$ pA/pF
Oscillation threshold is $I_{osc} = 0.18$ pA/pF

2.3   Models of a cell pair: a stem cell connected to a myocyte

A stem cell connected to a myocyte (a cell pair) is described by equations:

$$\frac{dE_s}{d_t} = \frac{-N\sigma_f}{C}g_1^s g_2^s(E_s + 40) + \frac{n\sigma_g}{C}(E_m - E_s) \tag{2.15}$$

$$\partial_t E_m = \frac{-I_{ion}}{C}(E_m, g_i^m) + \frac{n\sigma_g}{C}(E_s - E_m) \tag{2.16}$$

$$\partial_t g_i^m = \frac{F(g_i^m, E_m)}{\tau_i^m(E_m)}, \quad i = 1, ..., 6 \tag{2.17}$$

$$\partial_t[Ca] = -10^{-7}i_{Ca} + 0.07(10^{-7} - [Ca]) \tag{2.18}$$

$$\frac{dg_i^s}{dt} = \frac{F(g_2^s, E_s)}{\tau_2^s(E_s)}, \quad i = 1, 2 \tag{2.19}$$

C is the cell capacitance ~ 95 pF.

n is the number of gap junction channels per cell.

N is the number of pacemaker channels per cell.

σ_g is the conductivity of a single gap junction channel ~ 50 pS.

The term $n\sigma_g(E_m - E_s)$ in Eq.2.20 describes the current flowing from a myocyte to a stem cell through a gap junction channel.

The simplified model (Stem-mh) was incorporated similarly. The stem cell is described by a simplified model (Stem-h) with one gating variable g_2^s only.

$$\frac{dE_s}{d_t} = \frac{-N\sigma_f}{C}g_2^s(E_s + 40) + \frac{n\sigma_g}{C}(E_m - E_s) \tag{2.20}$$

$$\partial_t E_m = \frac{-I_{ion}}{C}(E_m, g_i^m) + \frac{n\sigma_g}{C}(E_s - E_m) \tag{2.21}$$

$$\partial_t g_i^m = \frac{F(g_i^m, E_m)}{\tau_i^m(E_m)}, \quad i = 1, ..., 6 \tag{2.22}$$

$$\partial_t [Ca] = -10^{-7} i_{Ca} + 0.07(10^{-7} - [Ca]) \tag{2.23}$$

$$\frac{dg_i^s}{dt} = \frac{F(g_2^s, E_s)}{\tau_2^s(E_s)} \tag{2.24}$$

2.4 Models for cardiac tissue with incorporated stem cells

We suppose that stem cells are injected to pacemaker region only and are connected to the myocytes only but not one to another. The tissue is described by the equations below.

$$\frac{dE_s}{d_t} = \frac{-N\sigma_f}{C} g_2^s(E_s + 40) + \frac{n\sigma_g}{C}(E_m - E_s) \tag{2.25}$$

$$\partial_t E_m = \frac{-I_{ion}}{C}(E_m, g_i^m) + D\nabla^2 E_m + \delta_{x,p} \frac{n\sigma_g}{C}(E_s - E_m) \tag{2.26}$$

$$\partial_t g_i^m = \frac{F(g_i^m, E_m)}{\tau_i^m(E_m)}, \quad i = 1, ..., 6 \tag{2.27}$$

$$\partial_t [Ca] = -10^{-7} i_{Ca} + 0.07(10^{-7} - [Ca]) \tag{2.28}$$

$$\frac{dg_i^s}{dt} = \frac{F(g_2^s, E_s)}{\tau_2^s(E_s)} \tag{2.29}$$

Where : $\delta_{x,p} = \begin{cases} 1, & x \in P \\ 0, & x \notin P \end{cases}$

A stem cell was unable to induce oscillations in normal ventricular myocytes (k=1) even in a cell pair. A stem cell normally induces oscillations in myocytes with k=0.3.

Oscillation threshold I_{osc} in one, two and three dimensional cardiac tissue is higher compared to a cell pair.

Following details show how changing k affects the excitation and oscillation thresholds in different kinds of the myocytes:

For $k = 1$, the excitation threshold is $I_{exc} = 2.0$ pA/pF and $2.01 < I_{oscil} < 2.6$ pA/pF.

For $k = 0.5$, the excitation threshold is $I_{exc} = 0.68$ pA/pF and $0.69 < I_{oscil} < 1.1$ pA/pF.

For $k = 0.3$, the excitation threshold is $I_{exc} = 0.17$ pA/pF and $0.18 < I_{oscil} < 0.77$ pA/pF.

For $k = 0.233$, the excitation threshold is $I_{exc} = 0.009$ pA/pF and $0.01 < I_{oscil} < 0.66$ pA/pF.

Chapter 3

Stem cells with HCN2 gene in cardiac tissue

3.1 Cell pair consisting of a stem cell connected to a myocyte

It was demonstrated [5] that stem cells make connexin proteins and form functional gap junctions that couple electrically with myocytes.

A cell pair is what we will call a stem cell transfected with HCN2 gene connected to the myocyte. In this chapter we will begin to employ the model of a stem cell transfected with HCN2 gene.

The goal is :

- To investigate HCN2 isoform as a gene delivery system

- To see how it acts as a pacemaker when is transplanted in a stem cell

- What factors can influence its efficiency

- What are its limitations

Besides, we will mimick the experiment [5] in which the stem cells transfected with HCN2 are connected to the myocytes and the experiment in which the expression of HCN2 in stem cells provides an I_f-based current sufficient to increase the beating rate of the cocultured neonatal myocytes. Then in this chapter, we will investigate one dimensional condition when stem cells are connected to a fiber of myocyte.

3.1.1   Current through gap junction channels

Fig.2.4 is an example when current flows from gap junctions between a myocyte and a stem cell. It is seen that the amplitude of oscillation and range of potential is different in a stem cell and a myocyte. It is also important to note that k is chosen for the myocyte relatively low.
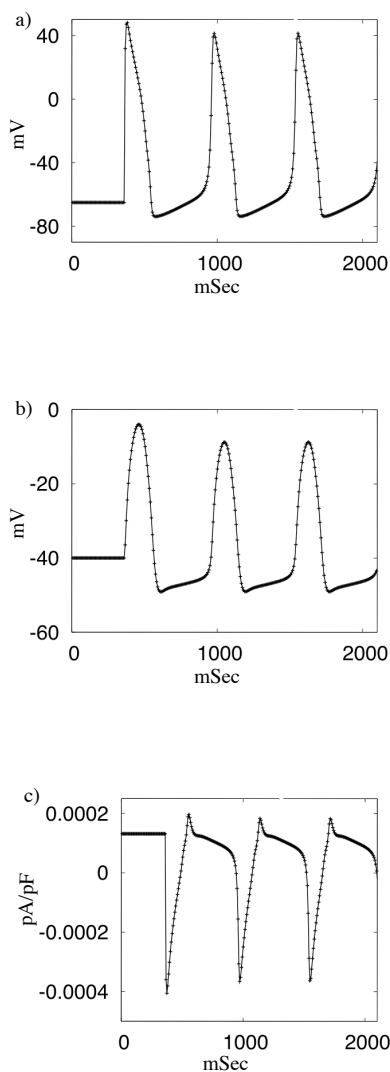
Figure 3.1: **A cell pair: Current flowing through gap junction channels.** a) Myocyte, b) Stem cell, c) Current through gap junction channels. Parameters: number of gap junction channels per cell $n = 10$, number of pacemaker channels per cell $N = 10^4$, level of expression of I_{K1}, k=0.233.

3.1.2 Oscillation induction and disappearance in a cell pair

Oscillations in a cell pair are shown in Fig.3.2. In Fig.3.2a, there are no oscillation for a myocyte with k=0.233(relatively a low k value). In Fig.3.2b oscillation appears when the myocyte is connected to a stem cell. In Fig.3.2c oscillation disappears when the number of gap junction channels per cell is increased. It is important to note that with k values larger than 0.43 the oscillation is never induced, independent of number of gap junction and pacemaker channels.
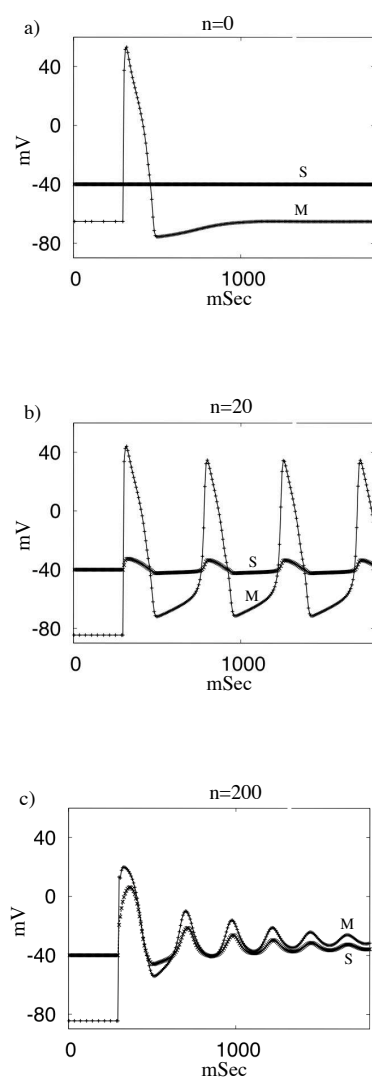
Figure 3.2: **A cell pair: oscillations induction (b) and disappearance (c).** Myocyte and stem cell potentials are marked by M and S. Number of gap junctions n is indicated above each image. Parameters: k=0.233, $N = 1.2 \times 10^5$ (see eqns 2.20,2.21).

Defining boundaries of the oscillation region

In the following Figs.3.4,3.5 we define the position of "disappearance of oscillations" boundary at parameters values where the upstroke of the AP decreases below ~ 0 mV and the oscillation amplitude is not inferior than ~ 50 mV. Fig.3.3a,b show what we have considered as oscillation and Fig.3.3 is defined as no oscillation.

To be accurate to find when the propagation will disappear, it would be better to use cardiac tissue models.
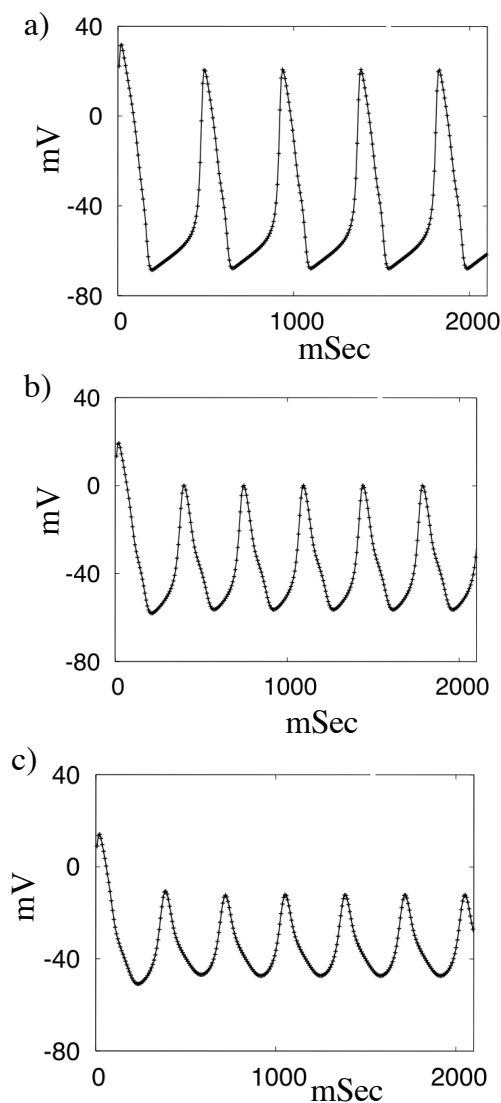
Figure 3.3: **Oscillation disappears**. a)Number of gap junction channels per cell $n = 40$, b)$n = 80$, c)$n = 100$. a),b) are considered as oscillation and not c). Parameters : $k = 0.3, N = 10^7$.

3.1.3 Oscillation regions for stem-mh and stem-h models

Oscillation region for stem-mh model

In Fig.3.4 the oscillation region is shown. It is seen that for large numbers of gap junction and pacemaker channels there is no oscillation. Stem cells can induce oscillations only in myocytes with decreased level of expression of current I_{K1} (= decreased k). We have observed that oscillation can not be induced in normal myocytes (k=1), no matter how large are number N of pacemaker channels or number n of gap junctions. Also, it is seen that oscillations here are robust, and oscillation period is almost constant for a wide range of changing number of pacemaker channels per cell.
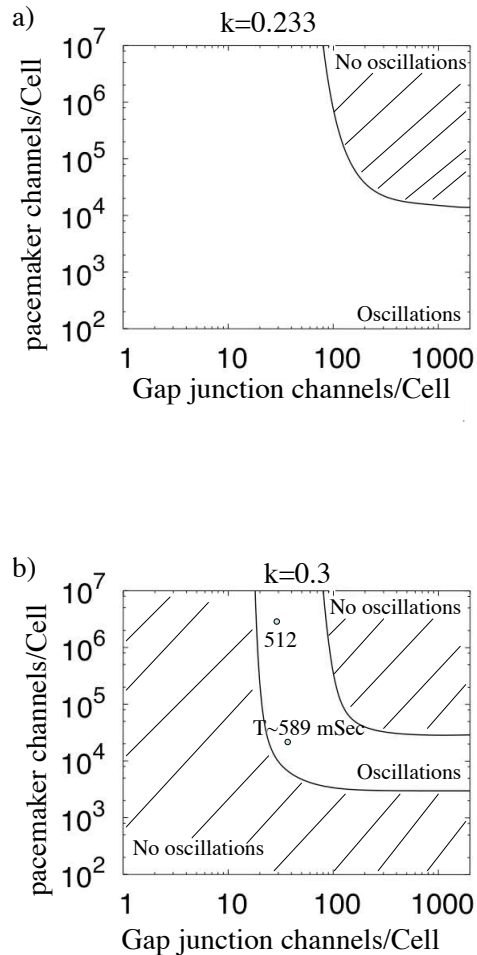
Figure 3.4: **Cell pair oscillations Stem-mh model**. a, b) Oscillation region. Note that the oscillation region shrinks fast with increasing k. (hatched is the region where there are no oscillations).

Oscillation region for stem-h model

Same investigation is done for oscillation region with simplified model in Fig.3.5. It is seen that increasing the number of pacemaker channels doesn't help for inducing oscillation. With increasing k in Fig.3.5b the oscillation region shrinks. This is observed in Fig.3.5c,d. For the myocytes with k larger than 0.43 the oscillation region will disappear.
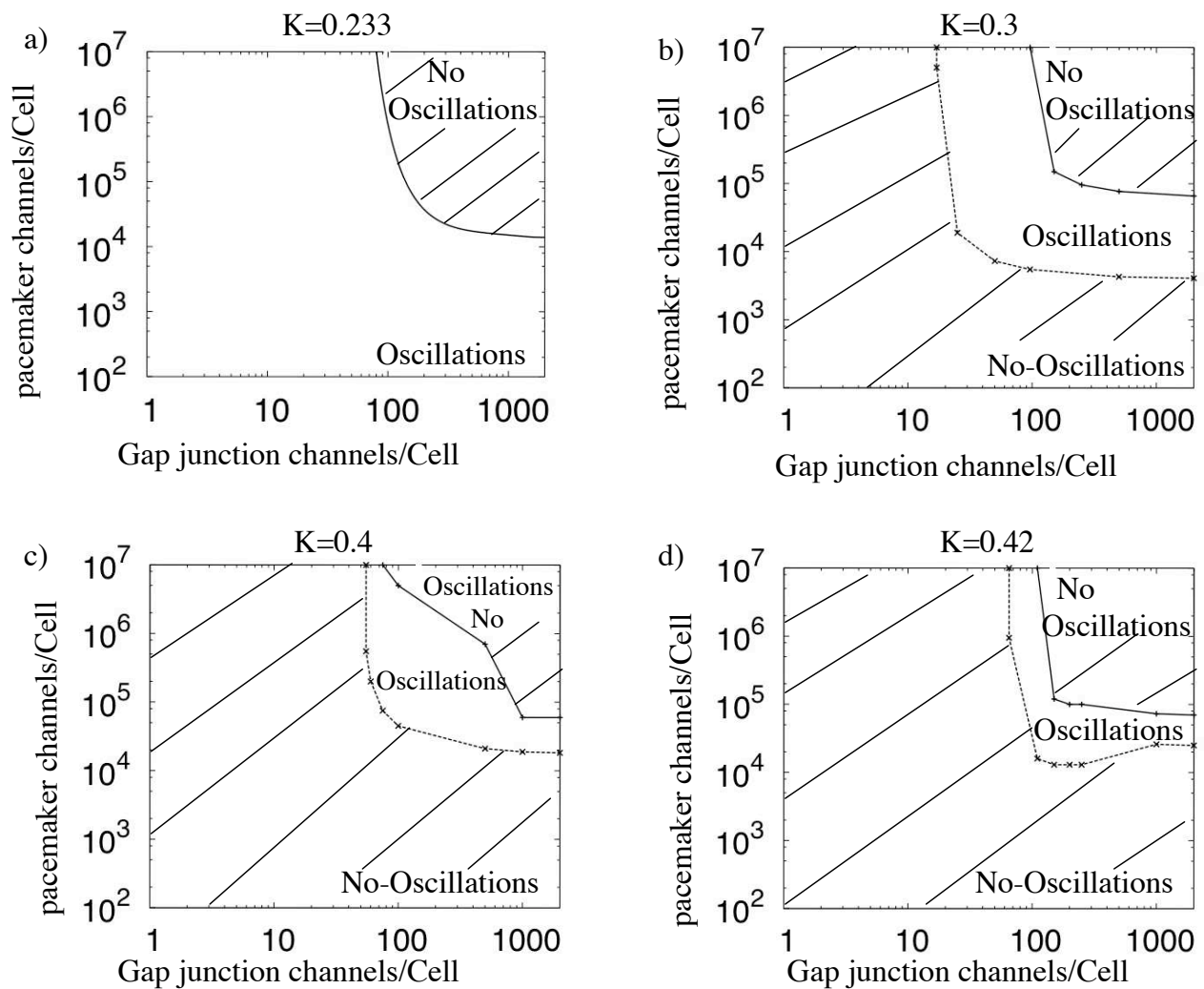
Figure 3.5: **Cell pair oscillations**. Oscillation region (hatched is the region where there are no oscillation).

Oscillation region compared for two stem cell models

In Fig.3.6 the oscillation region is compared for two stem cell models for two values of expression level of I_{K1}. Since the ratio $\epsilon = \frac{\tau_1}{\tau_2} << 1$ the result of two models are close. From here, only simplified model is the base of all following the investigations.

The oscillation region is empty for k values larger than 0.43. This emphasizes the role of k in induction of oscillations in a cell pair.
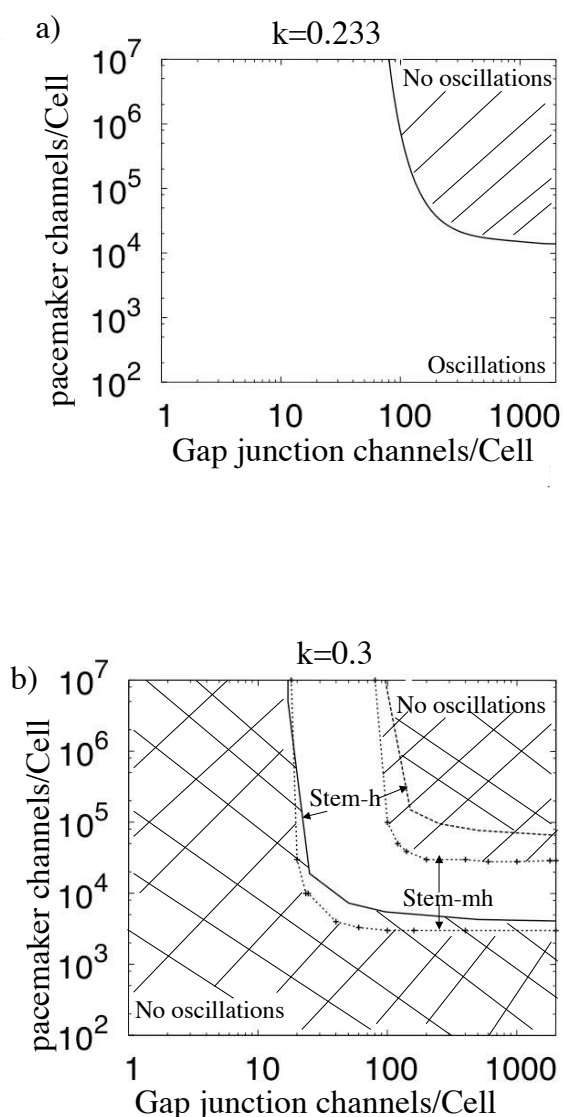
Figure 3.6: **Cell pair oscillations compared**.

3.1.4   Dependance of period of oscillation on parameters

In a pair of stem cell and myocyte connected, the period of the oscillation depends on level of expression of I_{K1} (or k), number of gap junction channels per cell (or n) and number of pacemaker channels per cell (or N) Fig.3.7.

Increasing the number of gap junction channels stabilizes the period of oscillation, except in Fig.3.7b that oscillation disappears for large number of gap junction and pacemaker channels.
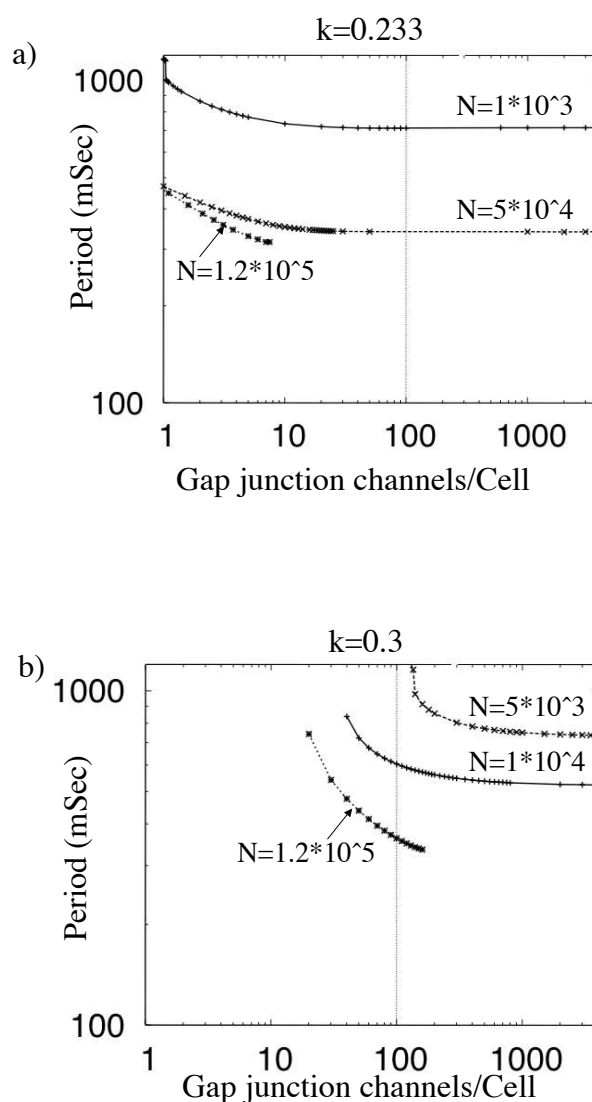
Figure 3.7: Period of oscillation dependance on number of gap junction channels/Cell and number of pacemaker channels/Cell. Dashed vertical line shows number of gap junctions in experiment [5].

3.2 Stem cells as a pacemaker in a fiber

For one dimensional calculations we took a fiber of 201 myocytes Fig.3.8($L = 20.1$ mm is considered as infinitely long). Pacemaker region consists of stem cells connected to the myocytes and not connected together. We put this pacemaker region ($l = 4.3$ mm) in the middle of the fiber.

Note that we used cell dimension $100 \times 10 \times 10\mu$ so $dx = 100\mu$. Myocyte and stem cell capacitance is ~ 95pF and specific membrane capacitance is $\sim 1\mu F/Cm^2$.

In Fig.3.9 induction of oscillation in a fiber is shown. Threshold for inducing oscillations increases much more in a fiber (see chapter: two and three dimensional cardiac tissue).
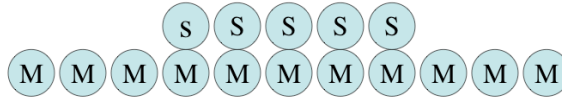
Figure 3.8: A Schema of fiber of myocytes with a pacemaker region in the middle.
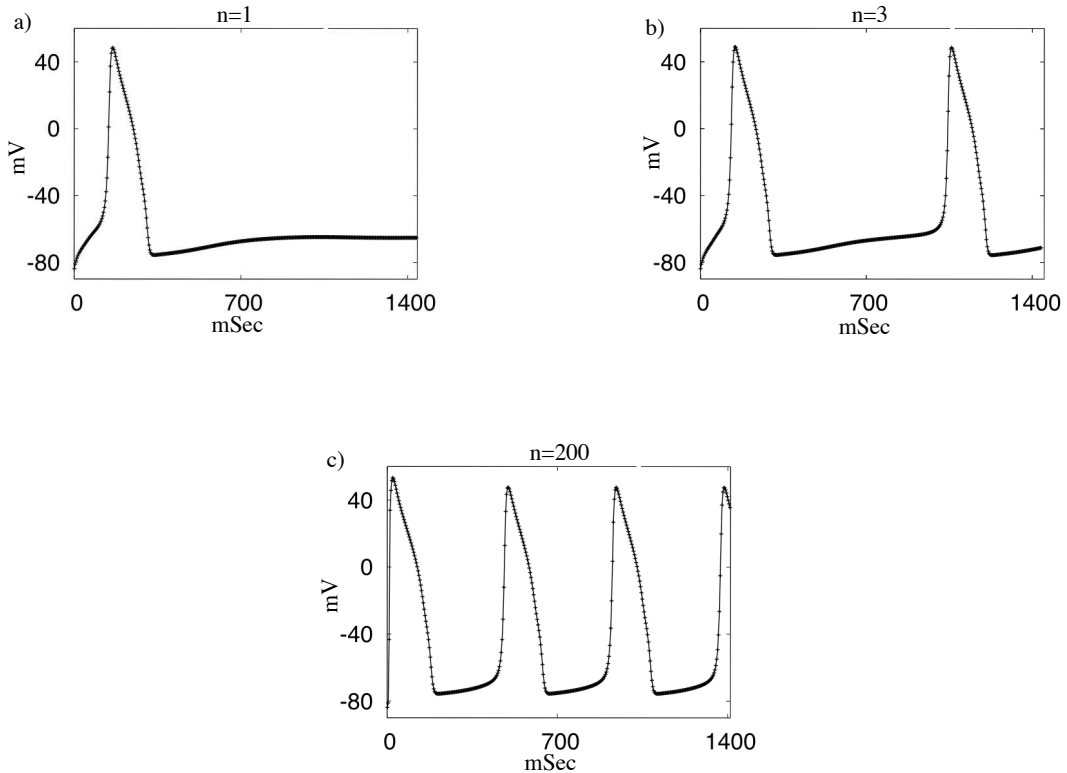
Figure 3.9: **Fiber: Induction of oscillations by stem cells**. a-c) Pacemaker length $l = 4.3$ mm, $N = 5 \times 10^4$,k=0.233.

3.2.1   Pacemaker length in a fiber

In Fig.3.10, it is seen that for a longer fiber, a longer pacemaker region is needed to induce oscillation. This length is different for different number of gap junction and pacemaker channels.
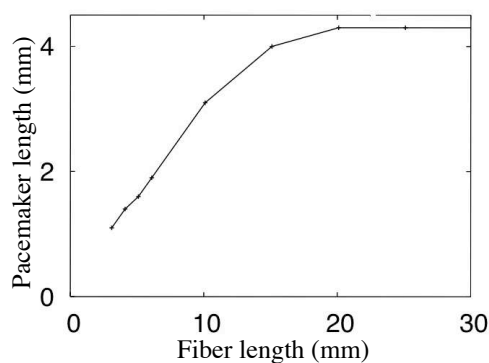
Figure 3.10:   **Pacemaker length needed to induce oscillations in a fiber**. Parameters: $n = 100, N = 6 \times 10^4$, k=0.233.

3.2.2   Oscillation's amplitude in the fiber

In Fig.3.11 oscillations amplitude increases with the distance from the pacemaker region. It is observed in a case of a small source-sink mismatch: a current load for the pacemaker channels decreases oscillation amplitude, but it remains above the propagation threshold. While propagating, AP gaines its normal amplitude 100mV.
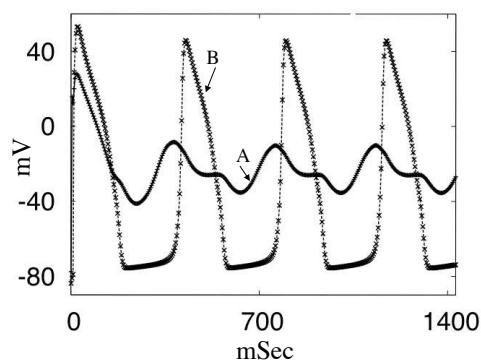
Figure 3.11: **Amplitude of oscillations increases with the distance from the pacemaker region.** Potential was recorded inside pacemaker region (point A) and at a remote point B.

3.2.3 Oscillation region for a fiber

Oscillation region for stem-mh model

Oscillation region for stem-mh model is shown in Fig.3.12. It is seen that in a fiber (same as in a cell pair) increasing k will result in shrinking the oscillation region.
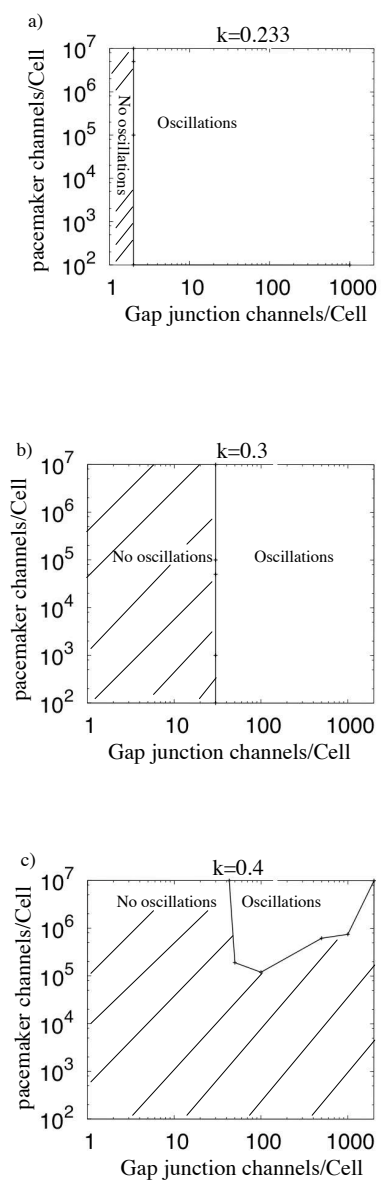
Figure 3.12: Oscillation region compared for Stem-mh model.

Oscillation regions for stem-h model

Same investigation is done for stem-h model. Same is seen that increasing k will result in shrinking the oscillation region.
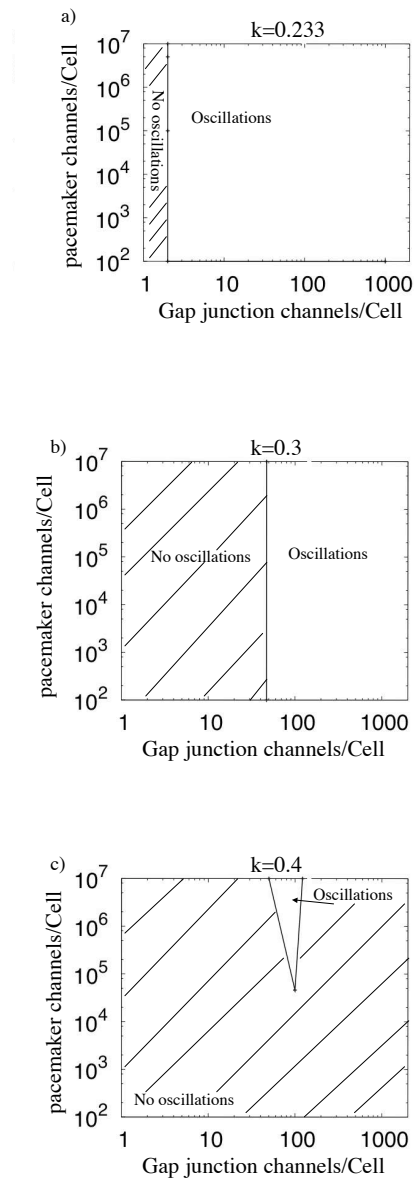
Figure 3.13: Oscillation region compared for Stem-h model.

Comparison of the oscillation regions for two stem cell models

In Fig.3.14 the oscillation regions are compared for two models. With $k = 0.4$, oscillations region shrinks so strongly that with $k > 0.4$, oscillations are not possible anymore. Note that it means that stem cells can never induce oscillations in normal myocytes (described by BR model).
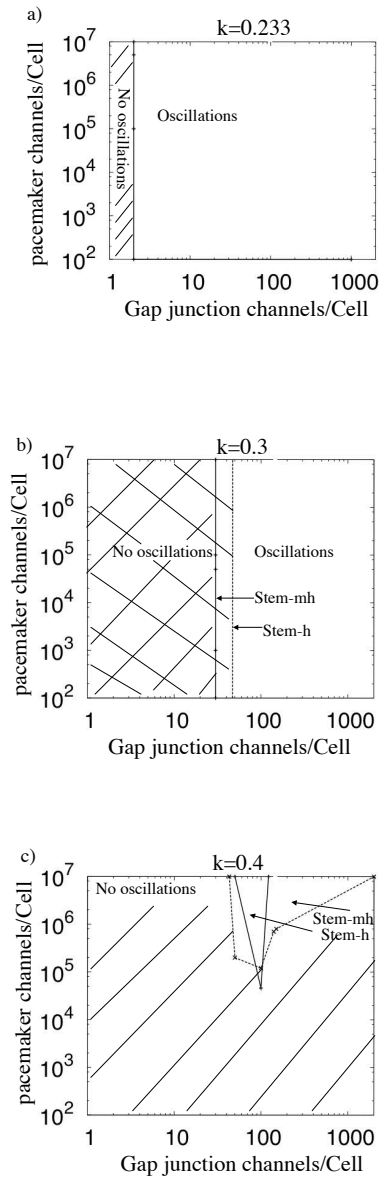
Figure 3.14: Oscillation region compared for two models

3.2.4   A paradox: Oscillation region is larger for the fiber than for a stem cell

Intuitively, It is expected that it is more difficult to induce oscillations in a fiber than in a cell pair or in other words, more current is needed for a certain number of myocytes than only one. It is not the case. Why?

Also, oscillation region in a fiber is larger than in a cell pair. It looks like a paradox, but it is not.

Explanation is that oscillation region is larger only for large currents from a stem cell (large N, large n). In a cell pair, such large currents abolish oscillations.

In a fiber, the myocytes are not connected to stem cells directly. In such myocytes, the current delivered from stem cells is smaller, and therefore for some of myocytes it appears inside the oscillation region. Threshold for inducing oscillations increases much more in a fiber (see chapter: Result: two and three dimensional cardiac tissues).

3.2.5   Reducing period of oscillation by connecting stem cells to neonatal myocytes

In experiments [5], they observed that transfected stem cells (hMSCs) influenced beating rate *in vitro* when plated onto a localized region of a coverslip and overlaid with neonatal rat ventricular myocytes. The coculture beating rate was 93 ± 16 when hMSCs were transfected with control plasmid and 161 ± 4 bpm when hMSCs were expressing mHCN2. In Fig.3.15b the same is obtained.

We investigated the dependence of oscillation period on both: number of pacemaker channels per cell N and number of gap junction channels per cell n for a large interval of their variation that is even not accessible in todays experiment in Fig.3.15a.

It is seen that for auto-oscillating myocytes ($k = 0.215$), oscillation is affected by number of gap junction channels n only and is almost independent on number of pacemaker channels N.

In other experiments [37], they observed a long-term survival of transplanted neonatal rat myocytes and the contribution of these cells to improve cardiac function.

3.3   Multiple connection

Experimentalists expected that having multiple connection between a myocyte and a stem cell increases the possibility of having oscillation. In the experiment Fig.2.4, different kinds of connection was observed: a stem cell to two(many) myocytes and a myocyte to two(many) stem cells.
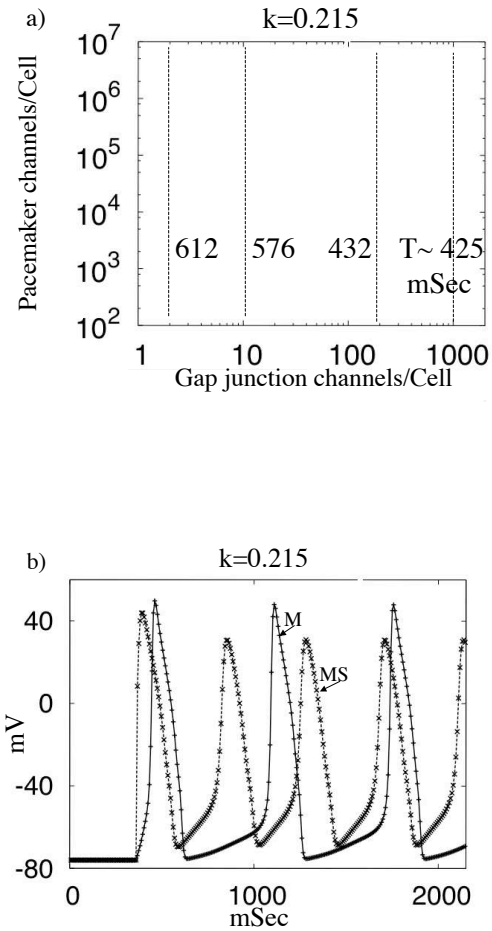
Figure 3.15: **Fiber: Decrease of oscillations period by stem cells.** a) Dependence of oscillation period T on N and n. Note that the period is the same along every vertical line. b) An example of record with n=320, $N = 1.1 \times 10^6$. M- myocytes alone; MS- myocytes and stem cells. Pacemaker length $l = 4.3$ mm.

Several stem cells connected to one myocyte

We will investigate a case when two stem cells are connected to a myocyte. By connecting two stem cells to a myocyte, oscillation will disappear later than when there is only one stem cell connected to a myocyte, Fig.3.17.

In Fig.3.18 oscillation is compared between cases when one or two stem cells are connected to one myocyte. It is seen that oscillation will disappear for larger k in case of two stem cells connected to a myocyte. This confirms that large number of stem cells are needed to induce oscillation in a real heart. (Meanwhile, only 50 stem cells made gap junctions over 10^6 injected [5]).

Several stem cells connected to myocytes in a pacemaker region

In the pacemaker region, stem cells may be connected either to every myocyte, or to every second, every third, etc. myocyte. Respectively, we call stem cell concentration in the pacemaker region: 100%, 50%, 33% etc. In Fig3.19a a schema of such concentration of stem cells in the pacemaker region is shown.

Fig3.19b shows that a moderate decreasing of stem cells concentration in a pacemaker does not destroy oscillations, but increases the oscillation period.

In Fig3.19c the period of oscillation is shown according to the number of stem cells connected to one myocyte. Stem cell concentration $100\%, 50\%$, means one stem cell per 1 myocyte or 2 myocytes, respectively 200% means 2 stem cells per one myocyte.

Several myocytes connected to one stem cell

Real problem appears when one wants to induce oscillations in a real heart, when number of myocytes are increased. Fig.3.16 is an example to show how one stem cell can induce oscillations in two myocyte with low k but as soon as k increases, oscillation disappears.
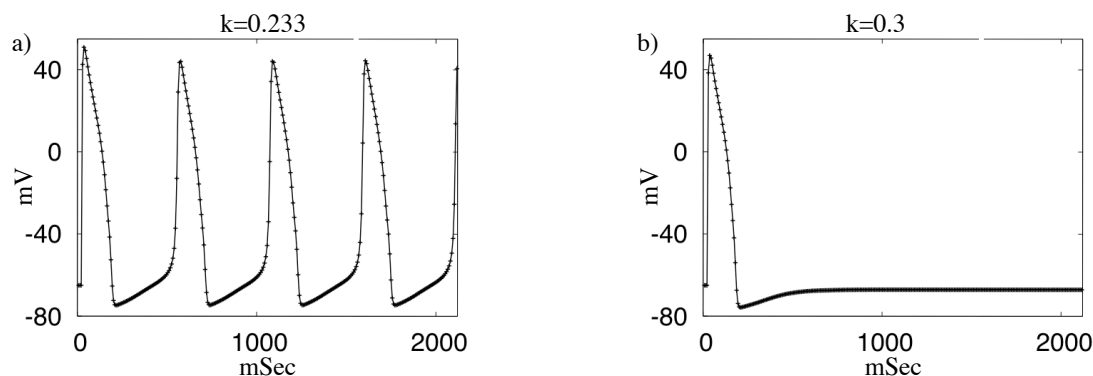
Figure 3.16: one stem cell can induce oscillations in two myocyte with low k but as soon as k increases, there would be no oscillations. Parameters: number of gap junction channels $n = 100$, number of pacemaker channels $N = 10^4$.
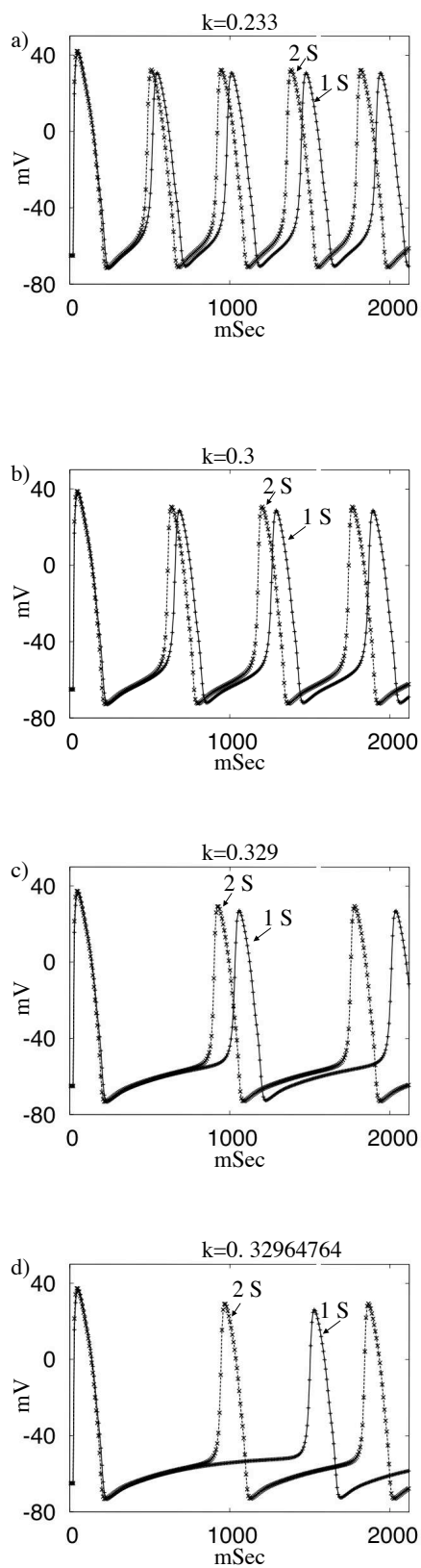
Figure 3.17: Oscillations compared for one or two stem cells connected to one myocyte. In a,b and c) period of oscillation decreases. Parameters in stem cell: number of gap junction channels $n = 100$, $N = 10^4$.
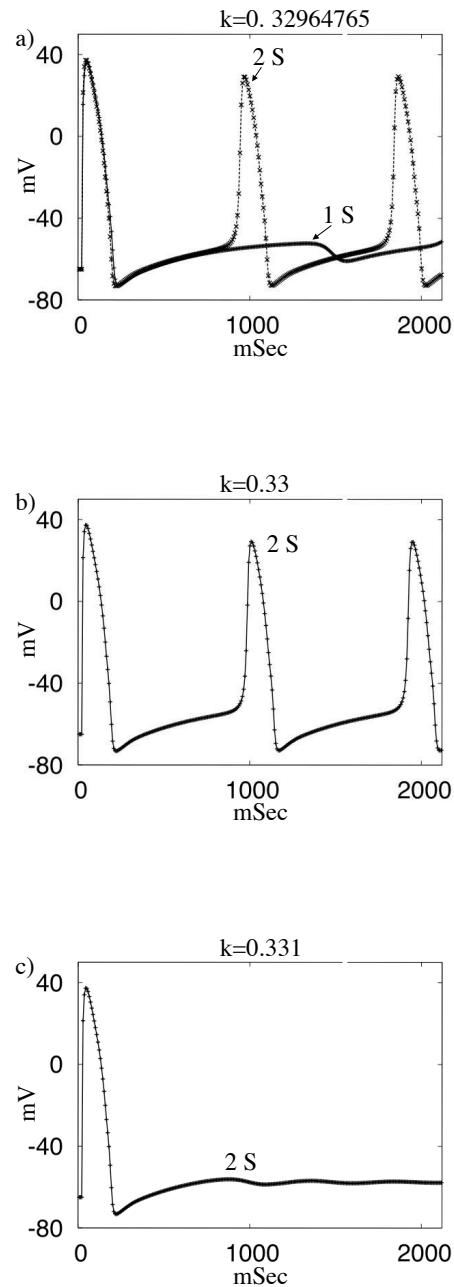
Figure 3.18: a) Oscillation disappears when only one stem cell is connected to the myocyte while having 2 stem cells maintains oscillation. In b,c) it is showed that how oscillation disappears for two stem cells connected to the myocyte. Note that k is larger when there are two stem cells when oscillation disappears. Parameters in stem cell: number of gap junction channels $n = 100$, $N = 10^4$.

a)

b)

c)
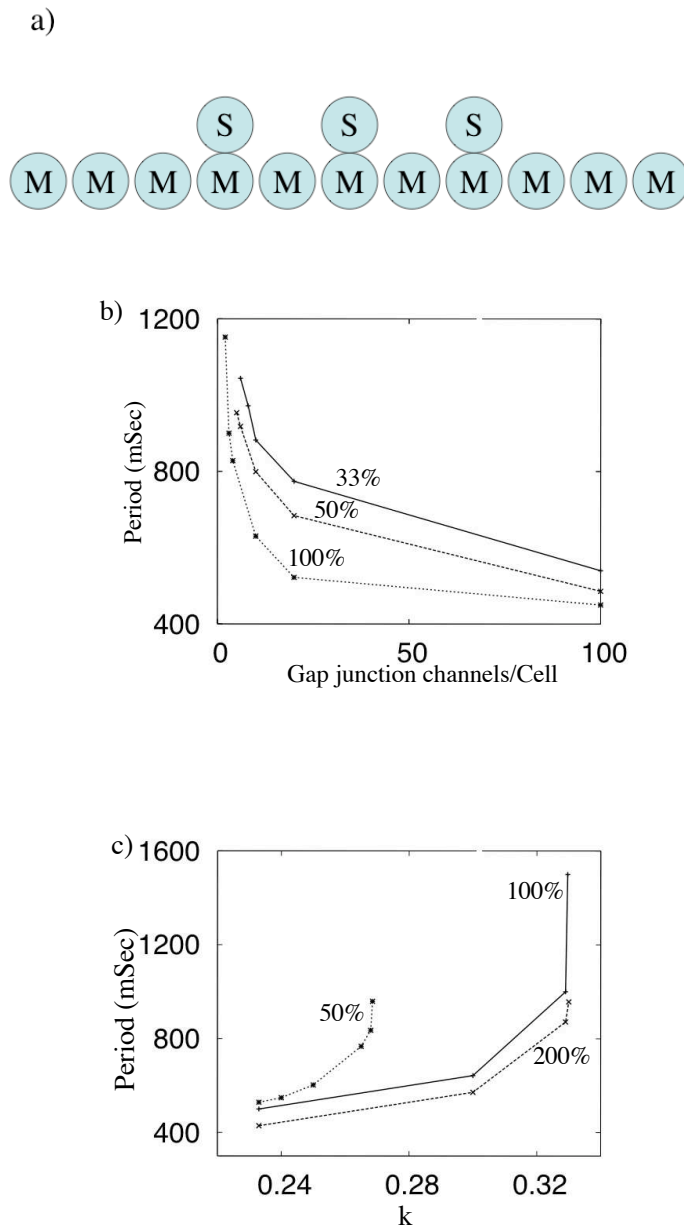
Figure 3.19: **Decreasing stem cells concentration(dilution) in a pacemaker increases the oscillations period**. a) shows stem cell dilution of 50% inside the pacemaker region. b) Period of oscillation for different stem cell dilutions in the pacemaker region in a Fiber. c) Stem cell concentration $100\%, 50\%$, means one stem cell per 1 myocyte or 2 myocytes, respectively 200% means 2 stem cells per one myocyte. A pacemaker $l = 4.3$ mm length is composed of stem cells connected to myocytes. Fiber length $L = 20.1$ mm , $k = 0.233$, $N = 5 \times 10^4$.

Chapter 4

Stem cells with HCN1 gene in cardiac tissue

4.0.1 HCN1 isoform

The theoretical predictions for future experiments to incorporate HCN1, HCN4 isoforms into the biological pacemakers is presented in the current and the following chapters. Since the experimentalists have already chosen HCN2 as a successful choice and HCN1, HCN4 have similar characteristics, they might be considered same successful.

We will only investigate HCN1, HCN4 since HCN3 is almost not present in cardiac muscle (only low level traces of HCN3 are found in embryonic pacemaker cells [13]).

HCN1 channels display fast gating properties and are expressed at low levels in SA node and largely absent in ventricle.

We used experiment [8],[9] when Xenopus oocyte transfected by HCN1 (when a voltage step is applied to it, similar to the experiment [5]), as far as no experiment was performed by transfecting stem cells with HCN1 [1] (one reason that HCN1 was not chosen for experiments instead of HCN2 might be that it is almost unaffected by cAMP[9]).

4 Sec test potential was done [8],[9] varying from -40 to -110 mV in 10 mV steps holding potential and tail potentials were -40 mV. To adapt an experiment when a Xenopus oocyte is transfected by HCN1 to an experiment for a stem cell transfected by HCN1, we considered the difference between experiment conditions in both cases. It is important to note that stem cell experiments are performed at body temperature ($36°$C) and Oocyte experiments are done at the room temperature ($20°$C).

The records that are used for construction of the model are shown in Fig.4.1.

---

[1]Even if the channel is considered to be expressed with the same characteristics in all platform cells, the activation depends although to cell type specificty [14] and this might be a general characteristic of this gene family.
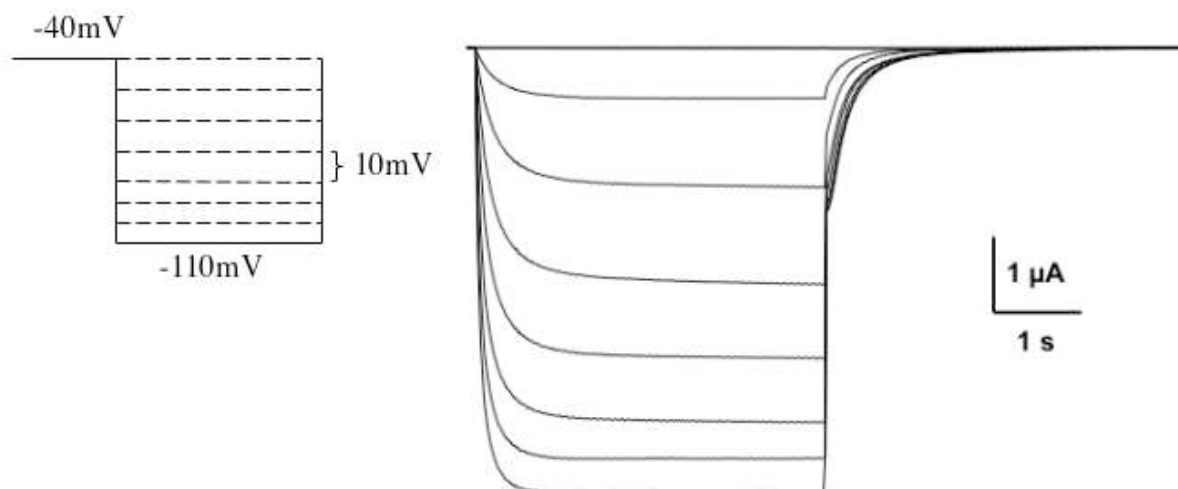
Figure 4.1: Voltage step applied to Xenopus oocyte transfected by HCN1

4.1 Constructing a model of a stem cell transfected with HCN1

We constructed a simplified model (with inactivation only) for a stem cell transfected with HCN1 gene from experimental data [8],[9].

Figure 4.2: Inactivation time constants (τ_2).
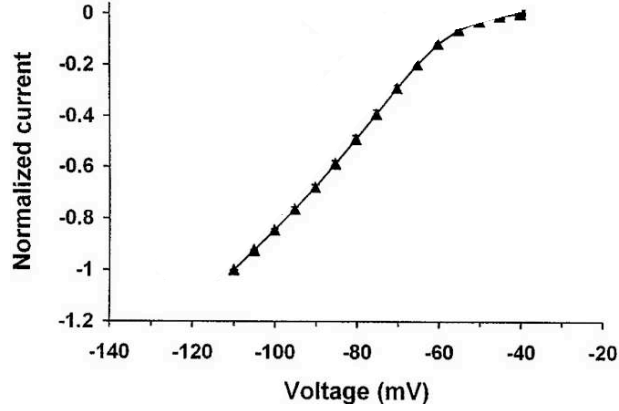
Figure 4.3: current records from [8]

Estimating the time constant $\tau_2(E)$

Time constants for the inactivation gating variable $\tau_2(E)$ for HCN1 and HCN2 genes [8] are shown in Fig.4.2.

To adapt data [8] from $20°$C to $36°$C.

There is a very steep temperature dependence to the kinetics such that the time constant decreases between 3 and 6 fold for a $10°$C change in the temperature. We may use this Q_{10} to estimate τ_2 at $36°$C. But because of decreasing of lipid layer viscosity with temperature, more accurate data can be obtained by calculating the ratio of time constants of HCN2 and HCN1 from [8].

As seen from Fig.4.5 the ratio is:

$$\frac{\tau_{HCN2}}{\tau_{HCN1}} = \begin{cases} 11, & E = -85\,mV \\ 33, & E = -125\,mV \end{cases}$$

The total dependance is shown in Fig.4.4. From previously created model for HCN2, Fig.2.1, using this ratio, we obtained the time constants for HCN1 Fig.4.5b.

Estimation of inactivation variable $g_2(E)$

Experimentally measured dependence of the current on voltage Fig.4.3 gives inactivation variable g_2 dependance on voltage Fig.4.5a. It is important to note that since both currents are negative,

we transformed the normalized current to a standard coordinates and the curve looks like Fig.4.5a.

This completes determination of the functions needed for the model of a stem cell transfected with HCN1 gene.

$$dE_s/dt = -N\sigma_f\, g^s(E_s - E_r)/C \tag{4.1}$$
$$dg^s/dt = (\bar{g}^s - g^s)/\tau_2^s(E_s) \tag{4.2}$$

where the reversal potential for HCN1 is -30 ± 2 mV (external solution 2 mM K^+)[8].
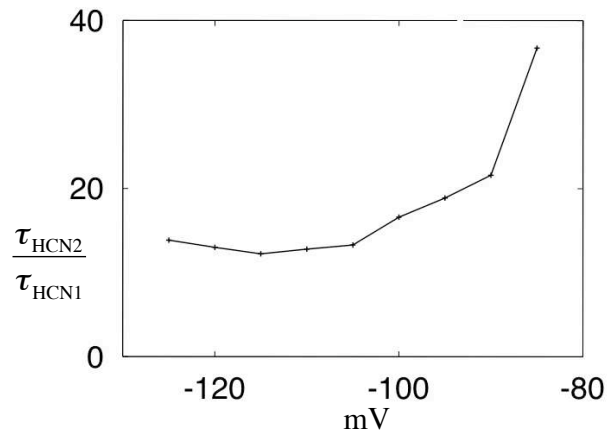
Figure 4.4: Ratio of $\frac{\tau_{HCN2}}{\tau_{HCN1}}$

Appendix to construction of HCN1 model

To adapt data [8] from 20°C to 36°C, a traditional approach is to use Q_{10} - the coefficient of increasing the velocity of a chemical reaction by increasing the temperature by 10°C. Velocity of a chemical reaction depends on temperature as:

$$V = e^{\frac{-W}{KT}}$$

This permits to obtain the value Q_{16} for transition from 20°C to 36°C, using a known value of Q_{10}.

For transition from 20°C to 30°C the Q_{10} expression is:

$$\frac{e^{\frac{-W}{K303}}}{e^{\frac{-W}{K293}}} = Q_{10}$$

Taking $Q_{10} = 3$ we obtain: $\frac{-W}{K} = 9753.37$ and $Q_{16} = 15$. This does not much deviate from Fig.4.5b.

But we obtained τ_2 of HCN1 at 36°C as follows : In Fig.4.2 we calculated the ratio τ_2 of $\frac{HCN2}{HCN1}$ for each voltage. As far as we had exact τ_2 for HCN2 [6], we used this ratio obtained for obtaining τ_2 of HCN1. τ_2 obtained by Q_{10} is the same as τ_2 above.
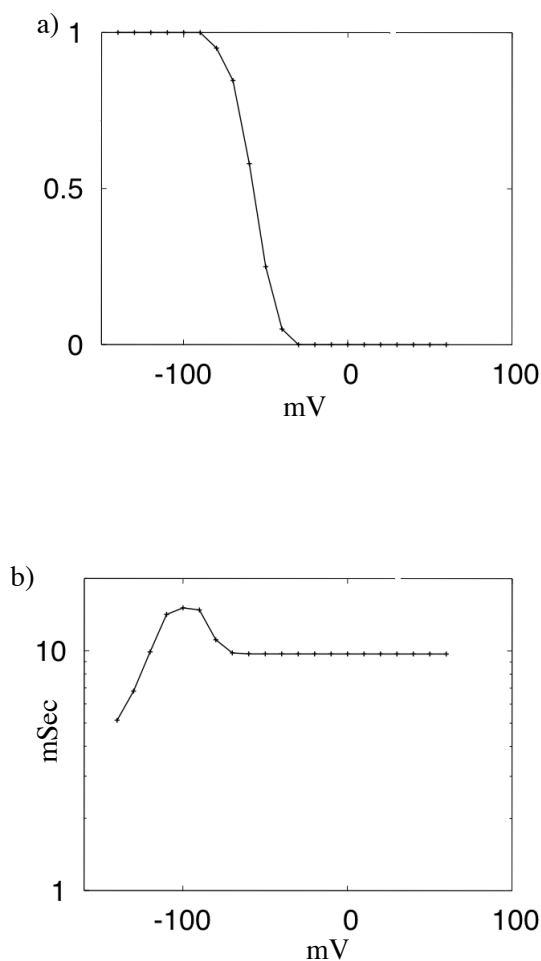
Figure 4.5: model for HCN1 with inactivation. a) Inactivation gating variable (g_2 or h). b) time constants.

4.2 Investigating model of a stem cell transfected with HCN1

4.2.1 Oscillation region for a cell pair

In Fig.4.6 oscillation region for a stem cell with HCN1 is shown.
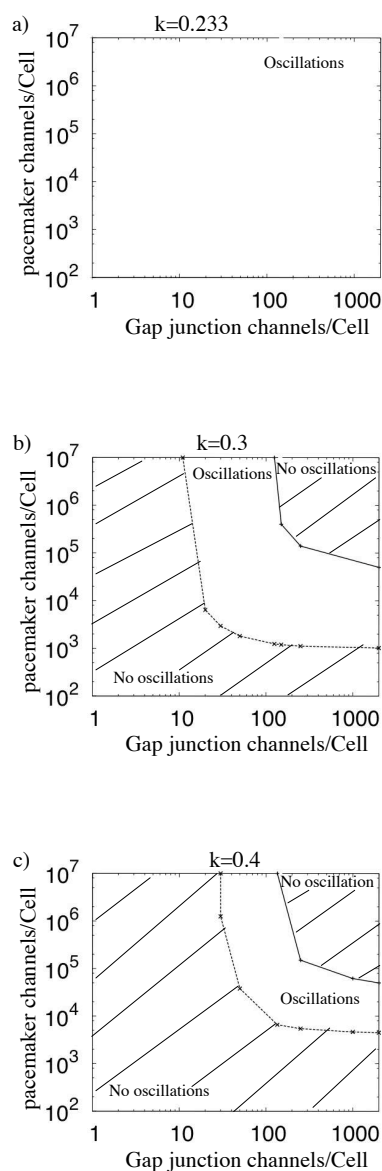
Figure 4.6: Oscillation region for HCN1 done with stem-h model. Hatched is no oscillation region.

4.2.2 Oscillation region for stem cells with HCN1 in a fiber

In Fig.4.7 Oscillation region for a fiber connected to stem cell transfected to HCN1 is shown.
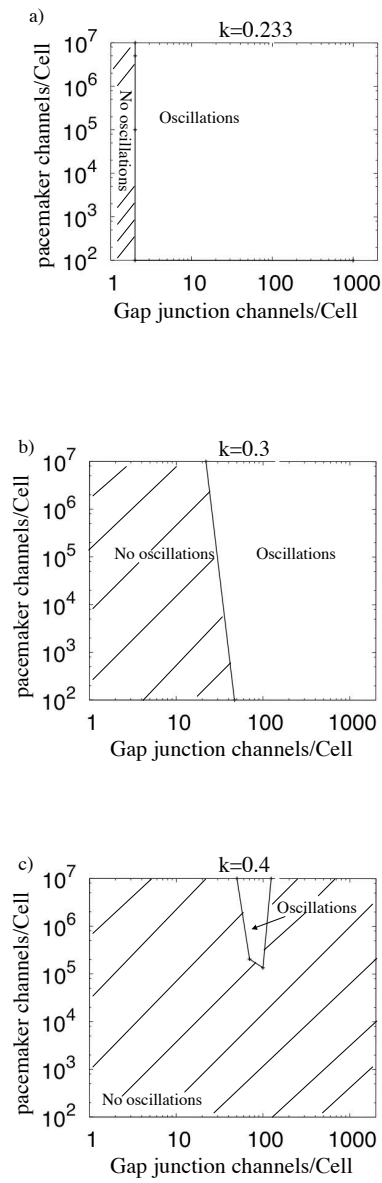
Figure 4.7: Oscillation region in a fiber when stem cells are transfected with HCN1.

4.3   Result of transfecting stem cells with HCN1

To draw a conclusion of transfecting stem cells with HCN1, it is observed that their behavior is similar to what was observed with HCN2.

If these channels are installed in stem cells, they provide similar I_f-based current during a voltage step applied to the cell pair. This current is the lowest among four isoforms.

They have approximately the same oscillation region as HCN2. Meanwhile they are almost unaffected by cAMP which means that it is difficult to use them in the future experiments as far they can not be regulated easily.

Chapter 5

Stem cells transfected with HCN4 gene in cardiac tissue.

In this chapter, we will investigate when the stem cells are transfected with HCN4 for designing a biological pacemaker. HCN4 is highly expressed in the sino-atrial node and it is the major channel mediating sympathetic simulation of the pacemaker activity. Also HCN4 is the first ion channel that within the heart and is found also in neurons. The slowly activating HCN4 contributes to the pacemaker activity and the modulation of the heart rate by β-adrenergic stimulation (cAMP) [11], [12]. Fig.5.1 shows the source experiment that we used for obtaining data concerning HCN4. In this experiment, HEK293 (Human Embryonic Kidney) cells was used to be transfected by HCN4.
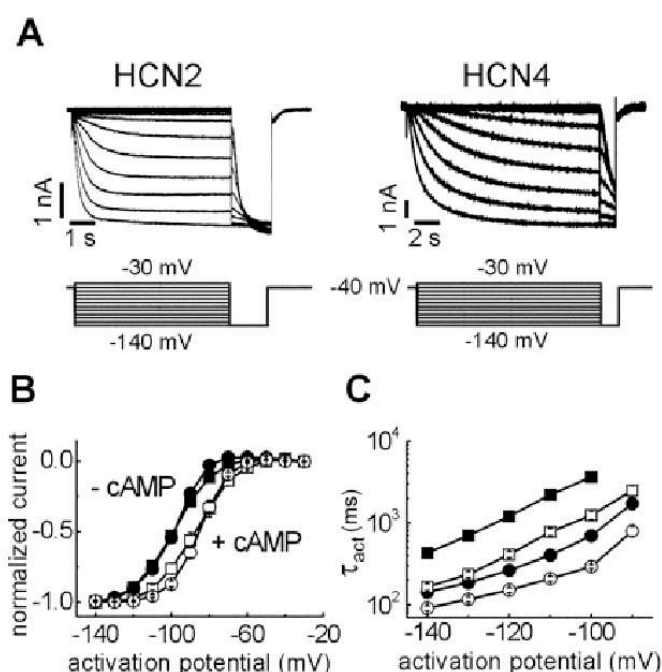
Figure 5.1: Basic properties of HCN4 [11]. A. current recorded holding potential from -40 mV to the range of -140 to -30 mV. B. Normalized current. C. Inactivation time constants (Filled squares correspond to HCN4).

5.1 Constructing a model of a stem cell with HCN4

Similar to HCN1, we constructed a simplified model (with inactivation only) for a stem cell transfected with HCN4 gene from experimental data [11] Fig.5.1.
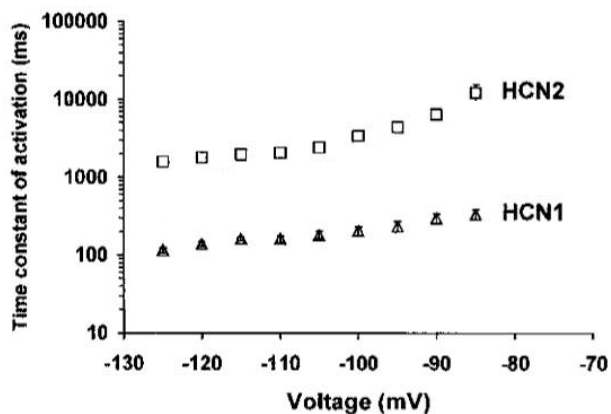
Estimating the time constant $\tau_2(E)$ and inactivation variable $g_2(E)$

In Fig.5.1C current records for HCN4 and comparison to HCN2 are shown. In Fig.5.1B normalized current induced by HCN4 (filled squares) is shown. It describes *increasing* of the current with negative voltages- note that the vertical axis is shown with unusual notaions : maximum of the current (1) is below and (0) of the current is above that should not be the case for a normalized current I/I_{max} since both of them are negative. When transformed to standard coordinates I/I_{max} this curve looks as shown in Fig.5.2a. It gives voltage dependance of inactivation gating variable g_2 or h.
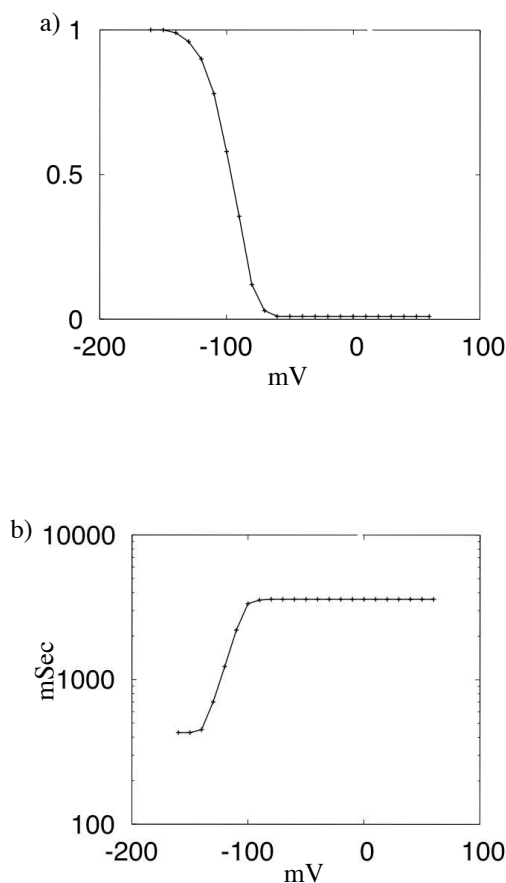
Figure 5.2: model for HCN4 with inactivation. a) Inactivation gating variable (g_2 or h). b) time constants.

5.2 Investigating a model of a stem cell transfected with HCN4

5.2.1 Oscillation region for a cell pair

The oscillation regions for a cell pair are shown in Fig.5.3. Region shrinks by increasing k same as the isoforms investigated before.
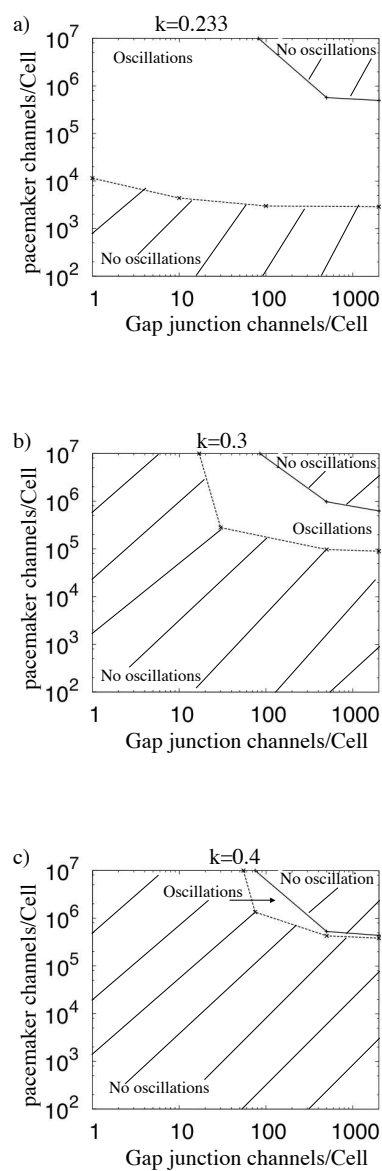
Figure 5.3: Oscillation region for HCN4 done with stem-h model. Hatched is no oscillation region.

5.2.2 Oscillation region for stem cells with HCN4 in a fiber

The oscillation regions for a fiber are shown in Fig.5.4.
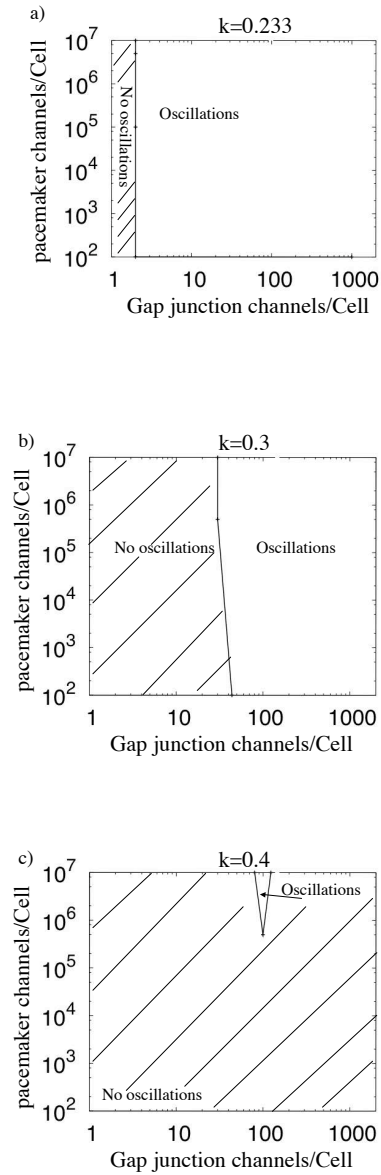
Figure 5.4: Oscillation region for HCN4 done with stem-h model. Hatched is no oscillation region.

5.3 Result of transfecting stem cells with HCN4

To draw a conclusion of transfecting stem cells with HCN4, it is observed that their behavior is similar to what was observed with HCN2.

If these channels are installed in stem cells, they provide similar I_f-based current during a voltage step applied to the cell pair. This current is the largest among four isoforms.

They have approximately the same oscillation region as HCN2.

Chapter 6

Generic features of HCN genes family

Biological data

The gene family encoding Hyperpolarization-activated Cyclic Nucleotide-gated cation channels is called HCN family. There are four isoforms of the gene, labeled HCN1 to HCN4 [32][27][19].

All four isoforms give rise to pacemaker (funny) current I_f current. The predominant isoform in the SA node is HCN4 (followed by HCN2) and in ventricle is HCN2. HCN1 is the fastest isoform but it produces least pacemaker current in a voltage clamp experiment while HCN4 produces largest current but it is the slowest isoform.

HCN1 transcripts are expressed at low levels in the SA node and largely absent in ventricle. This differential expression raises the possibility that pacemaker activity in one cardiac region could be altered without the necessity of changing it in another[25].

The slowly activating HCN4 is controlled by β-adrenergic stimulation, whereas the less expressed, faster activated HCN2 and HCN1 may have additional functions such as maintaining the resting potential of pacemaker and other cells[11], [12].

Researchers dealing with installing these isoforms into the stem cells for designing the biological pacemaker expected [6] that HCN1 might be better than HCN2 and might help inducing oscillation (or a shift in g_2 by $10 - 15$ mV to the negative direction in HCN1 compared to the already studied HCN2).

Expectations of the experimenters were that absence of oscillations is not due to sufficiently large number of gap junction channels. In Experiments *in vitro*[5], cells had about 12 hours to develop gap junctions connections, the hope was that more time will result in a larger number of gap junctions. An additional hope was that the experiments were done *in vitro*, while in *in vivo*, the number of gap junctions may be even more. Figs.3.6, 4.6, 5.3,3.14,4.7,5.4 show that increasing number of gap junctions can not help inducing oscillations for large k. We have shown that reducing k helps inducing oscillations. We tried to identify properties which are common to all isoforms.

6.1   Oscillation induced by HCN1,2,4

We will compare oscillation region for HCN1,2,4. For large numbers of gap junction and pace-maker channels, there are no oscillations with any value of k (except k resulting in auto-oscillatory myocytes).

6.1.1   Oscillation regions in a cell pair: Comparing genes HCN1,HCN2, HCN4

As seen in Fig.6.1, oscillation region for a cell pair is larger for stem cell transfected with HCN1 than with HCN2 for all values of k.
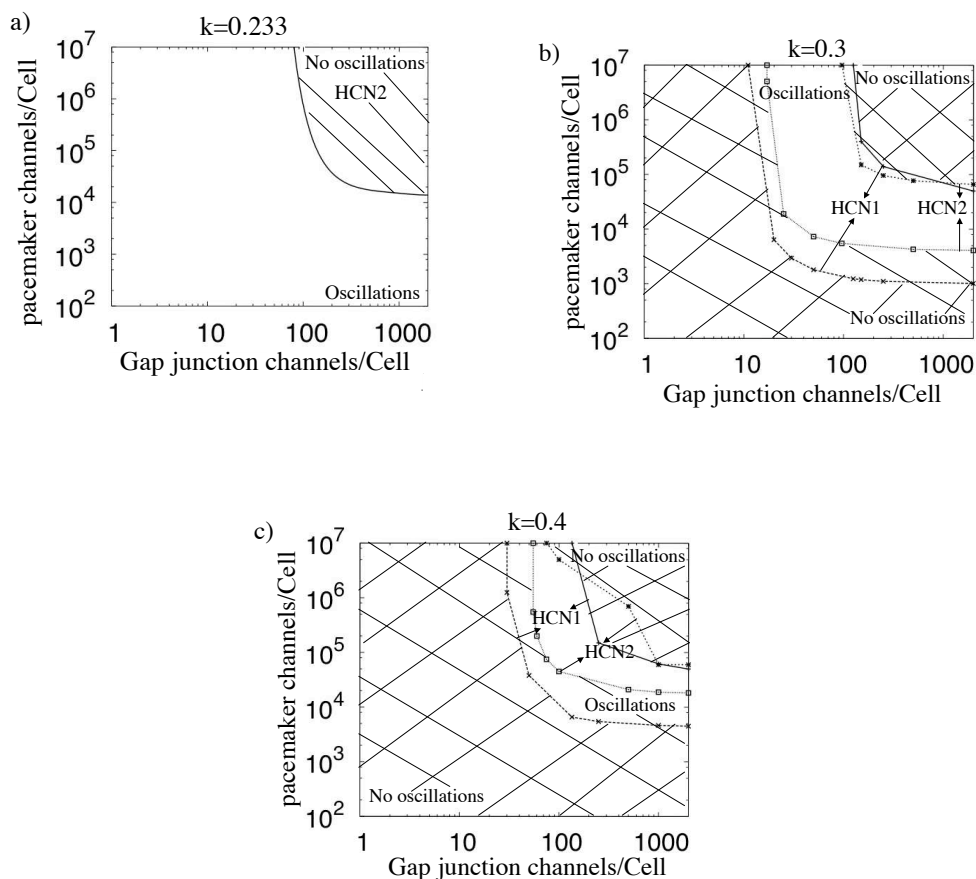
Figure 6.1: **Comparing oscillation regions for HCN1 and HCN2.** Notations are clear from b): hatching with a negative slope denotes no oscillations for HCN2 as in a). Hatching with a positive slope denotes no oscillations for HCN1. It is seen that oscillation region for HCN1 is larger than that for HCN2 for all values of k.

oscillations induced by stem cells transfected by HCN4 and HCN2 in a cell pair are compared in Fig.6.2. It is seen that the largest difference exists for larger k.
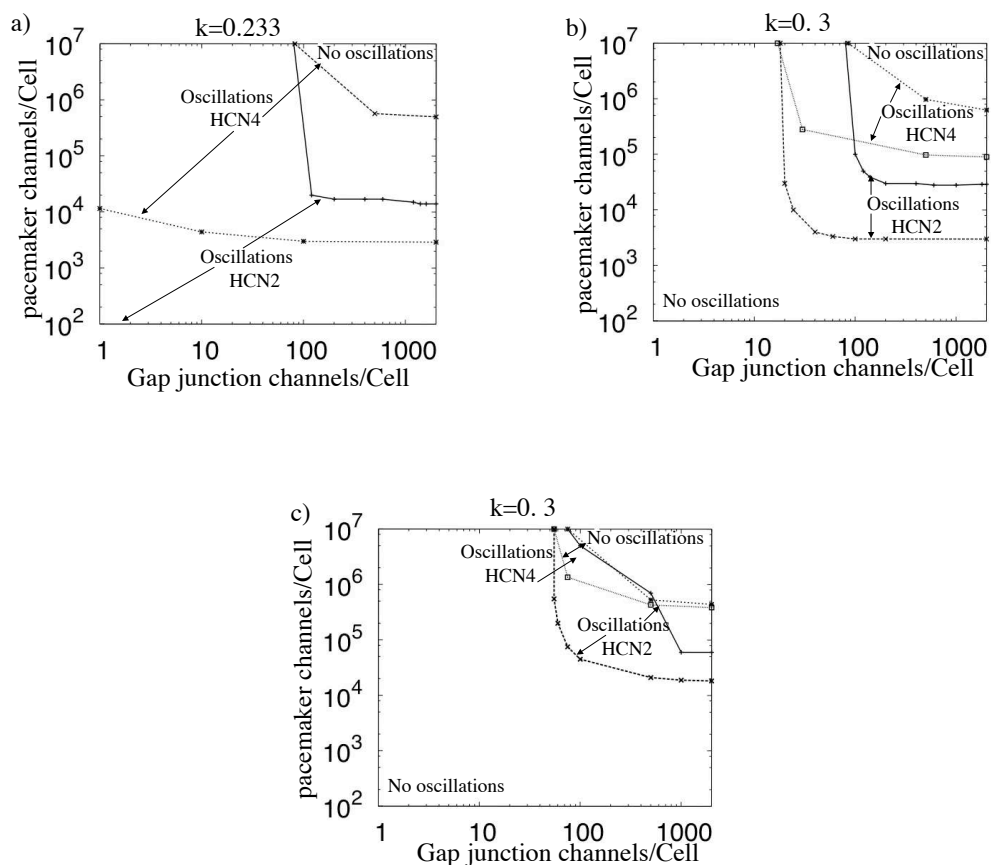
Figure 6.2: **Comparing oscillation regions for HCN1 and HCN2.** Specially here, figures are not hatched not to make it difficult to find regions. It is seen that oscillation region for HCN1 is larger than that for HCN2 for all values of k.

6.1.2   Oscillation regions in a fiber: Comparing genes HCN1,HCN2, HCN4

The oscillation region in a fiber is compared in HCN1 and HCN2 in Fig.6.3.
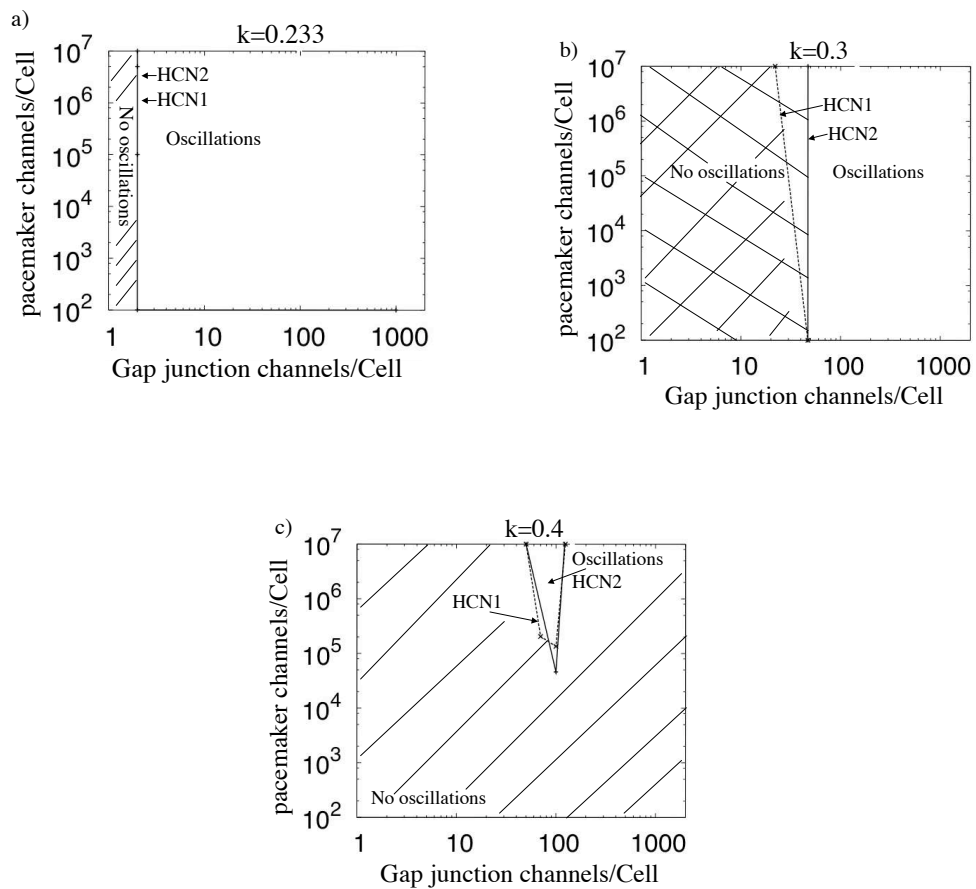
Figure 6.3: Comparing oscillation regions in a fiber when stem cells are transfected with HCN1 and HCN2.

The oscillation region in a fiber is compared in HCN4 and HCN2 in Fig.6.4.
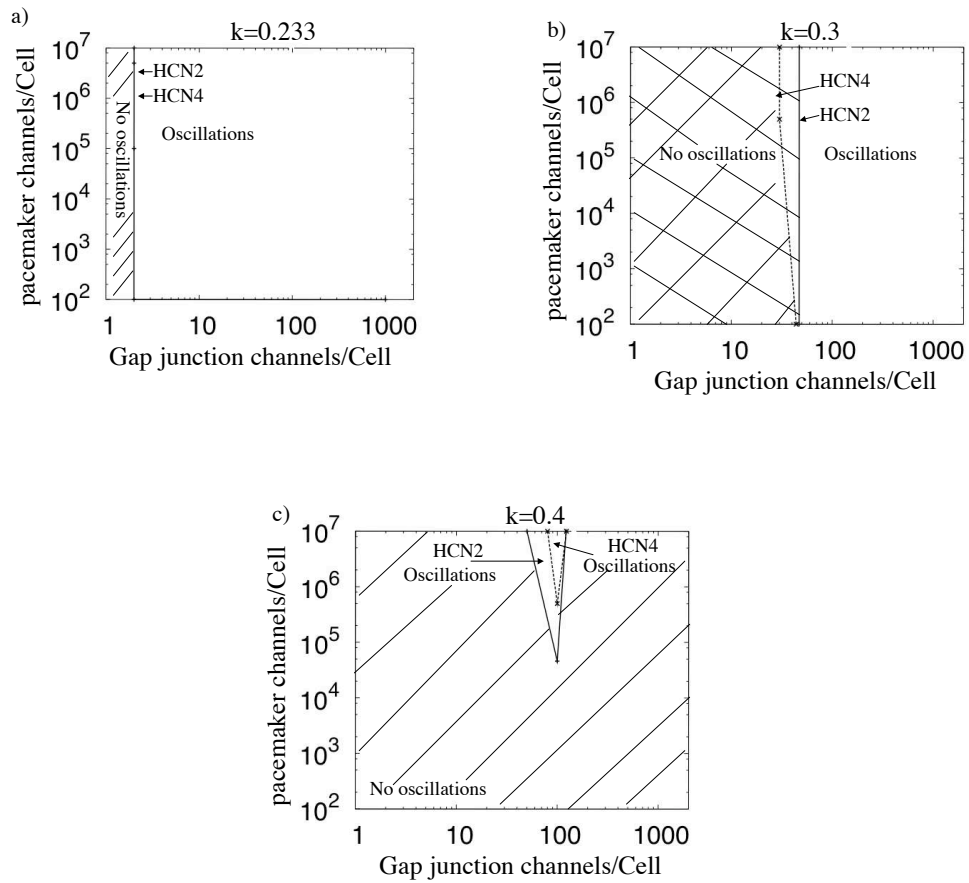
Figure 6.4: Comparing oscillation regions in a fiber when stem cells are transfected with HCN4 and HCN2.

Result of investigating HCN1, HCN2, HCN4 are summarized in Figs.6.1, 6.2,6.3, 6.4. They show the dependance of oscillations on expression level of I_{K1}, number of gap junction channels per cell, number of pacemaker current channels per cell and gating variable time constants.

A common feature of all these dependencies is: neither of isoforms is able to induce oscillations in myocytes with high level of expression of I_{K1}, e.g. in ventricular myocytes (k=1).

6.2   HCN can't induce oscillations in a ventricular myocyte

We want to understand if inability to induce oscillations in ventricular cells (k=1) :

A. is a model dependent phenomenon? what model independent mechanisms could be found?

B. is it due to the stem cells? or due to the HCN channels?

C. how to modify properties of HCN channels so that they could induce oscillations in myocytes with higher levels k of expression of I_{K1}.

We will start with a striking observation that an external current contrary to the current of HCN channels can induce oscillations in ventricular myocytes (k=1).

6.2.1   An electric current can induce oscillation in a ventricular myocyte (k=1)

Oscillation induced in ventricular myocytes with $k = 1$ by an external electric current are shown in Fig.6.5. In Fig.6.5a oscillation range for different amount of external electric current is seen. It is important to note that this oscillation range is narrow. In Fig.6.5b-f, it is observed that by increasing external electric current to the myocyte, the shape of AP is changed in addition to the period of oscillation.

An external current also changes the resting potential, for $I < I_{oscil}$ where I_{oscil} is the oscillation threshold Fig.6.6a.

To make the difference between an external electric current and a connection to a stem cell and clarify why an electric current can induce oscillation in a ventricular myocyte (k=1), we obtained oscillations in both cases and decreased the amplitude to investigate the factors playing a role here.

The oscillation amplitude can be decreased in both cases: either when an external electric current is injected to the myocyte or when myocyte is connected to a stem cell. But it is important to note that in case of external current Fig.6.6b, this happens with a much larger k (here even with k=1), while when stem cell is connected to the myocyte k is 0.42 Fig.6.6c.

In Fig.6.6b, it is seen that oscillation amplitude decreases with increasing the external electric current.

In Fig.6.6c , it is observed that oscillation amplitude decreases with increasing the number of gap junction channels per cell n for a constant number of pacemaker channels per cell.

Fig.6.7 is a more detailed example of Fig.6.6c. In a cell pair, amplitude and period of oscillation decrease with increasing number of pacemaker channels per cell N. This will result in disappearing the oscillation when the number of pacemaker channels becomes large.
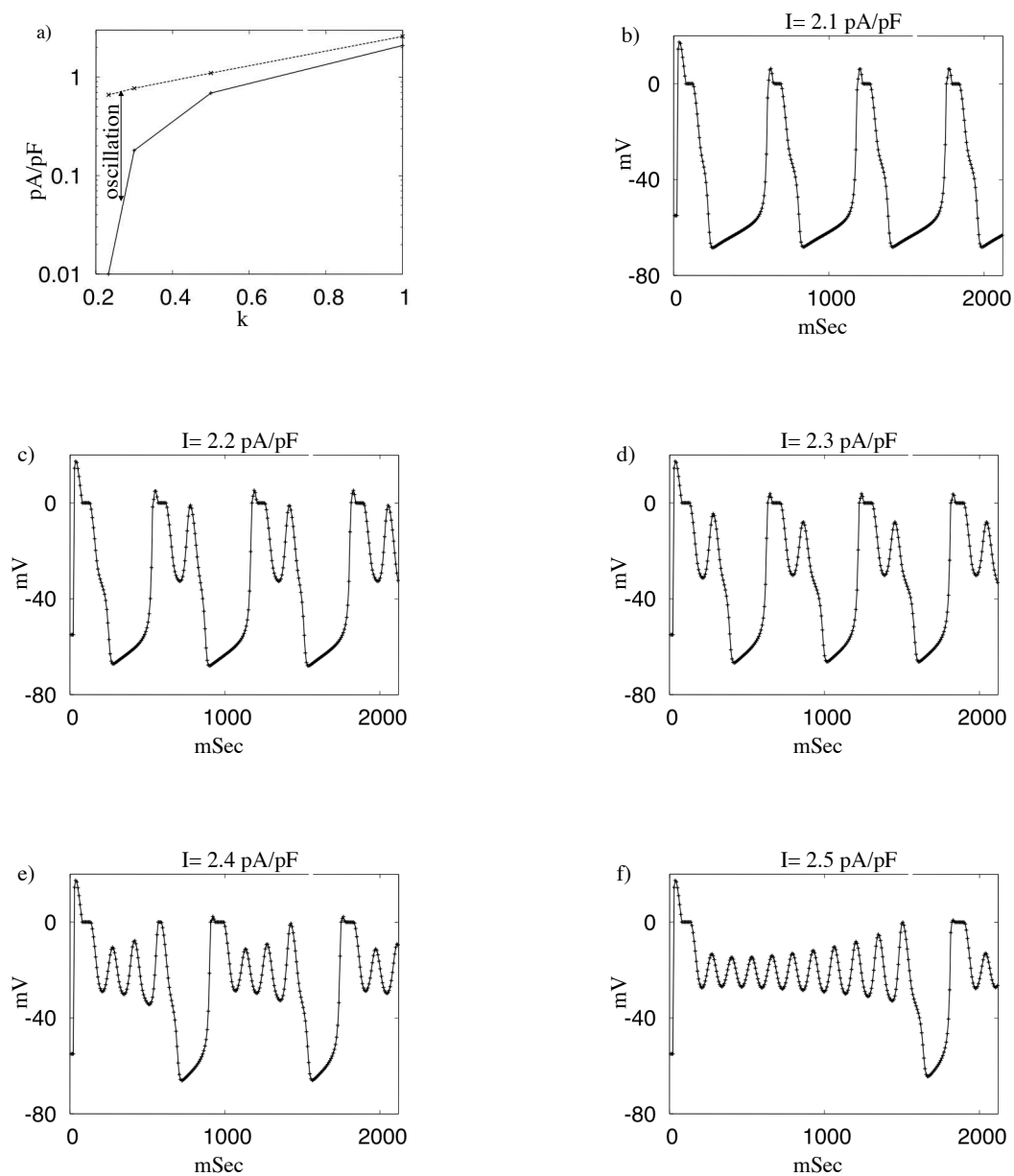
Figure 6.5: **External current induces oscillation in a ventricular myocyte.** a) Oscillation region as a function of the expression level k of I_{K1}. b, c, d, e, f) oscillations induced in a ventricular myocyte (k=1).
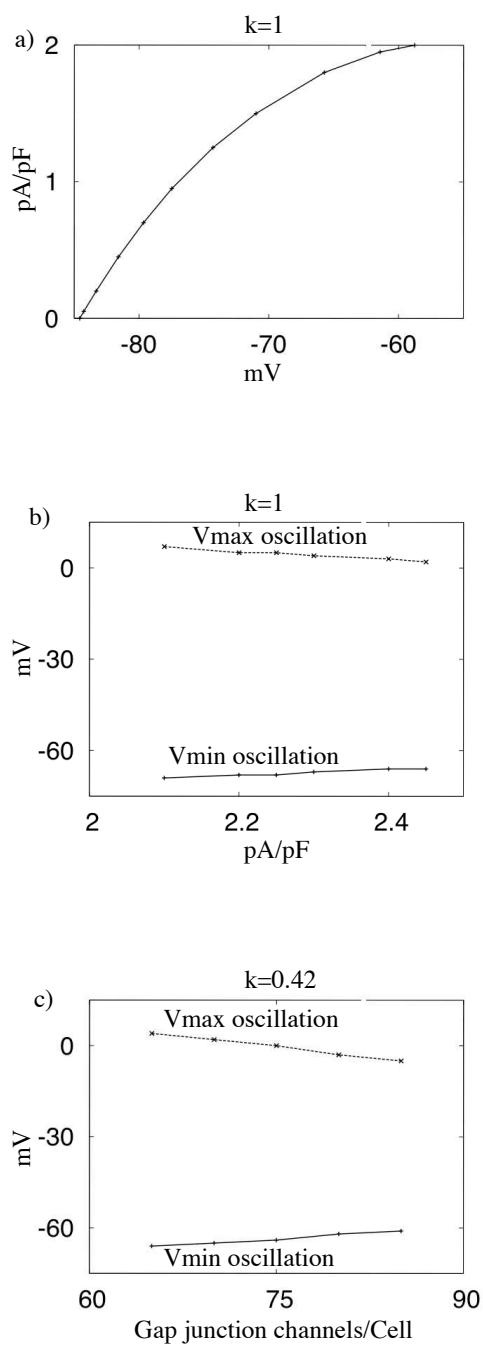
Figure 6.6: a) External electric current changes resting potential for $I_{ext} < 2.1$ pA/pF. Amplitude of oscillation. b) in a myocyte, c) in a cell pair $N = 10^7$.
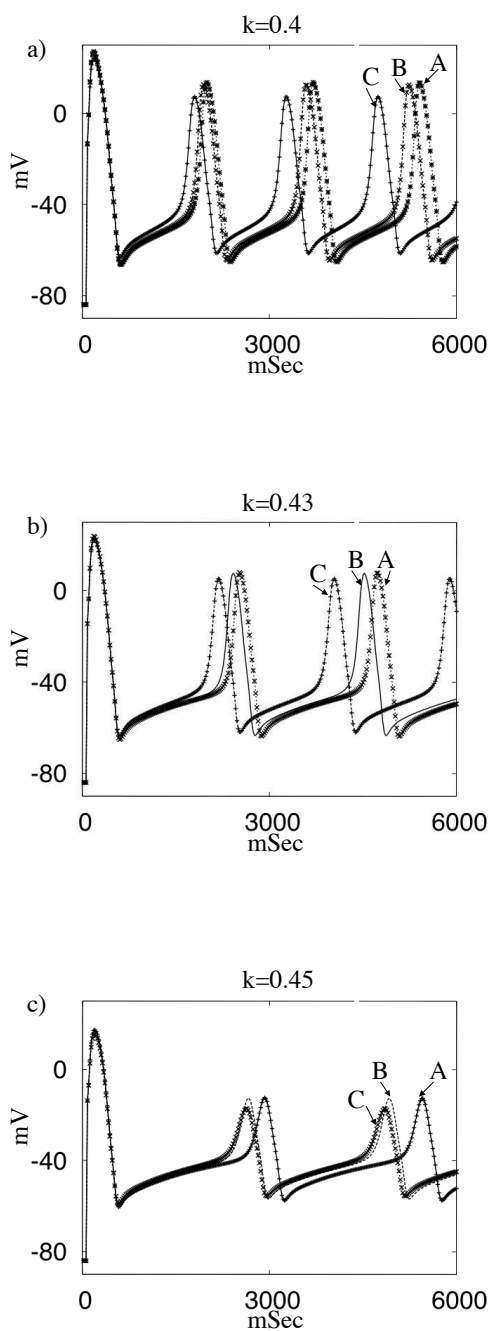
Figure 6.7: The amplitude of oscillation decreases with increasing k in a cell pair. Parameters: $n = 500$, a) A :$N = 2.8 \times 10^4$, B : $N = 3 \times 10^4$, C :$N = 4 \times 10^4$, b) A :$N = 3.4 \times 10^4$, B :$N = 3.5 \times 10^4$, C :$N = 4 \times 10^4$, c) A :$N = 5.7 \times 10^4$, B :$N = 6 \times 10^4$, C :$N = 6.5 \times 10^4$.

6.2.2   A simple model independent mechanism

As Fig.6.5 shows, to induce oscillations in ventricular myocytes (k=1), it is enough to deliver an external electric current 2.1 pA/pF. For a cell pair, this can be easily achieved by increasing the number n of gap junction channels and number N of pacemaker channels per cell. But with any values of N, n oscillations are not induced. What is the mechanism?

Below are the qualitative, model independent arguments explaining this strange phenomenon. The two experiments are compared in Fig.6.8. It is seen that when a stem cell induces oscillations, to start an AP, a larger inward current (I_{Na}, I_{Ca}) is required, because:

- It should charge the capacitance that is twice larger $(C_m \sim C_s \sim 100 \text{ pF})$.

- A part of the current will leak through pacemaker channels with conductivity σ_f .

To increase the current delivered by a stem cell, one needs to increase n, N, since $\sigma_g = n \times \sigma_g^1$ and $\sigma_f = n \times \sigma_f^1$. This results in increasing the percentage of the inward current (I_{Na}, I_{Ca}) that is not used to charge the myocyte capacitance C_m.
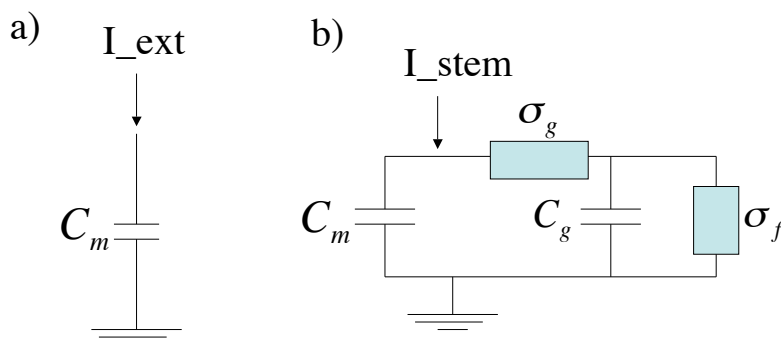
Figure 6.8: a) **Comparing induction of oscillations by an electric current (a), and by a stem cell (b).** C_m is the myocyte membrane capacitance, C_s is the stem cell membrane capacitance, σ_f and σ_g are conductances of pacemaker and gap junction channels.

These arguments suggest that:

(1) It is not the stem cell but the HCN2 pacemaker channels are mainly responsible for not having oscillations.

(2) It is not only HCN2 property but is common to all members of the HCN family.

The generic arguments are qualitative, not quantitative. The computer simulations to verify them are shown.

Item (1) was checked by a direct transfection of a myocyte with HCN2 gene, without using a stem cell, Fig.6.13b,6.14b,6.15b.

Item (2) was checked by numerical calculations of oscillation regions for all members of the HCN family Figs.3.6,4.6, 5.3,3.14,4.7,5.4.

6.2.3 Ionic mechanism of the phenomenon

An external current can induce oscillation in ventricular myocytes while a stem cell connected to it can not do it. The ionic mechanism of this phenomenon is illustrated in Figs.6.10, 6.11, 6.12.

It is seen that:

- *Statement A*. During oscillations, the APs are generated by I_{Ca} and not by I_{Na} as is usually expected (compare amplitudes of I_{Ca} and I_{Na} in Fig.6.10b, 6.11b, 6.12b). Then, to induce oscillations the HCN currents should depolarize the myocyte much stronger, to $E_{thr}^{Ca} \sim -25$mV instead of usual $E_{thr}^{Na} \sim -50$ mV, compare $m(E)$ and $d(E)$ in Fig.6.9b.

- *Statement B*. An important difference between the pacemaker current I_f and an injected external electric current I_{ext} is that I_{ext} can compensate any value of I_{K1} (simply by increasing it's amplitude). On the contrary, I_f can not do it.

The reason is that I_f has a reversal potential E_r. It is equal to ~ -40 mV for HCN2, HCN4 and -30 mV for HCN1.

Near the reversal potential E_r, any increase in number N of pacemaker channels will not help compensating I_{K1}, Figs.6.10c, 6.11c, 6.12c. Increasing its amplitude will create very large currents far from E_r that will suppress oscillations, Fig.6.1.

More detailed: The pacemaker current is an Inward current, i.e. having same direction as I_{Na}, and no matter what is the resistance of the channels, seems should not counteract the I_{Na} current. But for HCN2 and HCN4, the reversal potential of $E_r \sim -40$ mV and for HCN1, it is $E_r \sim -30$ mV. The current itself is:

$$I_f \propto (E - E_r)$$

So, with potentials more positive than -30 mV, the pacemaker current changes direction, and now it flows in opposite direction to I_{Na} (whose reversal potential is $+50$ mV).
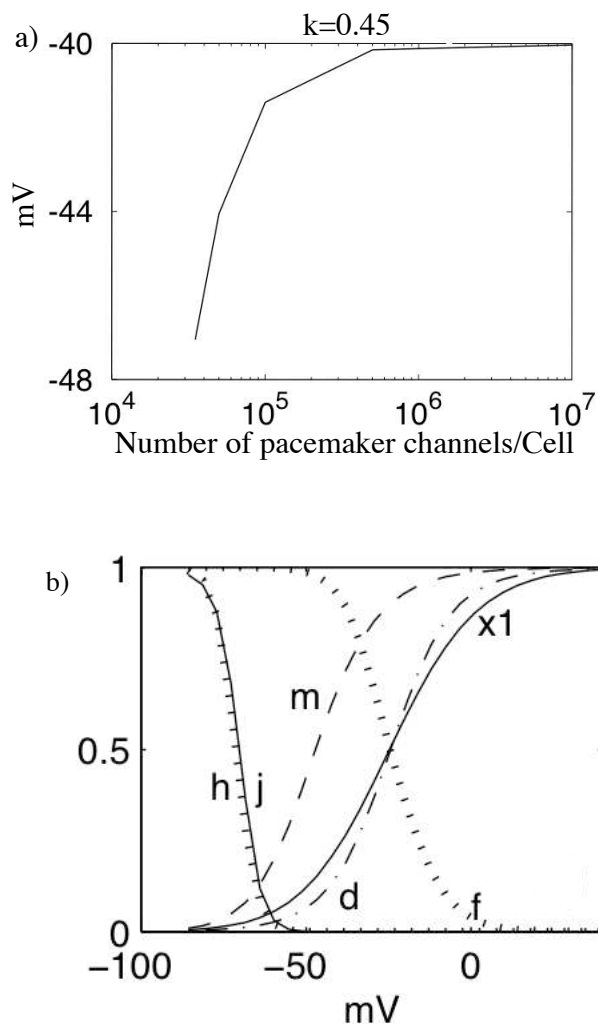
Figure 6.9: a) Dependance of the resting potential on the pacemaker channels per cell ,$n = 10^4$. b) BR gating variables.
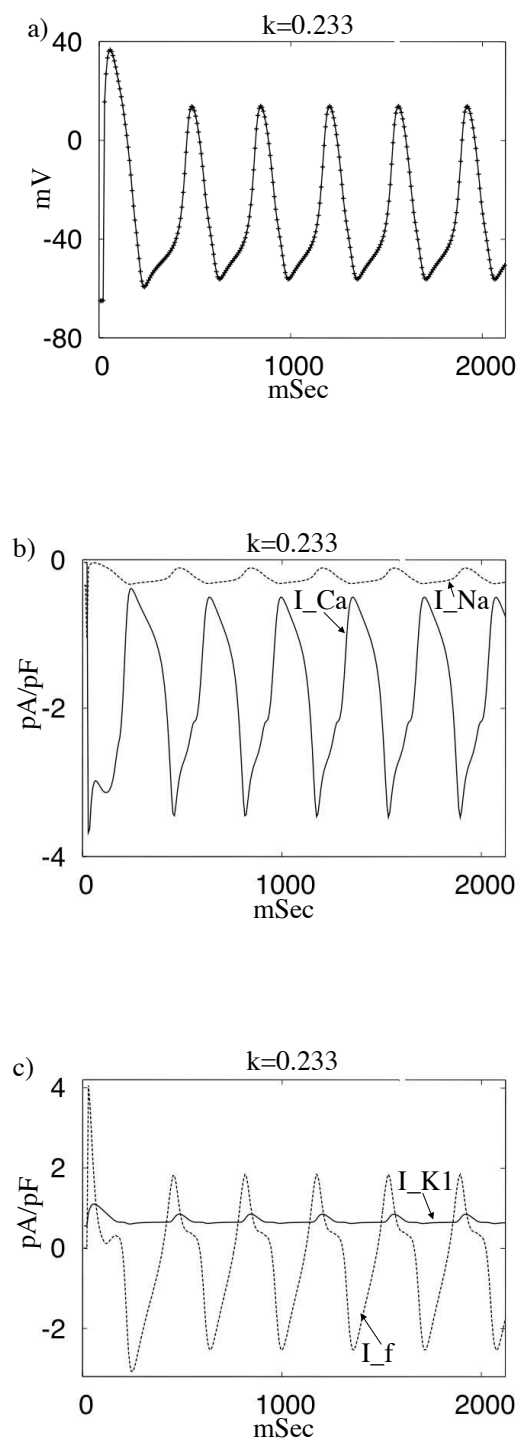
Figure 6.10: a) Oscillations, b) I_{Ca} and I_{Na} currents, c) I_f and I_{K1} currents. Parameter: $n = 10^4$, $N = 3.5 \times 10^4$
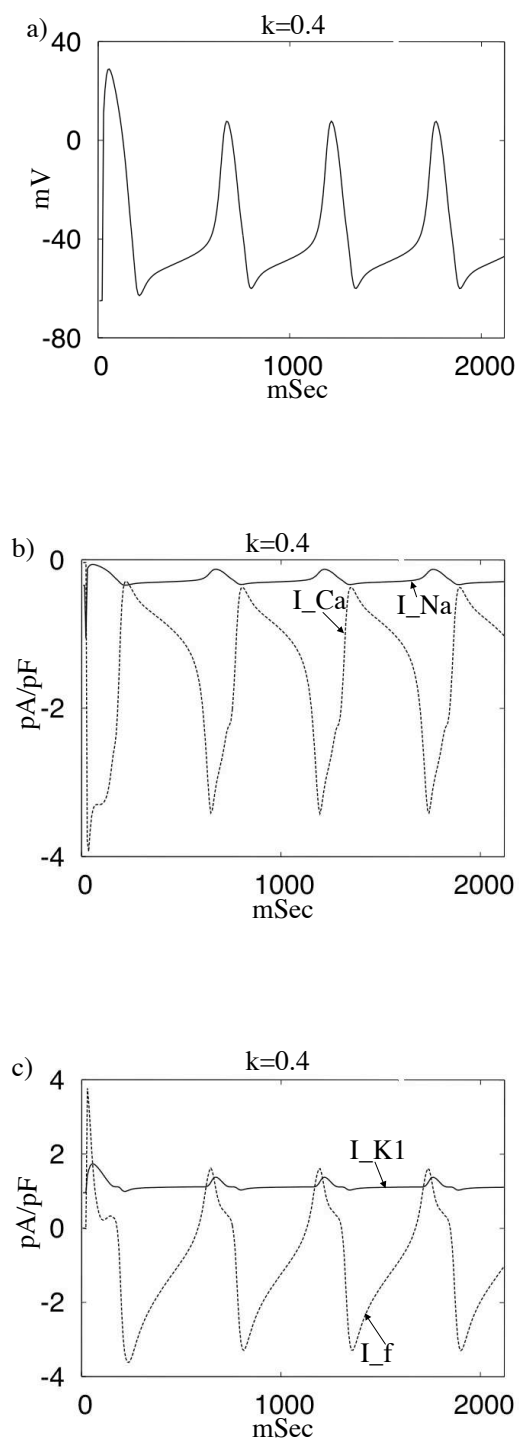
Figure 6.11: a) Oscillations, b) I_{Ca} and I_{Na} currents, c) I_f and I_{K1} currents. Parameter: $n = 10^4$, $N = 3.5 \times 10^4$
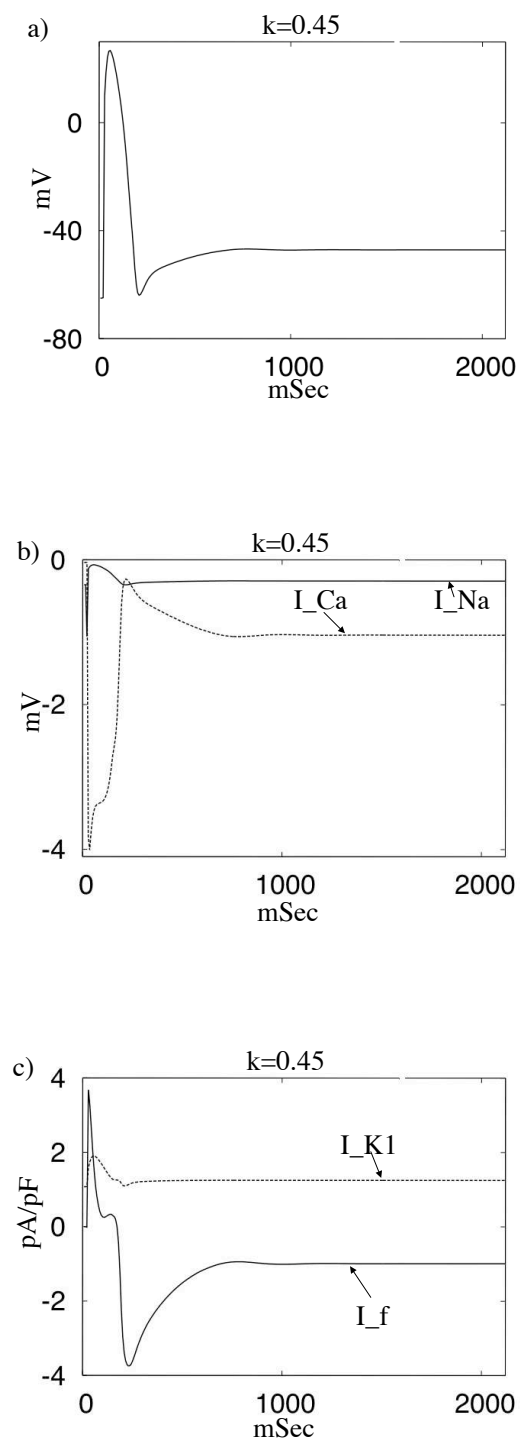
Figure 6.12: a) Oscillations, b) I_{Ca} and I_{Na} currents, c) I_f and I_{K1} currents. Parameter: $n = 10^4$, $N = 3.5 \times 10^4$

6.3   Expressing HCN1,2,4 in a myocyte or in a stem cell

We have found significant limitations of oscillation regions specific to all the isoforms. In Figs.3.14, 4.7, 5.4 oscillations are limited by many parameters, namely: expression level of I_{K1}, number of gap junction channels per cell, number of pacemaker current channels per cell and gating variable time constants.

An important question is: Is it because of the stem cells? Should they be replaced by some other platform?

To investigate this, we incorporated HCN2, HCN1 and HCN4 into the myocyte directly[1], and compared the oscillations. Figs.6.13, 6.14, 6.15 compare effectiveness of both ways of expression for HCN2, HCN1, HCN4.

Fig.6.13 shows oscillation regions for HCN2 expressed in a stem cell (a), and in a myocyte (b). The oscillation regions superimposed are shown in fig (c). It is seen that oscillation regions are almost the same, and there is no effect on oscillations in which platform HCN2 is expressed.

Figs.6.14, 6.15 compare the expression of HCN1 and HCN4 respectively in a stem cell and in a myocyte, presented in the same way as Fig.6.13.

It is seen that for all isoforms (HCN1, HCN2, HCN4), the platform of the expression (in a myocyte or in a stem cell) does not affect oscillation, for large enough number of gap junctions per cell ($n = 10^4$). For small enough n, the oscillation regions will be more narrow, similar to Fig3.6.

This result confirms what was found in the previous chapters as an important property of stem cells transfected with HCN2 (or HCN channels family generally). Stem cells transfected by HCN channels can induce oscillations only in myocytes with sufficiently low level ($k < 0.4$) of expression of I_{K1} and this is not a characteristic of the stem cell as a mean of gene delivery but the HCN gene itself.

Here, we wanted to show that the "defects" or limitations that we have found do not characterize stem cells, but are generic features of HCN gene family coding the pacemaker current. Our modeling results suggest that same limitations will be found in experiments with HCN delivered into myocytes using viruses as vectors[2], for example.

---

[1]Myocytes were not taken as the first platform and to be transfected with HCN channels because in practice they have this disadvantage that they must be extracted from patients heart, manipulated in the laboratory and then injected in patients heart, while stem cells are available from cell banks

[2]Even if for the moment viruses are not an ideal vector because of risk of causing cancer.
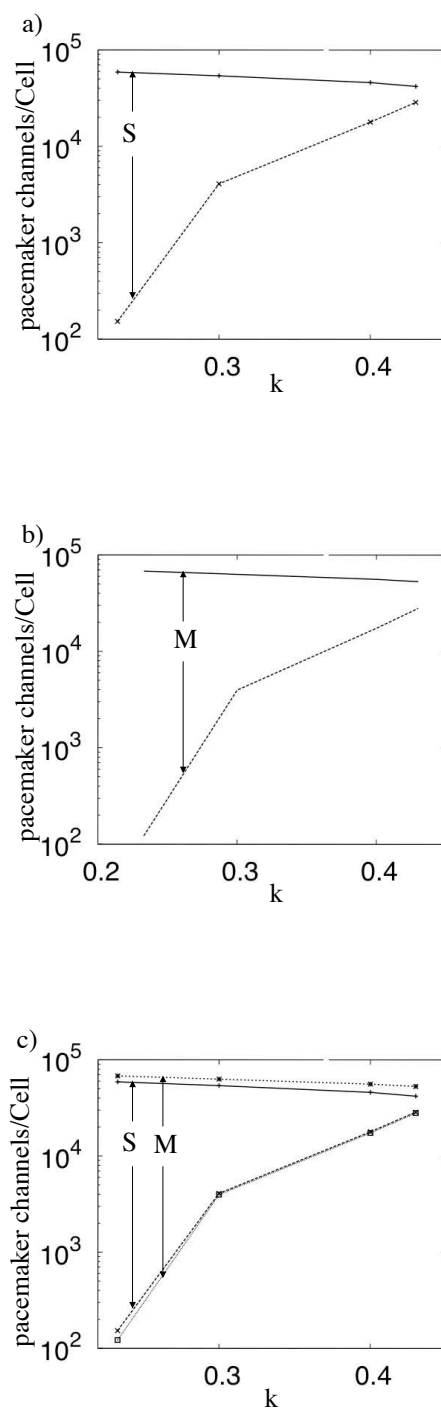
Figure 6.13: Oscillation regions for HCN2 expressed a) in a stem cell, b) in a myocyte, c) superimposed figures a) and b). Parameter: $n = 10^4$. It is seen that oscillation regions are almost the same.
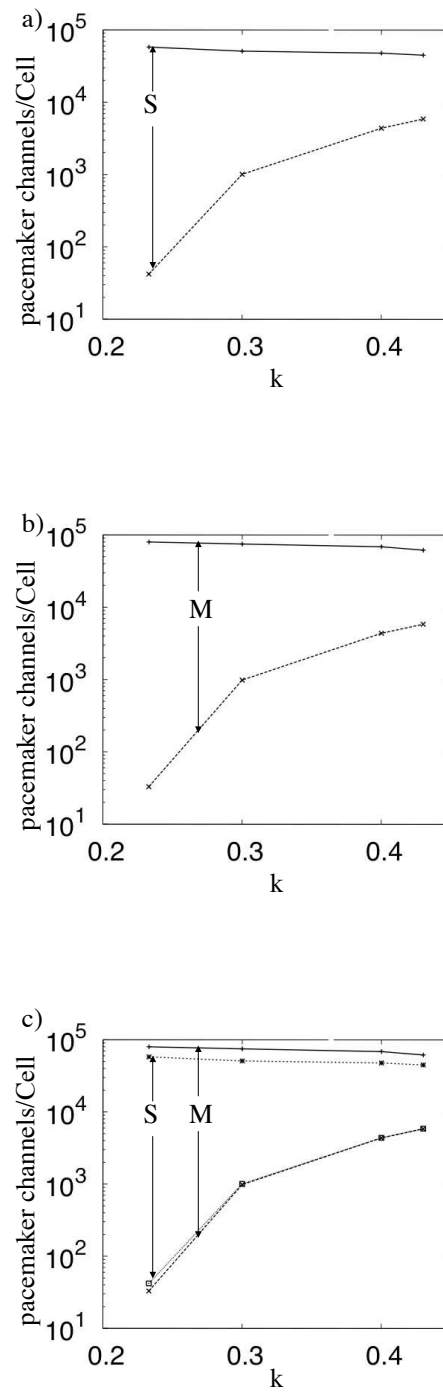
Figure 6.14: Oscillation regions for HCN1 expressed in a) a stem cell, b) a myocyte, c) superimposed figures a) and b). Parameter: $n = 10^4$. It is seen that oscillation regions are almost the same.
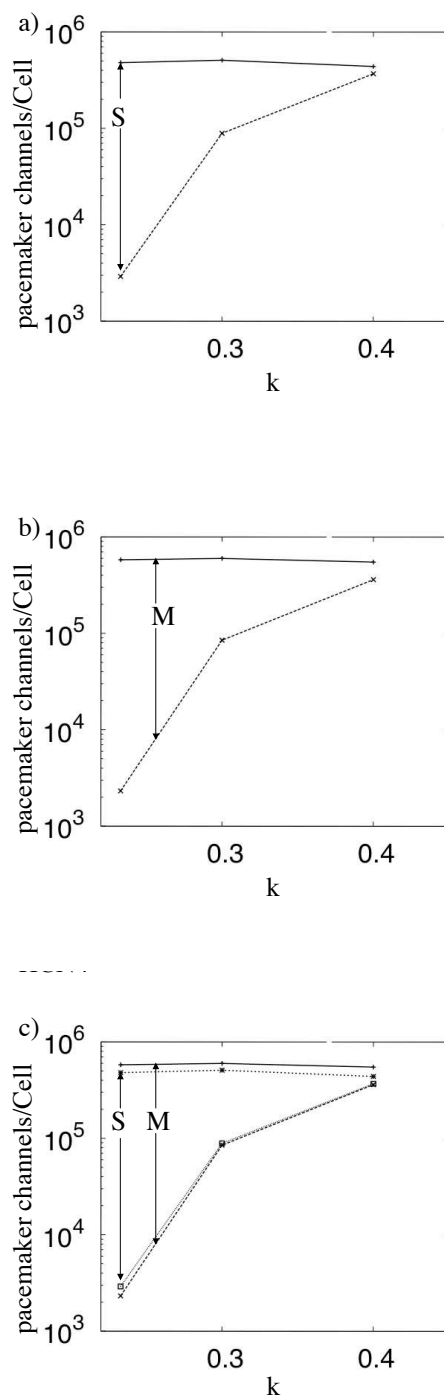
Figure 6.15: Oscillation regions for HCN4 expressed in a) a stem cell, b) a myocyte, c) superimposed figures a) and b). Parameter: $n = 10^4$. It is seen that oscillation regions are almost the same.

6.4   Modifying HCN genes properties

Reversal potential

Pacemaker currents generated by HCN channels can induce oscillations only in a myocyte with a low level k of expression of I_{K1} only Figs.6.13,6.14,6.15.

How these genes should be modified so that they can induce oscillations in myocytes with a higher level k of expression of I_{K1}? Statement B in the previous section indicates a path for this: a shift of the reversal potential E_r to more positive values, so that :

$$E_r > E_{thr}^{Ca}$$

It will not help to compensate I_{K1} everywhere but the total ionic current will change its sign *after* the front of AP is generated and will not prevent induction of oscillations.

Fig.6.16 shows oscillations induced by setting the reversal potential of the gene HCN2 in a myocyte with k=0.56 to -30 mV while there was no oscillation with same k and $E_r = -40$ mV. As Fig.6.13 shows the natural HCN2 can not induce oscillation for $k > 0.435$.
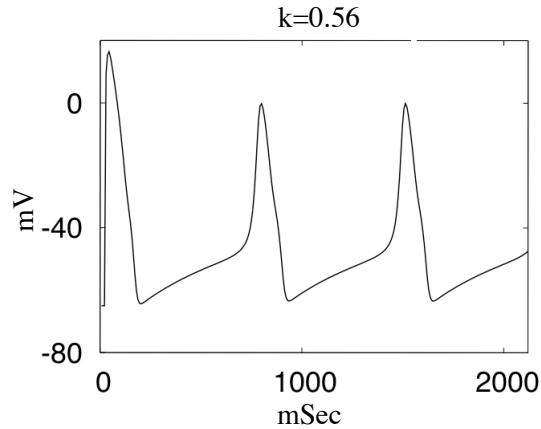
Figure 6.16: Oscillation for a cell pair k=0.56 when stem cells are transfected with a modified HCN2 where the reversal potential was set to -30 mV. Note that oscillation were never observed with such a value of k for HCN2.

Inactivation time constant

A simple analysis shows that oscillation region could be significantly increased by selective decreasing characteristic inactivation time in the voltage range corresponding to the front of the action

potential.

Here we show that with choosing another gene with same inactivation characteristic as HCN2 for example but respectively very low inactivation time, makes oscillation possible when it's impossible with HCN2.

This is due to AP upstroke time that is about 5 mSec. We checked this by changing inactivation time contant τ_2 of HCN2 to 1 mSec for all voltages.

Result shows that this helps widening oscillation range for constant N number of pacemaker channels per cell and k expression level of I_{K1} values Fig.6.17a. More important result is that there are oscillation with very fast inactivation time constant while there is no oscillation with τ_2 of HCN2 Fig.6.17b.
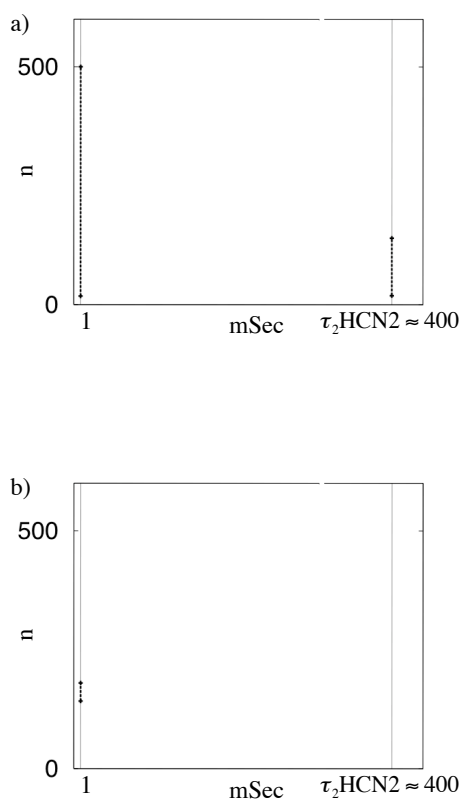
Figure 6.17: Oscillation region is shown in thick dashed line. a) k=0.3, b) k=0.45. It is seen that decreasing the inactivation time contants below the AP front duration increases oscillation region. Parameter: $N = 10^5$

6.5   Connecting stem cells to myocytes via transitional regions

In Fig.3.14 oscillation regions limit the parameters inside a pacemaker region only. A pacemaker can trigger oscillation in any tissue where an action potential (AP) can propagate.

Fig.6.18c shows a fiber consisting of ventricular myocytes (k=1) where periodical AP are induced by a stem cell based pacemaker. With k=1 oscillation was never observed before.

An important condition to satisfy is that the tissue connected to a pacemaker should not suppress oscillation in the pacemaker. Any tissue connected to a pacemaker is a sink for it. Too large sink suppresses oscillation. A sufficiently large sink decreases oscillation amplitude in the pacemaker region and kills oscillation in transitional and a remote point from the pacemaker region Fig.6.18a.

To avoid this difficulty, the natural pacemaker sinus (SA) node, is connected to the atrial tissue via a transitional region with different excitability that is a small load for the pacemaker. This ensures a safe connection to the cardiac tissue. Same exists for AV node and bundle branches.

The easiest way to connect a biopacemaker to the cardiac tissue is via any natural existing transitional regions. This was performed for example in [3], where the stem cells transfected with HCN2 were injected into the left bundle branch.

When neither of these natural transitional regions can be used, it should be created. Fig.6.18a show an unsuccessful transitional region where the amplitude of oscillation is decreased and becomes zero outside of the pacemaker region, while Fig.6.18b is an example of successful one.

The model permits to design such transitional regions, choose stem cell characteristics, myocytes parameters and connections between stem cells and myocytes.
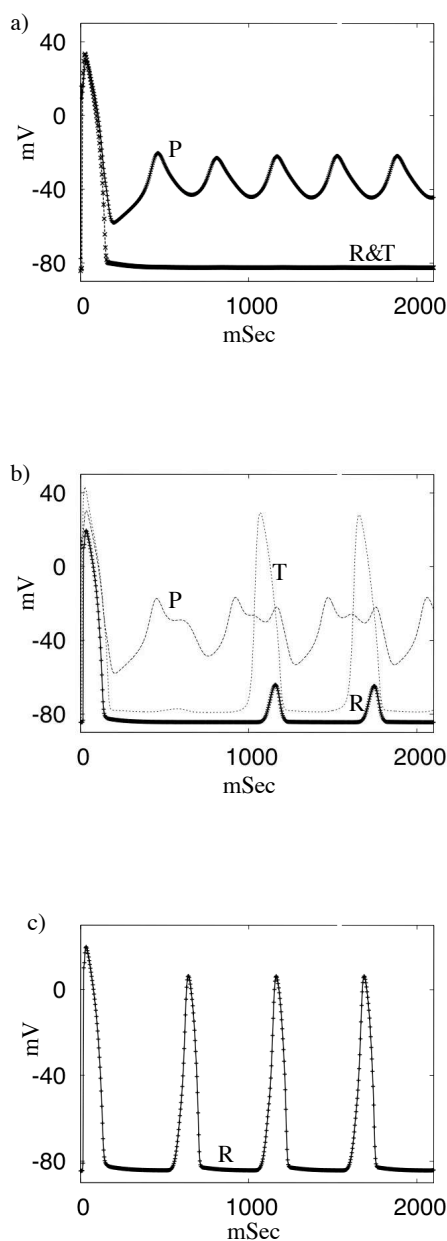
Figure 6.18: **Stem cells induce oscillations in a fiber consisting of ventricular myocytes, k=1.** P- records from the pacemaker, R -from the remote point of the fiber, T- from the transitional region. **a)** Oscillation amplitude in the pacemaker is decreased due to connection with cardiac tissue. No action potentials (AP) are seen on T or R electrodes. The pacemaker is connected to cardiac tissue (k=1) via a transitional region composed of myocytes with k=0.6. **b)** The pacemaker is connected to cardiac tissue (k=1) via a transitional region composed of myocytes with k=0.4. Oscillation amplitude in the pacemaker is above the propagation threshold. Action potentials (AP) are seen on T but not on R electrodes. **c)** Successful connection. Action potentials (AP) are seen on the remote electrode R. The transitional region composed of myocytes with k=0.3. In all images, the pacemaker consists of stem cells and myocytes k=0.233. Parameters: $n = 100, N = 10^4$

Chapter 7

Two and three dimensional cardiac tissue

Here I include results from our joint article [36]; analytical calculations are performed by Dr.Pumir.

The aim of the calculations is to estimate currents needed from a small size artificial pacemaker to induce oscillations in two and three dimensional tissues.

We study here the response of a tissue initially at rest, when a current of a given intensity is applied over a restricted volume of the tissue. Important information can be obtained by studying the purely passive case, where the membrane potential remains close to the resting potential. The response of the tissue crucially depends on the space dimension, d.

In the cable approximation, the equations governing the membrane potential thus simply read :

$$\nabla^2 e - \frac{e}{\lambda^2} = j\rho_d \tag{7.1}$$

The scale, λ, is the usual electrotonic length; $\lambda \approx 1mm$ in cardiac tissue. The source term in Eq.7.1 is the product of the current density, j, dimensionally a current divided by a d-dimensional volume, by the resistivity, ρ_d, dimensionally a resistance multiplied by a length to the power $d - 2$, so the product has the appropriate dimension (V/m^2).

We assume here that a 1-dimensional cable is made of aligned cells, and a 2-dimensional preparation is made of a monolayer arrangement of cells. Ignoring the anisotropy of the tissue, and assuming that the cells are cubic, of size $\sim a^3$, $a \approx 30\mu m$, the values of the resistivities are related by :

$$\rho_1 = \rho_3/a^2 \ , \ \ \rho_2 = \rho_3/a \tag{7.2}$$

To simplify, we consider the case of a source of current axisymmetric (j depends only on the distance

of the point to a center, O), and localized in a small volume ($j(r) = 0$ when $r \gg L$), when L is typically of the size of a cell ($100 \mu m$).

Equation 7.1 thus reduces to the simple ordinary differential equation :

$$\frac{d^2}{dr^2}e + \frac{d-1}{r}\frac{d}{dr}e - \frac{e}{\lambda^2} = j\rho_d \tag{7.3}$$

In this form, the space dimension simply appears as a parameter.

By using known solutions of the homogeneous problem ($j = 0$), the problem can be completely solved, using the variation of parameters method [38]. We consider in turn the dimensions $d = 1$, $d = 2$ and $d = 3$.

In 1 spatial dimension (case of a string of cells), Eq.7.3 reduces to :

$$\frac{d^2}{dr^2}e - \frac{e}{\lambda^2} = j\rho_1 \tag{7.4}$$

The solutions of the homogeneous problem are simply $u_1(r) = \exp(r/\lambda)$ and $u_2(r) = \exp(-r/\lambda)$. Imposing the physical constraint that the solution does not grow when $r \to \pm\infty$, one finds that

$$e(r) = -\frac{\lambda\rho_1}{2}\left(\int_r^\infty j(r')e^{(r-r')/\lambda}dr' + \int_{-\infty}^r j(r')e^{(r'-r)/\lambda}dr'\right) \tag{7.5}$$

We consider here the case where the injected current has a step function form : $j(x) = j_0$ for $-L \le x \le L$, and $j(x) = 0$ for $|x| > L$. A straightforward analysis of the solution given by Eq.7.5 shows that the maximum of e is located at $x = 0$:

$$e_{max,1} = -j_0\lambda\rho_1 \times \lambda(1 - \exp(-L/\lambda)) \tag{7.6}$$

Introducing the total amount of current injected into the fiber :

$I_{tot} = \int_{-L}^L j(x')dx'$, Eq.7.6 reduces to :

$$e_{max,1} = -\frac{\lambda\rho_1 I_{tot}}{2}(\lambda/L)(1 - \exp(-L/\lambda)) \tag{7.7}$$

which simply reduces, when $L/\lambda << 1$, to :

$$e_{max,1} \approx -\frac{\lambda\rho_1 I_{tot}}{2} \tag{7.8}$$

Graphs on the Fig.7.1 were calculated as follows. From Eq.7.7,7.11,7.15 the current I_{tot} was calculated needed to achieve the threshold depolarization to initiate a propagating action potential (AP). This is needed to drive the whole cardiac muscle from a small region with injected stem cells. The total current I_{tot} divided by number of stem cells injected is shown on the ordinate. A case when a stem cell is connected to every myocyte is shown. (Compare with data of [5], showing that only 0.005% of injected stem cells are connected to myocytes).

Myocytes with $100 \times 10 \times 10 \mu m$ size were considered to be densely packed inside the "pacemaker" region of size L ; stem cells were taken of zero size. $\lambda = 1mm$.

In 2-dimensions (case of a cells monolayer), the solution can be expressed in terms of the Bessel function K_0 and I_0 :

$$e(r) \quad = \quad -\rho_2 \Big(K_0(r/\lambda) \int_0^r j(r')I_0(r'/\lambda)r'dr' + I_0(r/\lambda) \int_r^\infty j(r')K_0(r'/\lambda)r'dr' \Big) \tag{7.9}$$

The largest value of the membrane potential, given by Eq.7.9, is reached at $r = 0$. In the case of a step function distribution of current ($j(r) = j_0$ when $r \leq L$, and $j(r) = 0$ when $r > L$), the largest value of the membrane potential, given by Eq.7.9, is reached at $r = 0$:

$$e_{max,2} \quad = \quad -j_0\rho_2 \int_0^L j(r')r'K_0(r'/\lambda)dr' - j_0\rho_2\lambda^2(1 - (L/\lambda)K_1(L/\lambda)) \tag{7.10}$$

where K_1 is the modified Bessel function [39]. In terms of the total injected current, $I_{tot} = \pi L^2 j_0$, the expression for $e_{max,2}$ reads :

$$e_{max,2} = -\frac{I_{tot}\rho_2}{\pi}(\frac{\lambda}{L})^2(1 - (L/\lambda)K_1(L/\lambda)) \tag{7.11}$$

In the particular case where the current is injected over a region of size $L << \lambda$, Eq.7.11 reduces to :
$$e_{max,2} \approx \frac{\rho_2 I_{tot}}{\pi}(\ln(L/2\lambda) + \gamma - 1/2) \tag{7.12}$$
where I_{tot} is the total amount of injected current, and γ is the Euler constant [39]: $\gamma \approx 0.577$. where K_1 is the modified Bessel function [39].

In 3-dimensions (case of a whole tissue), the solutions of the homogeneous problem are $u_1(r) = \sinh(r/\lambda)/r$ and $u_2(r) = e^{-r/\lambda}/r$, and the solution that satisfies the physical constraints that the solution is bounded both when $r \to 0$ and $r \to \infty$:

$$e(r) \quad = \quad -\lambda\rho_3 \Big(\frac{\sinh(r/\lambda)}{r} \int_r^\infty r'e^{-r'/\lambda}j(r')dr' + \frac{e^{-r/\lambda}}{r} \int_0^r r' \sinh(+r'/\lambda)j(r')dr' \Big) \tag{7.13}$$

Assuming, as previously, that the distribution of current is uniform in the sphere of radius L : $j(r) = j_0$ when $r \leq L$ and $j(r) = 0$ otherwise, one finds that the membrane potential is maximal at $r = 0$:

$$e_{max,3} = \rho_3 j_0 \lambda^2 (1 - (1 + L/\lambda) \exp(-L/\lambda)) \tag{7.14}$$

In terms of the total injected current, $I_{tot} = 4\pi L^3 j_0 / 3$, Eq.7.14 reduces to :

$$e_{max,3} = \frac{3\rho_3 I_{tot}}{4\pi} \frac{\lambda^2}{L^3} (1 - (1 + L/\lambda) \exp(-L/\lambda)) \tag{7.15}$$

In the particular case where $L << \lambda$, expression 7.14 reduces to :

$$e_{max,3} \approx -\rho_3 \int_0^\infty j(r')r'dr' \approx -\frac{\rho_3 j_0 L^2}{2} \tag{7.16}$$

In terms of the total current injected in the tissue, $I_{tot} = 4\pi/3 j_0 L^3$, the maximum value of e_{max} is :

$$e_{max} \approx -\frac{3}{8\pi L} \rho_3 I_{tot} \tag{7.17}$$

From a mathematical point of view, it is interesting to remark that the maximum value of the membrane potential is independent of the scale λ in dimension 3 (in fact, in dimension $d > 2$). The estimate Eq.**??** could have been obtained by taking $\lambda = \infty$, contrary to what happens in dimension $d = 2$ and lower.

The expressions for $e_{max,d}$ allow us to estimate the required amount of injected current, I_{tot}, to reach the required threshold, e_{th}, to start an action potential. ¿From Eq.7.8, the critical currents is given, in 1-dimension by :

$$I_c^1 \approx -\frac{2}{\lambda \rho_1} \times e_{th} = -\frac{2a^2}{\lambda \rho_3} \times e_{th} \tag{7.18}$$

Similarly, one obtains from Eq.7.12 in 2-dimensions :

$$I_c^2 \approx \frac{\pi}{\rho_2} \frac{1}{\ln(L/2\lambda) + \gamma - 1/2} \times e_{th} \frac{\pi a}{\rho_3} \frac{1}{\ln(L/2\lambda) + \gamma - 1/2} \times e_{th} \tag{7.19}$$

and from Eq.7.17 in 3-dimensions :

$$I_c^3 \approx \frac{4\pi L}{\rho_3} \times e_{th} \tag{7.20}$$

For a given size of the injection zone, L, taken to be smaller than λ, the critical threshold, I_c^d thus depends very strongly on the dimension d of the system.

Reaching the critical threshold requires much less current in 1-dimension than in 2-dimensions (roughly by a factor $\sim \lambda \ln(L/\lambda)/a$). Similarly, reaching the threshold requires a stronger current in 3 dimensions than in 3-dimensions, roughly by a factor $\sim L/(a\ln(L/\lambda))$.

A conclusion: In order to drive the cardiac tissue, small size artificial pacemakers need to deliver currents orders of magnitude larger than those used in a cell pair or cell culture experiments (Fig. 7.1). To avoid this, size of the pacemaker created should be several times larger than the space constant λ.
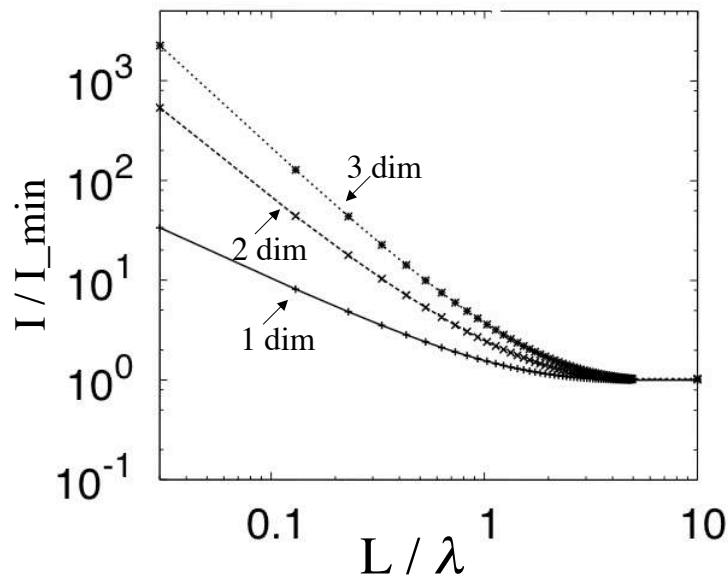
Figure 7.1: Current needed from a stem cell to drive cardiac tissue. I_{min} is the minimal current. L pacemaker size; stem cells are homogeneously distributed inside it. λ is the space constant. For pacemaker size L not big enough, the current should be increased several orders of magnitude in cardiac tissue (3 dim) compared with experiments in cell culture (2 dim) or 1 dim fiber.

Chapter 8

Conclusions

- As our mathematical models show, stem cells that are transfected with HCN genes, reliably induce oscillations in myocytes under appropriate conditions. The condition is that myocytes should be close to a spontaneous oscillatory state. It is possible to obtain oscillation with relatievly low numbers of gap junction and pacemaker channels in this case. These oscillations are robust and their period depends on the number of gap junction and pacemaker channels per cell.

- The mathematical models developed permit now to estimate how the oscillations induced depend on number of pacemaker channels N expressed in a stem cell and number of gap junctions per cell couple n. Obtaining a reliable model would greatly reduce the number of the experiments. They permit also to estimate the effect of expression levels that are not achieved in the experiments yet.

- We observed that in a pair of a myocyte-stem cell transfected by HCN gene, by modifying HCN properties, it is possible to obtain oscillations even in myocytes with a relatively large k (or with a low excitability). These modifications can be: changing the reversal potential, or changing inactivation time constant. This might be interpreted as searching for a different gene family to transfect the stem cells.

- The oscillations regions are found for isoforms HCN2, HCN1, HCN4. They are very close to one another. The regions guarantee robust oscillations can thus be selected. The common point between these regions of the isoforms is that for large numbers of gap junction and pacemaker channels, oscillations become impossible.

- Induction of oscillations in the ventricular myocytes (k=1) by connecting stem cells to them has not been found possible. So, alternative approaches should be used in the experiment.

- These approaches might include other types of cardiac cells such as bundle branch and purkinje cells, like buffers between the stem cells and the ventricular myocytes. This can explain the experiment in [3]. The developed model permits to describe the transitional region between the small pacemaker and the working myocardium, by taking into account a gradual change of the excitability in the cardiac tissue to obtain oscillation.

- Increasing the number of stem cells versus myocytes will help obtaining oscillation but in the experiments the number of stem cells making gap junctions with the myocytes is about

0.005% so this issue may not help the future experiments unless a new method for increasing the number of stem cells making gap junctions with the myocytes is found. Also increasing the number of stem cells versus myocytes will lead to decreasing the period of oscillation.

- To study the induction of oscillation, stem cell descriptions should include both activation and inactivation of pacemaker current, contrary to the tradition in the field used by the biologists. Even if the result given by the simplified model including only inactivation is close to the result of the complete model including inactivation and activation, we observed differences between their various oscillation regions. It is better to use the complete model.

- To drive cardiac muscle, the small size artificial biological pacemakers may need deliver currents with orders of magnitude larger than that in a cell pair or cell culture experiments. This is the most serious question ask by this thesis.

Chapter 9

Appendix

9.1 List of relevant biological terms

Gap junction channels: Channels between two connected cells. Conductivity of a single channel $\sigma_1 \sim 50$ pS. Number of channels per cell is $\sim 10^2 - 10^4$.

Pacemaker channels: Conductivity of a single channel $\sigma_f \sim 1$ pS. Number of channels per cell is $\sim 10^5 - 10^7$

Reversal potential: Voltage at which there is no ion exchange through the membrane. For myocyte ~ -40 mV.

9.2 Verifying the stem cell models

9.2.1 Comparing membrane resistance calculated from BR model and from our cell pair model

We verified our stem cell model by measuring and comparing the memebrane resistance of the myocyte with BR model and our stem cell model when the myocyte is connected to the stem cell.

With the stem cell model , the membrane resistance of the myocyte measured was only 6 percent different from measured in BR model.

A numerical simulation of the BR model

An external electric current $I = 0.00675$ pA/pF was injected into a ventricular myocyte with an expression level $k = 0.233$ of I_{K1}. It induced a change in resting potential E_r^m from -65.29 to -63.67 mV. This permits to estimate the membrane resistance of the myocyte:

$\sigma_m = \frac{I}{\Delta E} = \frac{0.00675(pA/pF)}{1.62mV} = 4.16$ pS/pF

$\sigma_m = 416$ pS per cell (with membrane capacitance C_m=100 pF.

A numerical simulation of the cell pair model

A stem cell connected to a myocyte is shown in Fig.9.1a. In the model of this cell pair , we measured resting potentials of a stem cell, $E_s^r = -40$ mV and of a myocyte, $E_m^r = -65.29$ mV and modified values $E_s = -45.5$ mV and $E_m = -63.5$ mV after the cells are connected.

This permits to calculate the membrane resistance of a myocyte:

$$R_m = \frac{E_m^r - E_m}{I} \tag{9.1}$$

where I is a current flowing through gap junctions resistance R_{gap}, Fig.9.1b. Current I is easily found as $I = \frac{E_m - E_s}{R_{gap}}$.

This gives membrane conductivity $\sigma_m = \frac{1}{R_m} = 468$ pS, only 6 percent difference with value estimated from BR equations directly.

Here, we used evident relations: $R_{gap} = \frac{1}{\sigma_{gap}}, \sigma_{gap} = n\sigma_{gap}^1$ and $\sigma_{gap}^1 = 50$ pS. Parameters of the numerical simulations: $k = 0.233$, $N = 10^3$, $n = 0.75$ (to have a very small current I, we used a very small value of n not achievable in the real experiment).
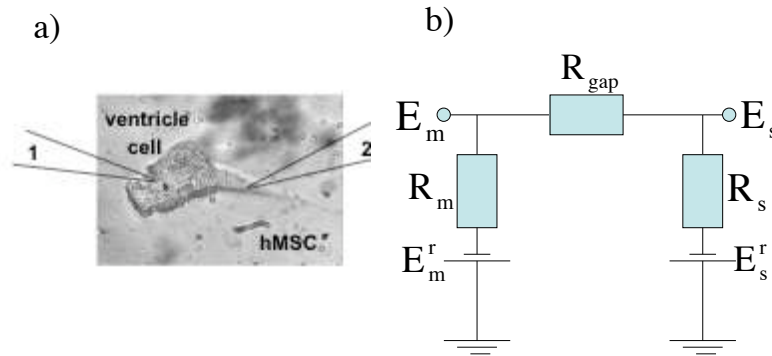
Figure 9.1: **A cell pair**. a) an image, b) an equivalent electric circuit. E_s and E_m are resting potentials of a stem cell and of a myocyte, respectively. R_{gap} is the gap junction resistance, R_m is the membrane resistance of the myocyte.

9.3   Fortran programs

0 dimension : cell pair (a stem cell connected to a myocyte)- Stem-h model

```fortran
      PROGRAM MAIN
      IMPLICIT REAL*8 (A-H,O-Z)
      PARAMETER (nxo = 1, nyo = 1)
      PARAMETER (no = nxo*nyo)
      COMMON/isize/nx,ny
      COMMON/VSTEP/N_vstp,N_vstpf
      COMMON/paramV/V_min,V_max,dv_inv,V_minf,V_maxf,dv_invf
      COMMON/membcap/cap,couplef,funch
      COMMON/TIME/t,dt
      COMMON/TBLytau/xy_inf(1:300,1:7),tau(1:300,1:7),xX_i(1:300),
     1 xI_k1(1:300)
      COMMON/TBLdytau/dxy_inf(1:300,1:7),dtau(1:300,1:7),dxX_i(1:300),
     1 dxI_k1(1:300)
      COMMON/itime/in,io
      COMMON/Iions/xI_X1, xI_Na, xxI_k1
      DIMENSION gate(1:7,1:no)!1=x,2=m,3=h,4=j,5=d,6=f,
      DIMENSION gate_inf(1:7,1:no)1=x_inf,2=m_inf,3=h_inf,4=j_inf,5=d_inf,6=f_inf
      DIMENSION tau_g(1:7,1:no)!1=tau_x,2=tau_m,3=tau_h,4=tau_j,5=tau_d,6=tau_f
      DIMENSION X_i(1:no)!,xK1_inf(1:n),xKp(1:n)
      DIMENSION c_Cai(1:no)
      DIMENSION Vm(1:no,1:2)    ! 2: i_new,i_old
      DIMENSION xI_ion(1:no,1:2),xI_si(1:no,1:2) ! 2:i_new,i_old
      DIMENSION xIext(1:no)
      COMMON/TBLytauf/gbar(1:30,1:3),tauf(1:30,1:3)
      COMMON/TBLdytauf/dgbar(1:30,1:3),dtauf(1:30,1:3)
      DIMENSION xI_fun(1:no)
      DIMENSION gatef(1:3,1:no)
      DIMENSION taug(1:3,1:no)
      DIMENSION Vmf(1:no,1:2)
      integer ntotal,i_time,nsave

      n = no
      nx = nxo
      ny = nyo

      V_min = -200.d0
      V_max =  190.d0
      N_vstp = 300

      V_minf = -160.d0
      V_maxf =  100.d0
      N_vstpf = 53
```

```
      OPEN(8,file='ctrl.dat',status='old')
      READ(8,*)tinit, dt, ntotal, nsave

      OPEN(10,file='myo.dat')
      OPEN(11,file='stem.dat')

      cap = 95.d0   !pF

      t = tinit

! make a table of constants
      CALL TABLE()
      CALL TBLCST()

! initialization
      in = 1
      io = 2

      CALL INITIAL(Vmf,gatef)
      CALL funnyC(Vmf,xI_fun,gatef)

      CALL INIT(Vm,gate,c_Cai)
      CALL CURRENT(Vm,xI_ion,xI_si,gate,X_i,c_Cai,xIext)
      in = 3 - in
      io = 3 - io

      CALL INITIAL(Vmf,gatef)
      CALL funnyC(Vmf,xI_fun,gatef)

      CALL INIT(Vm,gate,c_Cai)
      CALL CURRENT(Vm,xI_ion,xI_si,gate,X_i,c_Cai,xIext)
      in = 3 - in
      io = 3 - io

      do  i_time = 1, ntotal

c      ------------- when n=0  --------------
        if (i_time.lt. ntotal/6) then
 do k=1,nx*ny
           if(Vm(k,in).lt.0.d0)then
             xIext(k) = 0.0d0 ! to add electric current
           else
             xIext(k) = 0.d0
           endif
        enddo
        couplef=100. !number of gap junction channels per cell
        funch= 100000.  !number of pacemaker current channels per cell
```

```
            if(mod(i_time,nsave).eq.0)then
               do k=1,1
                 WRITE(10,'(2e14.4)')t, Vm(k,in)
                 WRITE(11,'(2e14.4)')t, Vmf(k,in)
               enddo
            endif


c       ------------ when n=couplef  --------------

        ELSE
 do k=1,nx*ny
            if(Vm(k,in).lt.0.d0)then
               xIext(k) = 0.d0
            else
               xIext(k) = 0.d0
            endif
          enddo

          couplef= 100.
          funch= 100000.

        CALL CNST_V(Vm,gate_inf,tau_g,X_i) !tau & gate_inf at n+1/2 timestep
        CALL UPDTGV(gate,gate_inf,tau_g) !integration of gating variables
        CALL CONC_Ca(c_Cai,xI_si) !integration of calcium
        CALL UPDTV(Vm,Vmf, xI_ion) ! integration of potential
        CALL CURRENT(Vm,xI_ion,xI_si,gate,X_i,c_Cai,xIext)!update of currents

        CALL INTERPOL(Vmf,g_inf,taug) !tau & g_inf at n+1/2 timestep
        CALL UP_G(gatef,g_inf,taug) !integration of gating variables
        CALL UP_V(Vmf,Vm,xI_fun) ! integration of potential
        CALL funnyC(Vmf,xI_fun,gatef)!,xIext)!update of Current

        if(mod(i_time,nsave).eq.0)then
            do k=1,1
               WRITE(10,'(2e14.4)')t,Vm(k,in)
               WRITE(11,'(2e14.4)')t,Vmf(k,in)
            enddo
        endif
           in = 3 - in
           io = 3 - io


         endif
          t=t+dt
        ENDDO !time integration

        CLOSE(10)
```

```
        CLOSE(11)


        end program

**********************************************************************
        SUBROUTINE TABLE()
        IMPLICIT REAL*8 (A-H, O-Z)
        COMMON/VSTEP/N_vstp,N_vstpf
        COMMON/isize/nx,ny
        COMMON/paramV/V_min, V_max, dv_inv,V_minf,V_maxf,dv_invf
        COMMON/TBLytauf/gbar(1:30,1:3),tauf(1:30,1:3)
        COMMON/TBLdytauf/dgbar(1:30,1:3),dtauf(1:30,1:3) !,dxI_f(1:30)

        dvf = (V_maxf - V_minf)/float(N_vstpf-1)
        dv_invf = 1.d0/dvf

c*      open(80,file='tau1_04.dat',status='old')
c*      do l=1,14
c*      read(80,*)thing,tauf(l,1)
c*      enddo
c*      close(80)


c*      open(81,file='g1_04.dat',status='old')
c*      do l=1,14
c*      read(81,*)thing,gbar(l,1)
c*      enddo
c*      close(81)


        open(82,file='tau2_HCN2-2005.dat',status='old')
        do l=1,53
        read(82,*)thing,tauf(l,2)
        enddo
        close(82)

        open(83,file='g2_HCN2-2005.dat',status='old')
        do l=1,53
        read(83,*)thing,gbar(l,2)
        enddo
        close(83)

***     calculate difference
        do 40 i = 1, N_vstpf -1
 do 30 j = 2,2 !1, 2

            dtauf(i,j) = tauf(i+1, j) - tauf(i, j)
            dgbar(i,j) = gbar(i+1, j) - gbar(i, j)
```

```
30       continue
40    continue

      end

******************************************************************

      SUBROUTINE TBLCST()
      IMPLICIT REAL*8 (A-H, O-Z)
      COMMON/VSTEP/N_vstp,N_vstpf
      COMMON/paramV/V_min, V_max, dv_inv,V_minf,V_maxf,dv_invf
      COMMON/TBLytau/xy_inf(1:300,1:7),tau(1:300,1:7),xX_i(1:300),
    1 xI_k1(1:300)
      COMMON/TBLdytau/dxy_inf(1:300,1:7),dtau(1:300,1:7),dxX_i(1:300),
    1 dxI_k1(1:300)

      dv = (V_max - V_min)/float(N_vstp)
      dv_inv = 1.d0/dv

      do 10 i = 1, N_vstp
      v = dble(i)*dv + V_min
*****  X1
      c1 = 0.0005d0
      c2 = 0.083d0
      c3 = 50.d0
      c4 = 0.0d0
      c5 = 0.0d0
      c6 = 0.057d0
      c7 = 1.d0

      a = alpbeta(v,c1,c2,c3,c4,c5,c6,c7)

      c1 = 0.0013d0
      c2 = -0.06d0
      c3 = 20.d0
      c4 = 0.0d0
      c5 = 0.0d0
      c6 = -0.04d0
      c7 = 1.0d0

      b = alpbeta(v,c1,c2,c3,c4,c5,c6,c7)

      tau(i,1) = 1.d0/(a + b)

      xy_inf(i,1) = a/(a + b)

      xX_i(i) = 0.8d0*(dexp(0.04d0*(v + 77.d0)) - 1.d0)
    1          /dexp(0.04d0*(v + 35.d0))
```

```
***** Parameters of Sodium current
*****  m
      c1 = 0.0d0
      c2 = 0.0d0
      c3 = 47.d0
      c4 = -1.0d0
      c5 = 47.d0
      c6 = -0.1d0
      c7 = -1.0d0

      a = alpbeta(v,c1,c2,c3,c4,c5,c6,c7)

      c1 = 40.d0
      c2 = -0.056d0
      c3 = 72.d0
      c4 = 0.d0
      c5 = 0.d0
      c6 = 0.d0
      c7 = 0.d0

      b = alpbeta(v,c1,c2,c3,c4,c5,c6,c7)

      tau(i,2) = 1.d0/(a + b)

      xy_inf(i,2) = a/(a + b)

***** h
      c1 = 0.126d0
      c2 = -0.25d0
      c3 = 77.d0
      c4 = 0.d0
      c5 = 0.d0
      c6 = 0.d0
      c7 = 0.d0

      a = alpbeta(v,c1,c2,c3,c4,c5,c6,c7)

      c1 = 1.7d0
      c2 = 0.d0
      c3 = 22.5d0
      c4 = 0.d0
      c5 = 0.d0
      c6 = -0.082d0
      c7 = 1.d0

      b = alpbeta(v,c1,c2,c3,c4,c5,c6,c7)
```

```
      tau(i,3) = 1.d0/(a + b)

      xy_inf(i,3) = a/(a + b)

***** j
      c1 = 0.055d0
      c2 = -0.25d0
      c3 = 78.d0
      c4 = 0.d0
      c5 = 0.d0
      c6 = -0.2d0
      c7 = 1.d0

      a = alpbeta(v,c1,c2,c3,c4,c5,c6,c7)

      c1 = 0.3d0
      c2 = 0.0d0
      c3 = 32.d0
      c4 = 0.d0
      c5 = 0.d0
      c6 = -0.1d0
      c7 = 1.d0

      b = alpbeta(v,c1,c2,c3,c4,c5,c6,c7)

      tau(i,4) = 1.d0/(a + b)

      xy_inf(i,4) = a/(a + b)

***** d
      c1 = 0.095d0
      c2 = -0.01d0
      c3 = -5.d0
      c4 = 0.d0
      c5 = 0.d0
      c6 = -0.072d0
      c7 = 1.d0

      a = alpbeta(v,c1,c2,c3,c4,c5,c6,c7)

      c1 = 0.07d0
      c2 = -0.017d0
      c3 = 44.d0
      c4 = 0.d0
      c5 = 0.d0
      c6 = 0.05d0
      c7 = 1.d0
```

```fortran
      b = alpbeta(v,c1,c2,c3,c4,c5,c6,c7)

      tau(i,5) = 1.d0/(a + b)

      xy_inf(i,5) = a/(a + b)

***** f
      c1 = 0.012d0
      c2 = -0.008d0
      c3 = 28.d0
      c4 = 0.d0
      c5 = 0.d0
      c6 = 0.15d0
      c7 = 1.d0

      a = alpbeta(v,c1,c2,c3,c4,c5,c6,c7)

      c1 = 0.0065d0
      c2 = -0.02d0
      c3 = 30.d0
      c4 = 0.d0
      c5 = 0.d0
      c6 = -0.2d0
      c7 = 1.d0

      b = alpbeta(v,c1,c2,c3,c4,c5,c6,c7)

      tau(i,6) = 1.d0/(a + b)

      xy_inf(i,6) = a/(a + b)

**********
      a_K1 = 4.d0*(dexp(0.04d0*(v + 85.d0)) - 1.d0)
     1       /(dexp(0.08d0*(v + 53.d0))+exp(0.04d0*(v + 53.d0)))
      b_K1 = 0.2d0*(v + 23.d0)/(1.d0 - exp(-0.04d0*(v+23.d0)))
      xI_k1(i) = 0.35d0*(a_K1 + b_K1)
C      write(18,'(2e16.8)')V_min + dv*dble(i),xI_k1(i)
 10   continue

***   calculate difference

      do 20 i = 1, N_vstp -1
         do 30 j = 1, 6
            dtau(i,j) = tau(i+1, j) - tau(i, j)
            dxy_inf(i,j) = xy_inf(i+1, j) - xy_inf(i, j)
 30      continue
         dxX_i(i) = xX_i(i+1) - xX_i(i)
         dxI_k1(i) = xI_k1(i+1) - xI_k1(i)
```

```
 20    continue

       end

*******************************************************************

       REAL*8 FUNCTION alpbeta(v,c1,c2,c3,c4,c5,c6,c7)
       IMPLICIT REAL*8 (A-H, O-Z)

       x = c1*dexp(c2*(v + c3)) + c4*(v + c5)
       y = dexp(c6*(v + c3)) + c7

       alpbeta = x/y

       return
       end



*******************************************************************

       SUBROUTINE INTERPOL(Vmf,g_inf,taug)
       IMPLICIT REAL*8 (A-H, O-Z)
       COMMON/isize/nx,ny
       COMMON/paramV/V_min, V_max, dv_inv,V_minf,V_maxf,dv_invf
       COMMON/TBLytauf/gbar(1:30,1:3),tauf(1:30,1:3)
       COMMON/TBLdytauf/dgbar(1:30,1:3),dtauf(1:30,1:3)
       COMMON/itime/in,io
       DIMENSION g_inf(1:3,1:nx*ny)
       DIMENSION taug(1:3,1:nx*ny)
       DIMENSION Vmf(1:nx*ny,1:2)


c*     do k=1,nx*ny

c*         v_extrap=( 3.d0*Vmf(k,io)-Vmf(k,in) )/2.d0
c*         v_extrap=v_extrap - 20.d0
c*         i = int( (v_extrap-V_minf)*dv_invf ) + 1
c*         di = (v_extrap-V_minf)*dv_invf +1.d0- dble(i)

c*         g_inf(1,k) = gbar(i,1) + di*dgbar(i,1)
c*         taug(1,k)  = tauf(i,1) + di*dtauf(i,1)
c*     enddo
       do k=1,nx*ny
          v_extrap=( 3.d0*Vmf(k,io)-Vmf(k,in) )/2.d0
          v_extrap=v_extrap - 0.d0
          ih = int( (v_extrap-V_minf)*dv_invf ) + 1
          dih = (v_extrap-V_minf)*dv_invf +1.d0- dble(ih)
```

```fortran
        g_inf(2,k) = gbar(ih,2) + dih*dgbar(ih,2)
        taug(2,k)  = tauf(ih,2) + dih*dtauf(ih,2)

    enddo

    end

*******************************************************************
    SUBROUTINE CNST_V(Vm,gate_inf,tau_g,X_i)
    IMPLICIT REAL*8 (A-H, O-Z)
    COMMON/isize/nx,ny
    COMMON/paramV/V_min, V_max, dv_inv,V_minf,V_maxf,dv_invf
    COMMON/TBLytau/xy_inf(1:300,1:7),tau(1:300,1:7),xX_i(1:300),
   1 xI_k1(1:300)
    COMMON/TBLdytau/dxy_inf(1:300,1:7),dtau(1:300,1:7),dxX_i(1:300),
   1 dxI_k1(1:300)
    COMMON/itime/in,io
    DIMENSION gate_inf(1:7,1:nx*ny)
    DIMENSION tau_g(1:7,1:nx*ny)
    DIMENSION Vm(1:nx*ny,1:2)

  do k=1,nx*ny
            v_extrap=(3.d0*Vm(k,io)-Vm(k,in))/2.d0
            i = int( (v_extrap-V_min)*dv_inv )
            di = (v_extrap-V_min)*dv_inv - dble(i)

         do j = 1,6  !this loop i-index is for 6 gates
            gate_inf(j,k) = xy_inf(i,j) + di*dxy_inf(i,j)
            tau_g(j,k)  = tau(i,j) + di*dtau(i,j)
         enddo

      enddo

    end

*******************************************************************

    SUBROUTINE UP_G(gatef,g_inf,taug)
    IMPLICIT REAL*8 (A-H, O-Z)
    COMMON/isize/nx,ny
    COMMON/TIME/t,dt
    COMMON/itime/in,io
    DIMENSION gatef(1:3,1:nx*ny)
    DIMENSION g_inf(1:3,1:nx*ny)
    DIMENSION taug(1:3,1:nx*ny)
    DIMENSION tauf(1:30,1:3),gbar(1:30,1:3)

    dtinv = 1.d0/dt
```

```
      do k=1,nx*ny
        do i = 2,2 !1, 2
       gatef(i,k)=( gatef(i,k)*(dtinv - 1.d0/(2.d0*taug(i,k)) )
     1  + ( g_inf(i,k))/(taug(i,k)) )
     1      /( dtinv+1.d0/(2.d0*taug(i,k)) )
        enddo
      enddo

      end


*********************************************************************

      SUBROUTINE UPDTGV(gate,gate_inf,tau_g)
      IMPLICIT REAL*8 (A-H, O-Z)
      COMMON/isize/nx,ny
      COMMON/TIME/t,dt
      COMMON/itime/in,io
      DIMENSION gate(1:7,1:nx*ny)
c       1=x, 2=m, 3=h, 4=j, 5=d,6=f,7=e
      DIMENSION gate_inf(1:7,1:nx*ny)
c       1=x_inf,2=m_inf,3=h_inf,4=j_inf,5=d_inf, 6=f_inf
      DIMENSION tau_g(1:7,1:nx*ny)
c      1=tau_x,2=tau_m,3=tau_h,4=tau_j,5=tau_d,6=tau_f
      DIMENSION tau_E(1:30),g_E(1:30),alpha_E(1:30)

      dtinv = 1.d0/dt

      do k=1,nx*ny

       do i = 1, 1

         gate(i,k)=( gate(i,k)*(dtinv - 1.d0/(2.d0*tau_g(i,k)) )
     1  +(gate_inf(i,k))/(tau_g(i,k)))/( dtinv+1.d0/(2.d0*tau_g(i,k)) )

       enddo

***adiabatic elimination of variable m
      gate(2,k)=gate_inf(2,k)

       do i = 3, 7
       gate(i,k)=( gate(i,k)*(dtinv - 1.d0/(2.d0*tau_g(i,k)) )
     1  + (gate_inf(i,k))/(tau_g(i,k)) )
     1      /( dtinv+1.d0/(2.d0*tau_g(i,k)) )
        enddo

      enddo
```

```fortran
      end

**********************************************************************
      SUBROUTINE funnyC(Vmf,xI_fun,gatef)
      IMPLICIT REAL*8 (A-H, O-Z)
      COMMON/isize/nx,ny
      COMMON/paramV/V_min, V_max, dv_inv,V_minf,V_maxf,dv_invf
      COMMON/TBLytauf/gbar(1:30,1:3),tauf(1:30,1:3)
      COMMON/TBLdytauf/dgbar(1:30,1:3),dtauf(1:30,1:3)
      COMMON/itime/in,io
      DIMENSION xI_fun(1:nx*ny)
      DIMENSION Vmf(1:nx*ny,1:2)
      DIMENSION gatef(1:3,1:nx*ny)
      DIMENSION g_inf(1:3,1:nx*ny)

      do k=1,nx*ny
       xI_fun(k) = 0.6363*gatef(2,k)*( Vmf(k,in)+40.d0 )
      enddo

      end
**********************************************************************
      SUBROUTINE CURRENT(Vm,xI_ion,xI_si,gate,X_i,c_Cai,xIext)
      IMPLICIT REAL*8 (A-H, O-Z)
      COMMON/isize/nx,ny
      COMMON/paramV/V_min, V_max,dv_inv,V_minf,V_maxf,dv_invf
      COMMON/TBLytau/xy_inf(1:300,1:7),tau(1:300,1:7),xX_i(1:300),
     1 xI_k1(1:300)
      COMMON/TBLdytau/dxy_inf(1:300,1:7),dtau(1:300,1:7),dxX_i(1:300),
     1 dxI_k1(1:300)
      COMMON/itime/in,io
      COMMON/Iions/xI_X1, xI_Na, xxI_k1
      DIMENSION Vm(1:nx*ny,2)
      DIMENSION gate(1:7,1:nx*ny)!1=x, 2=m, 3=h,4=j,5=d,6=f,7=e
      DIMENSION xI_ion(1:nx*ny,1:2), xI_si(1:nx*ny,1:2)
      DIMENSION X_i(1:nx*ny)!,xI_f(1:300),xI_fun(1:300)
      DIMENSION c_Cai(1:nx*ny)
      DIMENSION tau_E(1:30),g_E(1:30),alpha_E(1:30)
      DIMENSION xIext(1:nx*ny)

      do k=1,nx*ny

      iv = int((Vm(k,in) - V_min)*dv_inv)
      div = (Vm(k,in) - V_min)*dv_inv - dble(iv)

      X_i(k) = xX_i(iv)  + div*dxX_i(iv)
      xI_X1 = gate(1,k)*X_i(k)

      xI_Na = (4.0d0*gate(2,k)*gate(2,k)*gate(2,k)*gate(3,k)
```

```
1      *gate(4,k)+ 0.003d0 )*(Vm(k,in) - 50.d0)

 xI_si(k,in)=0.09d0*gate(5,k)*gate(6,k)
1          *(Vm(k,in) + 82.3d0 + 13.0287d0*dlog(c_Cai(k)))


 xxI_k1  = 0.233* ( xI_k1(iv)  + div*dxI_k1(iv) )

 xI_ion(k,in) = xI_X1 + xI_Na + xI_si(k,in) + xxI_k1 + xIext(k)

 enddo

 end


***************************************************************

      SUBROUTINE UP_V(Vmf ,Vm ,xI_fun)
      IMPLICIT REAL*8 (A-H, O-Z)
      COMMON/isize/nx,ny
      COMMON/membcap/cap,couplef,funch
      COMMON/TIME/t,dt
      COMMON/itime/in,io
      DIMENSION xI_fun(1:nx*ny)
      DIMENSION Vm(1:nx*ny,2)
      DIMENSION Vmf(1:nx*ny,2)

 c1 = dt*0.5d0/cap
 c2 = dt*0.5d0/cap

  do k=1,nx*ny

 Vmf(k,in)=Vmf(k,io)-2.d0*funch*0.001*xI_fun(k)*c1!.001 make N correct
1+c2*couplef*50*0.001
1 *((3.d0*Vm(k,io)-Vm(k,in)-(3.d0*Vmf(k,io)-Vmf(k,in))))

  enddo
 end


***************************************************************
      SUBROUTINE UPDTV(Vm, Vmf ,xI_ion)
      IMPLICIT REAL*8 (A-H, O-Z)
      COMMON/isize/nx,ny
      COMMON/membcap/cap,couplef,funch
      COMMON/TIME/t,dt
      COMMON/itime/in,io
      DIMENSION xI_ion(1:nx*ny,1:2)
      DIMENSION Vm(1:nx*ny,2)
      DIMENSION Vmf(1:nx*ny,2)
```

```fortran
      c1 = dt*0.5d0/1
      c2 = dt*0.5d0/cap

      do iy = 1, ny
      do ix = 1, nx

      k = (iy - 1)*nx + ix

      Vm(k,in) = Vm(k,io) - ( 3.d0*xI_ion(k,io)- xI_ion(k,in) )*c1
     1 + c2*couplef*50*0.001
     1 *( Vmf(k,in)+Vmf(k,io) - (3.d0*Vm(k,io)-Vm(k,in))  )

      enddo
      enddo

      end

************************************************************
      SUBROUTINE CONC_Ca(c_Cai,xI_si)
      IMPLICIT REAL*8 (A-H, O-Z)
      COMMON/isize/nx,ny
      COMMON/TIME/t,dt
      COMMON/itime/in,io
      DIMENSION xI_si(1:nx*ny,1:2)
      DIMENSION c_Cai(1:nx*ny)

       do k=1,nx*ny

      c_Cai(k) = 1.E-7 + ( (c_Cai(k) - 1.E-7)*(1.d0/dt - .035d0)
     1  - (.5E-7)*(3.d0*xI_si(k,io)-xI_si(k,in) ) )/(1.d0/dt+0.035d0)

       enddo

      end

************************************************************
      SUBROUTINE INITIAL(Vmf,gatef)
      IMPLICIT REAL*8 (A-H, O-Z)
      COMMON/isize/nx,ny
      COMMON/itime/in,io
      COMMON/paramV/V_min,V_max,dv_inv,V_minf,V_maxf,dv_invf
      COMMON/TBLytauf/gbar(1:30,1:3),tauf(1:30,1:3)
      COMMON/TBLdytauf/dgbar(1:30,1:3),dtauf(1:30,1:3)
      DIMENSION Vmf(1:nx*ny,1:2)
      DIMENSION gatef(1:3,1:nx*ny)
      DIMENSION taug(1:3,1:nx*ny)
```

```
      do k =1 ,nx*ny
       Vmf(k,in) = -40.d0
      enddo

c*      do k=1,nx*ny

c*          v_extrap=( 3.d0*Vmf(k,io)-Vmf(k,in) )/2.d0
c*          v_extrap=v_extrap - 20.d0
c*          i = int( (v_extrap-V_minf)*dv_invf ) + 1
c*          di = (v_extrap-V_minf)*dv_invf +1.d0- dble(i)

c*          gatef(1,k) = gbar(i,1) + di*dgbar(i,1)
c*          taug(1,k)  = tauf(i,1) + di*dtauf(i,1)
c*      enddo

      do k=1,nx*ny
          v_extrap=( 3.d0*Vmf(k,io)-Vmf(k,in) )/2.d0
          v_extrap=v_extrap - 0.d0
          ih = int( (v_extrap-V_minf)*dv_invf ) + 1
          dih = (v_extrap-V_minf)*dv_invf +1.d0- dble(ih)

          gatef(2,k) = gbar(ih,2) + dih*dgbar(ih,2)
          taug(2,k)  = tauf(ih,2) + dih*dtauf(ih,2)

      enddo

      end
**********************************************************************
      SUBROUTINE INIT(Vm,gate,c_Cai)
      IMPLICIT REAL*8 (A-H, O-Z)
      COMMON/isize/nx,ny
      COMMON/itime/in,io
      DIMENSION Vm(1:nx*ny,1:2)
      DIMENSION gate(1:7,1:nx*ny)!1=x,2=m,3=h,4=j,5=d,6=f,7=e
      DIMENSION c_Cai(1:nx*ny)

      do iy = 1, ny
      do ix = 1, nx
      k = (iy - 1)*nx + ix

      gate(1,k) = 0.42327701E-02
      gate(2,k) = 0.69985649E-02
      gate(3,k) = 0.99600418E+00
      gate(4,k) = 0.98634352E+00
      gate(5,k) = 0.22258681E-02
      gate(6,k) = 0.99999019E+00
      gate(7,k) = 1.50000000E+00
      c_Cai(k) = 0.15998270E-06
```

```
      Vm(k,in) = -0.76E+02
      enddo
      enddo
      end


**********************************************************
      SUBROUTINE SAVEDT(Vm,Vmf,gate,gatef,c_Cai,xI_si)
      IMPLICIT REAL*8 (A-H,O-Z)
      COMMON/TIME/t,dt
      COMMON/itime/in,io
      COMMON/isize/nx,ny
      COMMON/TBLytau/xy_inf(1:300,1:7),tau(1:300,1:7),xX_i(1:300),
    1 xI_k1(1:300)
      COMMON/Iions/xI_X1, xI_Na, xxI_k1
      COMMON/membcap/cap,couplef,funch
      DIMENSION Vm(1:nx*ny,1:2),c_Cai(nx*ny)
      DIMENSION gate(1:7,1:nx*ny)
      DIMENSION xI_ion(1:nx*ny,1:2)
      DIMENSION Vmf(1:nx*ny,1:2)
      DIMENSION gatef(1:3,1:nx*ny)
      DIMENSION xI_fun(1:nx*ny)

      DO k=1,nx*ny
       write(10,'(2e14.4)')t,Vm(k,in)
       write(11,'(2e14.4)')t,Vmf(k,in)
      ENDDO
      end
```

1 dimension : stem cells connected to myocytes as pacemaker in a fiber -Stem h model

```fortran
      PROGRAM MAIN
      implicit real*8 (a-h,o-z)
      PARAMETER (n_xo = 1, n_yo = 1)
      PARAMETER (no = n_xo*n_yo)
      COMMON/isize/n_x,n_y
      COMMON/VSTEP/N_vstpf
      COMMON/paramV/V_minf,V_maxf,dv_invf
      COMMON/membcap/cap,couplef,funch
      COMMON/TIME/t,dt
      COMMON/itime/in,io
      COMMON/TBLytauf/gbar(1:30,1:3),tauf(1:30,1:3)
      COMMON/TBLdytauf/dgbar(1:30,1:3),dtauf(1:30,1:3)
      DIMENSION xI_fun(1:no)
      DIMENSION gatef(1:3,1:no)
      DIMENSION taug(1:3,1:no)
      DIMENSION Vmf(1:no,1:2)

      parameter (nt=18000, vmin=-100,vmax=80,dvt=0.01)
      parameter (nx=201) !inifintely long fiber=201 myo*.1mm(dx)=20.1mm
c    these are the 8 variables for BR
      real x1,m,h,j,d,f,u,ca
   real u_old
      real ut
c       temporal voltage used to update voltage after laplacian been calculated
c    these are the alphas and betas
      real ax1,am,ah,aj,ad,af
      real bx1,bm,bh,bj,bd,bf
      real ik1,ix1,ina,is,es,gix1
      real ik1t
      real Iext,Iextt   !external current
      dimension ax1t(0:nt),bx1t(0:nt),amt(0:nt),bmt(0:nt)
      dimension aht(0:nt),bht(0:nt),ajt(0:nt),bjt(0:nt)
      dimension adt(0:nt),bdt(0:nt),aft(0:nt),bft(0:nt)
      dimension ik1t(0:nt),gix1t(0:nt)
      dimension u(0:nx+1),x1(nx),m(nx),h(nx),j(nx),d(nx)
   dimension u_old(0:nx+1)
      dimension f(nx),ca(nx),ut(nx)

        gna=4.0
        gnac=0.003
        ena=50
        gs=0.09

c------- delta t and delta x
        dt=0.02
```

```
      t=0
      dx=0.01 !dx --->0.1mm
      dx2=dx*dx
      Dlap=0.001

   open(15,status='unknown',name='stem.dat')
   open(16,status='unknown',name='myo.dat')

  n = no
  n_x = n_xo
  n_y = n_yo

  V_minf = -160.d0
  V_maxf =  100.d0
  N_vstpf = 53

  cap = 95.d0

  couplef = 100.   !number of gap junction channels per cell
  funch = 100000. !number of pacemaker current channels per cell

! make a table of constants
      CALL TABLE()
! initialization for stem values
      in = 1
      io = 2

      CALL INITIAL(Vmf,gatef)
      CALL funnyC(Vmf,xI_fun,gatef)

      in = 3 - in
      io = 3 - io

      CALL INITIAL(Vmf,gatef)
      CALL funnyC(Vmf,xI_fun,gatef)

      in = 3 - in
      io = 3 - io

c--------------- Initial Conditions (rest state for myocyte) ---------
      do i=0,nx+1
      u(i)=-84.5737
      u_old(i)=-84.5737
      ut(i)=u(i)
      enddo
      do i=1,nx
      ca(i)=0.0000001
      ax1=0.0005*exp(0.083*(u(i)+50))/(exp(0.057*(u(i)+50))+1.0)
```

```fortran
      bx1=0.0013*exp(-0.06*(u(i)+20))/(exp(-0.04*(u(i)+20))+1.0)

      am=-(u(i)+47)/(exp(-0.1*(u(i)+47))-1.0)
      bm=40*exp(-0.056*(u(i)+72))

      ah=0.126*exp(-0.25*(u(i)+77))
      bh=1.7/(exp(-0.082*(u(i)+22.5))+1.0)

      aj=0.055*exp(-0.25*(u(i)+78))/(exp(-0.2*(u(i)+78))+1.0)
      bj=0.3/(exp(-0.1*(u(i)+32))+1.0)

      ad=0.095*exp(-0.01*(u(i)-5))/(exp(-0.072*(u(i)-5))+1.0)
      bd=0.07*exp(-0.017*(u(i)+44))/(exp(0.05*(u(i)+44))+1.0)

      af=0.012*exp(-0.008*(u(i)+28))/(exp(0.15*(u(i)+28))+1.0)
      bf=0.0065*exp(-0.02*(u(i)+30))/(exp(-0.2*(u(i)+30))+1.0)

      x1(i)=ax1/(ax1+bx1)
      m(i)= am/(am+bm)
      h(i)= ah/(ah+bh)
      j(i)= aj/(aj+bj)
      d(i)= ad/(ad+bd)
      f(i)= af/(af+bf)
      enddo

c------------tables----------------
c   instead of using exponentials as above for  ax1, bx1, am, bm etc..
c   we tabulate their values for a range of voltage between -100 and 80
      do n=0,nt
      uu=vmin+n*dvt
      ax1t(n)=0.0005*exp(0.083*(uu+50))/(exp(0.057*(uu+50))+1.0)
      bx1t(n)=0.0013*exp(-0.06*(uu+20))/(exp(-0.04*(uu+20))+1.0)
      if(n.eq.5300)then
      amt(n)=10.
      else
      amt(n)=-(uu+47)/(exp(-0.1*(uu+47))-1.0)
      endif
      bmt(n)=40*exp(-0.056*(uu+72))

      aht(n)=0.126*exp(-0.25*(uu+77))
      bht(n)=1.7/(exp(-0.082*(uu+22.5))+1.0)

      ajt(n)=0.055*exp(-0.25*(uu+78))/(exp(-0.2*(uu+78))+1.0)
      bjt(n)=0.3/(exp(-0.1*(uu+32))+1.0)

      adt(n)=0.095*exp(-0.01*(uu-5))/(exp(-0.072*(uu-5))+1.0)
      bdt(n)=0.07*exp(-0.017*(uu+44))/(exp(0.05*(uu+44))+1.0)
```

```fortran
      aft(n)=0.012*exp(-0.008*(uu+28))/(exp(0.15*(uu+28))+1.0)
      bft(n)=0.0065*exp(-0.02*(uu+30))/(exp(-0.2*(uu+30))+1.0)

      if(n.eq.7700)then
      ik1t(n)=2.8178
      else
       ik1t(n)=0.35*0.233  !0.233 is level of IK1 expression
     &   *(4.0*(exp(0.04*(uu+85))-1.0)/(exp(0.08*(uu+53))
     &   +exp(0.04*(uu+53)))+0.2*(uu+23)/(1.0-exp(-0.04*(uu+23))))
      endif
       gix1t(n)=0.8*(exp(0.04*(uu+77))-1.0)/exp(0.04*(uu+35))

      enddo
      Iextt=-30   ! external current to produce AP
c---------------------------------------------------
c          time integration (for 5.0 sec)
c---------------------------------------------------
        do mt=0,5000     !this doloop makes 5.0 sec
         Iext= 0.

         do l=0,49     ! this doloop makes 1ms

c--------- updating boundary conditions for zero flux
        u(0)=u(2)
        u(nx+1)=u(nx-1)
c---------integration in space
      do i=1,nx

      CALL INTERPOL(Vmf,g_inf,taug) !tau & g_inf at n+1/2 timestep
      CALL UP_G(gatef,g_inf,taug) !integration of gating variables

      c1 = (dt*0.5d0)/cap

       do k=1,n_x*n_y

        Vmf(k,in) = Vmf(k,io) -2.d0*funch*0.001*0.63*gatef(2,k)*(Vmf(k,in)+40.d0)
     1 *c1+c1*couplef*50*0.001*( 3.*u_old(i)-u(i)-(3.*Vmf(k,io)-Vmf(k,in)) )

       enddo

      CALL funnyC(Vmf,xI_fun,gatef) !update Current

        ntab=nint((u(i)-vmin)/dvt)

        ik1=ik1t(ntab)
        gix1=gix1t(ntab)

c---------calculating the alphas and betas using the tabulated values--
```

```fortran
      ax1=ax1t(ntab)
      bx1=bx1t(ntab)

      am=amt(ntab)
      bm=bmt(ntab)

      ah=aht(ntab)
      bh=bht(ntab)

      aj=ajt(ntab)
      bj=bjt(ntab)

      ad=adt(ntab)
      bd=bdt(ntab)

      af=aft(ntab)
      bf=bft(ntab)
c---------updating the gates-----------
      x1(i)=x1(i)+dt*(ax1*(1.0-x1(i))-bx1*x1(i))
      m(i)= m(i)+dt*(am*(1.0-m(i))-bm*m(i))
      h(i)= h(i)+dt*(ah*(1.0-h(i))-bh*h(i))
      j(i)= j(i)+dt*(aj*(1.0-j(i))-bj*j(i))
      d(i)= d(i)+dt*(ad*(1.0-d(i))-bd*d(i))
      f(i)= f(i)+dt*(af*(1.0-f(i))-bf*f(i))
c----------updating the currents-----------
       es=-82.3-13.0287*log(ca(i))
       ix1=gix1*x1(i)
       ina=(gna*m(i)*m(i)*m(i)*h(i)*j(i)+gnac)*(u(i)-ena)
       is=gs*d(i)*f(i)*(u(i)-es)
       ca(i)=ca(i)+dt*(-0.0000001*is+0.07*(0.0000001-ca(i)))
c--------updating the voltage to ut
       xlap=u(i+1)+u(i-1)-2.*u(i)

    do p=1,n_x*n_y
    if( (i.gt.79).and.(i.lt.123) )then
       ut(i)=u(i)-dt*(ik1+ix1+ina+is+Iext)+dt*xlap*Dlap/dx2
   1 + dt*(0.5d0/cap)*couplef*50*0.001*
   1 ( Vmf(k,in)+Vmf(k,io) - ( 3.d0*u_old(i)-u(i) ) )
    else
       ut(i)=u(i)-dt*(ik1+ix1+ina+is)+dt*xlap*Dlap/dx2

    endif
    enddo

    enddo
c--------updating u from ut
       do i=1,nx
```

```
      u_old(i)=u(i)
           u(i)=ut(i)
         enddo
c---------updating time
         t=t+dt
         in = 3 - in
         io = 3 - io
         enddo
c--------write values of voltage at point 31 every 5 iterations-----
         if(mod(mt,10).eq.1)write(16,*)t,u(201)
c        if(mod(mt,10).eq.1)write(15,*)t,Vmf(k,in)


         enddo
         end
c------------------end of connected pair program------------------
c-----------------begin stem subroutines----------------------
**********************************************
      SUBROUTINE TABLE()
      IMPLICIT REAL*8 (A-H, O-Z)
      COMMON/VSTEP/N_vstpf
      COMMON/isize/n_x,n_y
      COMMON/paramV/V_minf,V_maxf,dv_invf
      COMMON/TBLytauf/gbar(1:30,1:3),tauf(1:30,1:3)
      COMMON/TBLdytauf/dgbar(1:30,1:3),dtauf(1:30,1:3)

      dvf = (V_maxf - V_minf)/float(N_vstpf-1)
      dv_invf = 1.d0/dvf

c*      open(80,file='tau1_04.dat',status='old')
c       do l=1,14
c       read(80,*)thing,tauf(l,1)
c       enddo
c       close(80)


c       open(81,file='g1_04.dat',status='old')
c       do l=1,14
c       read(81,*)thing,gbar(l,1)
c       enddo
c       close(81)

      open(82,file='tau2_HCN2-2005.dat',status='old')
      do l=1,53
      read(82,*)thing,tauf(l,2)
      enddo
      close(82)

      open(83,file='g2_HCN2-2005.dat',status='old')
      do l=1,53
```

```
      read(83,*)thing,gbar(l,2)
      enddo
      close(83)

***   calculate difference
      do 40 i = 1, N_vstpf -1
 do 30 j = 1, 1!2

          dtauf(i,j) = tauf(i+1, j) - tauf(i, j)
          dgbar(i,j) = gbar(i+1, j) - gbar(i, j)

30        continue
40     continue

       end


*****************************************************************

      SUBROUTINE INTERPOL(Vmf,g_inf,taug)
      IMPLICIT REAL*8 (A-H, O-Z)
      COMMON/isize/n_x,n_y
      COMMON/paramV/V_minf,V_maxf,dv_invf
      COMMON/TBLytauf/gbar(1:30,1:3),tauf(1:30,1:3)
      COMMON/TBLdytauf/dgbar(1:30,1:3),dtauf(1:30,1:3)
      COMMON/itime/in,io
      DIMENSION g_inf(1:3,1:n_x*n_y)
      DIMENSION taug(1:3,1:n_x*n_y)
      DIMENSION Vmf(1:n_x*n_y,1:2)

c     do k=1,n_x*n_y

c         v_extrap=( 3.d0*Vmf(k,io)-Vmf(k,in) )/2.d0
c         v_extrap=v_extrap - 0.d0
c         i = int( (v_extrap-V_minf)*dv_invf ) + 1
c         di = (v_extrap-V_minf)*dv_invf +1.d0- dble(i)

c         g_inf(1,k) = gbar(i,1) + di*dgbar(i,1)
c         taug(1,k)  = tauf(i,1) + di*dtauf(i,1)
c     enddo

      do k=1,n_x*n_y
          v_extrap=( 3.d0*Vmf(k,io)-Vmf(k,in) )/2.d0
          v_extrap=v_extrap - 0.d0
          ih = int( (v_extrap-V_minf)*dv_invf ) + 1
          dih = (v_extrap-V_minf)*dv_invf +1.d0- dble(ih)

          g_inf(2,k) = gbar(ih,2) + dih*dgbar(ih,2)
          taug(2,k)  = tauf(ih,2) + dih*dtauf(ih,2)
```

```
      enddo

      end

*********************************************************************

      SUBROUTINE UP_G(gatef,g_inf,taug)
      IMPLICIT REAL*8 (A-H, O-Z)
      COMMON/isize/n_x,n_y
      COMMON/TIME/t,dt
      COMMON/itime/in,io
      DIMENSION gatef(1:3,1:n_x*n_y)
      DIMENSION g_inf(1:3,1:n_x*n_y)
      DIMENSION taug(1:3,1:n_x*n_y)
      DIMENSION tauf(1:30,1:3),gbar(1:30,1:3)

      dtinv = 1.d0/dt

      do k=1,n_x*n_y
        do i = 1,1 !2
       gatef(i,k)=( gatef(i,k)*(dtinv - 1.d0/(2.d0*taug(i,k)) )
     1  + ( g_inf(i,k))/(taug(i,k)) )
     1     /( dtinv+1.d0/(2.d0*taug(i,k)) )
        enddo
      enddo

      end

*********************************************

      SUBROUTINE funnyC(Vmf,xI_fun,gatef)
      IMPLICIT REAL*8 (A-H, O-Z)
      COMMON/isize/n_x,n_y
      COMMON/paramV/V_minf,V_maxf,dv_invf
      COMMON/TBLytauf/gbar(1:30,1:3),tauf(1:30,1:3)
      COMMON/TBLdytauf/dgbar(1:30,1:3),dtauf(1:30,1:3)
      COMMON/itime/in,io
      DIMENSION xI_fun(1:n_x*n_y)
      DIMENSION Vmf(1:n_x*n_y,1:2)
      DIMENSION gatef(1:3,1:n_x*n_y)
      DIMENSION g_inf(1:3,1:n_x*n_y)

      do k=1,n_x*n_y

       xI_fun(k) = 0.6363*gatef(2,k)*( Vmf(k,in)+40.d0 )
      enddo
```

```
      end

***********************************

      SUBROUTINE INITIAL(Vmf,gatef)
      IMPLICIT REAL*8 (A-H, O-Z)
      COMMON/isize/n_x,n_y
      COMMON/itime/in,io
      COMMON/paramV/V_minf,V_maxf,dv_invf
      COMMON/TBLytauf/gbar(1:30,1:3),tauf(1:30,1:3)
      COMMON/TBLdytauf/dgbar(1:30,1:3),dtauf(1:30,1:3)

      DIMENSION Vmf(1:n_x*n_y,1:2)
      DIMENSION gatef(1:3,1:n_x*n_y)
      DIMENSION taug(1:3,1:n_x*n_y)

      do k =1 ,n_x*n_y
       Vmf(k,in) = -40.d0

      enddo

c      do k=1,n_x*n_y

c          v_extrap=( 3.d0*Vmf(k,io)-Vmf(k,in) )/2.d0
c          v_extrap=v_extrap - 0.d0
c          i = int( (v_extrap-V_minf)*dv_invf ) + 1
c          di = (v_extrap-V_minf)*dv_invf +1.d0- dble(i)

c          gatef(1,k) = gbar(i,1) + di*dgbar(i,1)
c          taug(1,k)  = tauf(i,1) + di*dtauf(i,1)
c      enddo

      do k=1,n_x*n_y
          v_extrap=( 3.d0*Vmf(k,io)-Vmf(k,in) )/2.d0
          v_extrap=v_extrap - 0.d0
          ih = int( (v_extrap-V_minf)*dv_invf ) + 1
          dih = (v_extrap-V_minf)*dv_invf +1.d0- dble(ih)

          gatef(2,k) = gbar(ih,2) + dih*dgbar(ih,2)
          taug(2,k)  = tauf(ih,2) + dih*dtauf(ih,2)

      enddo

      end

***********************************************************
      SUBROUTINE SAVEDT(Vmf,gatef)
      IMPLICIT REAL*8 (A-H,O-Z)
```

```
COMMON/TIME/t,dt
COMMON/itime/in,io
COMMON/isize/n_x,n_y
COMMON/membcap/cap,couplef,funch
DIMENSION Vmf(1:n_x*n_y,1:2)
DIMENSION gatef(1:3,1:n_x*n_y)

do k=1,n_x*n_y

write(10,'(10e14.4)')t,Vmf(k,in)

enddo
end
```

Bibliography

[1] Brown HF, DiFrancesco D, Noble SJ. How does adrenaline accelerate the heart? Nature 280:235-236;1979.

[2] Rosen MR, 15th annual Gordon K. Moe Lecture. Biological pacemaking: in our lifetime? Heart Rhythm. 2005 Apr;2(4):418-28.

[3] Plotnikov AN, Sosunov EA, Qu J, Shlapakova IN, Anyukhovsky EP, Liu L, Janse MJ, Brink PR, Cohen IS, Robinson RB, Danilo P, Rosen MR. Biological Pacemaker Implanted in Canine Left Bundle Branch Provides Ventricular Escape Rhythms That Have Physiologically Acceptable Rates. Circulation. 2004;109:506-512.

[4] Rosen MR,Brink PR, Cohen IS, Robinson RB. Genes, stem cells and biological pacemakers. Cardiovascular Research 64 (2004) 12 23.

[5] Potapova I, Plotnikov A, Lu Z, Danilo P, Jr, Valiunas V, Qu J, Doronin S, Zuckerman J, Shlapakova IN, Gao J, Pan Z, Herron AJ, Robinson RB, Brink PR, Rosen MR, Cohen IS. Human Mesenchymal Stem Cells as a Gene Delivery System to Create Cardiac Pacemakers. Circulation. 2004;94:952-959.

[6] Cohen IS, private commnication, 2. 20. 2005

[7] Valiunas V, Doronin S, Valiuniene L, Potapova I, Zuckerman J, Walcott B, Robinson RB, Rosen MR, Brink PR, Cohen IS. Human mesenchymal stem cells make cardiac connexins and form functional gap junctions. 2004.J Physiol 555.3 pp 617-626.

[8] Ulens C, Tytgat J Functional Heteromerization of HCN1 and HCN2 Pacemaker Channels. The Journal of Biological Chemistry Vol. 276, No. 9, Issue of March 2, pp. 60696072, 2001.

[9] Ulens C, Tytgat J. G_i and G_s-coupled receptors up-regulate the cAMP cascade to modulate HCN2, but not HCN1 pacemaker channels. Eur J Physiol (2001) 442:928942.

[10] Ulens C, Siegelbaum SA. Regulation of hyperpolarization-activated HCN channels by cAMP through a gating switch in binding domain symmetry. Neuron. 2003 Dec 4;40(5):959-70.

[11] Stieber J, Thomer A, Much B, Schneider A, Biel M and Hofmann F. Molecular Basis for the Different Activation Kinetics of the Pacemaker Channels HCN2 and HCN4. J. Biol. Chem., Vol. 278, Issue 36, 33672-33680, September 5, 2003.

[12] Stieber J, Herrmann S, Feil S, Lster J, Feil R, Biel M, Hofmann F, Ludwig A. The hyperpolarization-activated channel HCN4 is required for the generation of pacemaker action potentials in the embryonic heart. Proc Natl Acad Sci U S A. 2003 December 9; 100(25): 1523515240.

[13] Stieber J, Hofmann F, Ludwig A. Pacemaker channels and sinus node arrhythmia. Trends Cardiovasc Med. 2004 Jan;14(1):23-8.

[14] Qu J, Altomare C, Bucchi A, DiFrancesco D, Robinson RB. Functional comparison of HCN isoforms expressed in ventricular and HEK 293 cells. Pflugers Arch. 2002 Aug;444(5):597-601. Epub 2002 Jun 12.

[15] Qu J, Kryukova Y, Potapova IA, Doronin SV, Larsen M, Krishnamurthy G, Cohen IS, Robinson RB. MiRP1 modulates HCN2 channel expression and gating in cardiac myocytes. J Biol Chem. 2004 Oct 15;279(42):43497-502.

[16] Qu J, Barbuti A, Protas L, Santoro B, Cohen IS, Robinson RB. HCN2 Overexpression in Newborn and Adult Ventricular Myocytes Distinct Effects on Gating and Excitability. Circ Res. 2001;89:e8-e14.

[17] Miake J, Marban E, and Nuss HB. Functional role of inward rectifier current in heart probed by Kir2.1 overexpression and dominant-negative suppression. Journal Clin. Invest.111:15291536 (2003).

[18] Miake J, Marban E, H. Bradley Nuss. Biological pacemaker created by gene transfer. Nature. 2002;419:132-133.

[19] Azene EM, Xue T, Marban E, Tomaselli GF, Li RA. Non-equilibrium behavior of HCN channels: Insights into the role of HCN channels in native and engineered pacemakers. Cardiovascular Research. 67 (2): 263-273 AUG 1 2005.

[20] Xue T, Marban E, Li RA. Dominant-negative suppression of HCN1- and HCN2-encoded pacemaker currents by an engineered HCN1 construct - Insights into structure-function relationships and multimerization Circ Res. 90 (12): 1267-1273 JUN 28 2002.

[21] Xue T, Cho HC, Akar FG, Tsang SY, Jones SP, Marban E, Tomaselli GF, Li RA. Functional integration of electrically active cardiac derivatives from genetically engineered human embryonic stem cells with quiescent recipient ventricular cardiomyocytes - Insights into the development of cell-based pacemakers Circ Res. 111 (1): 11-20 JAN 4 2005.

[22] Henrikson CA, Xue T, Dong PH, Sang D, Marban E. Identification of a surface charged residue in the S3-S4 linker of the pacemaker (HCN) channel that influences activation gating JOURNAL OF BIOLOGICAL CHEMISTRY, 278 (16): 13647-13654 APR 18 2003

[23] Silva J, Rudy Y.Mechanism of Pacemaking in I_{K1}-Downregulated Myocytes. Circ Res. 2003;92:261-263.

[24] Yu H, Wu J, Potapova I, Wymore RT, Holmes B, Zuckerman J, Pan Z, Wang H, Shi W, Robinson RB, El-Maghrabi MR, Benjamin W, Dixon J, McKinnon D, Cohen IS, Wymore R. MinK-Related Peptide 1, A β Subunit for the HCN Ion Channel Subunit Family Enhances Expression and Speeds Activation. Circulation Research. 2001;88:e84.

[25] Yu HG, Lu Z, Pan Z, Cohen IS. Tyrosine kinase inhibition differentially regulates heterologously expressed HCN channels. Pflugers Arch. 2004 Jan;447(4):392-400.

[26] Kehat I, Khimovich L, Caspi O, Gepstein A, Shofti R, Arbel G, Huber I, Satin J, Itskovitz-Eldor J, Gepstein L. Electromechanical integration of cardiomyocytes derived from human embryonic stem cells. 2004; doi:10.1038/nbt1014.

[27] Santoro B, Tibbs GR. The HCN gene family: molecular basis of the hyperpolarization-activated pacemaker channels. Ann N Y Acad Sci. 1999 Apr 30;868:741-64.

[28] Beeler GW, Reuter H. Reconstruction of the action potential of ventricular myocardium fibers. J Physiol.1977; 268:177-210.

[29] Gepstein L. Derivation and potential applications of human embryonic stem cells. Circ Res. 2002;91:866876.

[30] Hodgkin AL, Huxley F. A quantitative description of memebrane current and it's application to conduction and excitation in nerve. J Physiol. 1952;117:500-544.

[31] Valiunas V, Weingart R, Brink PR. Formation of heterotypic gap junction channels by connexins 40 and 43. Circ Res. 2000;86:e42e49.

[32] Moosmang S, Stieber J, Zong X, Biel M, Hofmann F, Ludwig A. Cellular expression and functional characterization of four hyperpolarization-activated pacemaker channels in cardiac and neuronal tissues. Eur J Biochem. 2001;268:16461652.

[33] DiFrancesco D. A study of the ionic nature of the pacemaker current in calf Purkinje fibres. J Physiol. 1981;314:377393.

[34] Moore LK, Burt JM. Gap junction function in vascular smooth muscle: influence of serotonin. Am J Physiol. 1995 Oct;269(4 Pt 2):H1481-9.

[35] Liechty KW, MacKenzie TC, Shaaban AF, Radu A, Moseley AM, Deans R, Marshak DR, Flake AW. Human mesenchymal stem cells engraft and demonstrate site specific differentiation after in utero implantation in sheep. Nat Med 2002;6:12821286.

[36] Kanani S, Pumir A, Cohen IS, Krinski V. Incorporating stem cells into cardiac tissue. Hints from mathematical modeling. Submitted : Aug. 2005.

[37] Muller-Ehmsen J, Peterson KL, Kedes L, Whittaker P, Dow JS, Long TI, Laird PW, Kloner RA. Rebuilding a Damaged Heart Long-Term Survival of Transplanted Neonatal Rat Cardiomyocytes After Myocardial Infarction and Effect on Cardiac Function. Circulation. 2002;105:1720-1726.

[38] Bender CM and Orszag SA. Advanced mathematical methods for scientists and engineers. Mac Graw Hill, Singapore (1984).

[39] Abramowitz M, Stegun IA. Handbook of mathematical functions. Dover, 1972.